Investigation of the Ubiquitin Proteasome System in *Schizosaccharomyces pombe*

James S A Glover

Doctor of Philosophy
University of Edinburgh

2010

Abstract

Ubiquitin is an essential 76 amino acid protein which can be conjugated to lysine residues on a variety of substrates via its C-terminal diglycine motif. This conjugation allows the protein to act as a molecular tag in a range of processes, including regulation of chromatin compaction, signalling cascades and DNA repair. In addition, ubiquitin moieties are capable of forming chains through the successive conjugation to lysine residues within ubiquitin itself. One of the most well characterized functions of ubiquitin is its role in protein quality control and degradation. Tetra-ubiquitin chains, most commonly through a lysine-48 linkage, are responsible for directing proteins to the 26S proteasome for degradation. This process is of importance both in the removal of miss-folded proteins, and in the regulated destruction of specific targets, such as the cyclins.

The 90kDa AAA-ATPase Cdc48/p97/VCP is an essential protein that forms a hexameric complex, which interacts with a wide variety of ubiquitinated substrates. The specificity of Cdc48 is modulated by a series of different cofactors, which together allow Cdc48 to operate in several different contexts, from removal of misfolded proteins from the ER, to regulating securin stability. The role of two Cdc48 cofactors, Ubx4 and Ubx5, was studied in an attempt to dissect their function and to determine how they may modulate the function of Cdc48. Neither protein was found to be essential, as knockouts of either were found to be viable with no major defect in growth rate. The work also describes the findings of a yeast two-hybrid screen to identify potential substrates for both cofactors.

Delivery of ubiquitinated proteins to the proteasome is mediated by shuttling factors, which are able to bind to both ubiquitin and the proteasome, and hence mediate the interaction between both. The shuttling factor Dph1 binds ubiquitin via a C-terminal UBA domain, while its N-terminal UBL domain mediates its interaction with the proteasome. This work identified a novel interaction between the Sti1 domains of Dph1 and the N-terminal region of a mitochondrial localized AAA-ATPase, homologous to the Saccaromyces cerevisiae protein Msp1. In addition, cell fractionation experiments revealed the presence of Dph1 at the mitochondria. This interaction provides hints that Mlp1 may be involved in the removal of ubiquitinated proteins from the mitochondria, and their delivery to the proteasome. The thesis begins to try and attempt to identify possible substrates of this proposed mitochondria associated degradation pathway, and looks for ways in which the hypothesis may be tested.

Acknowledgements

The work shown in this thesis could not have been completed without the help of countless people in the human genetics unit and beyond. In particular, thanks need to go to the members of the Gordon lab, both past and present, who have helped the work progress. My supervisor, Colin Gordon, helped support the work in its earliest stages, and its latest, provided encouragement when things were going slowly, and urged caution when I was getting prematurely excited. Mairi Wallace and Morag Robertson not only both ensure that the lab keeps running smoothly, but also provided valuable advice, technical support, and helped with several of the experiments. The other members of the lab, Bethan Medina, David Girdwood and Kostas Paraskevopoulos, have proven excellent sources of company, advice and reagents. Similar thanks go to prior lab members as well: Jean O'Donoghue, Katalin Fullop and Jayne Miller, whose help in the early stages of the PhD helped me get settled in the lab. Particular thanks must also go to Ingo Amn, whose work provided a starting point for the second half of the thesis, without which this would be a substantially thinner, if not non-existent piece of work.

I also thank members of other labs, and support staff throughout the HGU. In particular, thanks to Paul Perry and Matthew Pearson for their assistance with the Microscopy, Steven Tait and Agnes Gallacher for sequencing support and Craig Nicol for imaging. Kevin Chalmers provided invaluable support and advice in the pull-down and immunoprecipitation experiments.

Yet the challenges of a PhD aren't only found in the laboratory. Fellow student Rachel Rigby offered assistance when moving flats on several occasions, including risking life and limb when it was necessary to do so in particularly icy conditions. Bob and Alison Hill were able to supply me with somewhere to live through the final months of my research, and the writing of the thesis, even though I didn't know if I'd be here for another three months, or another eight. Bob also helped with proofreading of the thesis, and providing advice with regards to its structure.

Finally, I must thank my parents, who shared the highs and lows of my PhD, through both regular phone-calls, and trips home when I needed an escape.

Document typeset in LaTeX 2$_\varepsilon$. Packages used include array, biocon, booktabs, fontenc, graphicx, lmodern, natbib, pdflscape, rotating, supertabular, TeXshade(Beitz, 2000) and textcomp. Processed using pdftex and based on an Edinburgh University thesis template by Mary Ellen Foster.

Declaration

I declare that this thesis was composed by myself, that the work contained herein is my own except where explicitly stated otherwise in the text. This work has not been submitted for any other degree or professional qualification except as specified.

(*James S A Glover*)

Table of Contents

List of Figures

List of Tables

Abbreviations

3-AT 3-amino-1,2,4-triazole

A Adenine

5mwt Five-marker wildtype

AAA ATPase ATPases associated with a number of cellular activities

ADP Adenosine diphosphate

ALS Amyotrophic lateral sclerosis

AMP Adenosine monophosphate

APC/C Anaphase promoting complex / cyclosome

APS Ammonium persulfate

apt1 AP-1 target gene

ATP Adenosine triphosphate

BFA Brefeldin A

bp Base pairs

BSA Bovine serum albumin

Cdc48 Cell division cycle protein 48

CPY* Carboxypeptidase Y*

C-terminal Carboxy-terminal

DNA Deoxyribonucleic acid

E1/2/3 Enzymes 1, 2 and 3 respectively in the ubiquitination cascade.

EMM Edinburgh minimal media

ER Endoplasmic reticulum

ERAD Endoplasmic reticulum associated degradation

FACS Fluorescence-activated cell sorting

H Histidine

HECT Homologous to E6-AP

IBMPFD Hereditary inclusion body myopathy, Paget's disease and frontotemporal dementia.

IMM Inner mitochondrial membrane

IMS Inter-membrane space

kDa Kilo-Daltons

LB Luria-Bertani media

MAD Mitochondria associated degradation

Mlp1 Msp1 like protein 1

MM Mitochondrial matrix

Msp1 Mitochondrial sorting of proteins 1

N-terminal Amino-terminal

NEM N-ethylmaleimide

NSF NEM-sensitive factor

NZF Npl4 zinc-finger

obr1 Overexpressed in brefeldin A resistant strains 1

OMM Outer mitochondrial membrane

PCNA Proliferating cell nuclear antigen

PEG Polyethylene glycol

RING Really interesting new gene

rpm Revolutions per minute

SDS Sodium dodecyl sulphate

SDS-PAGE SDS polyacrylamide gel electrophoresis

SILAC Stable isotope-labeled amino acids

SNAP Soluble NSF attachment protein

SNARE SNAP receptor

SOD Superoxide dismutaste

Sti Stress inducible

TEMED N,N,N',N'-Tetramethylethylenediamine

TRL Thioredoxin-like

Uba1 Ubiquitin activating enzyme 1

UBA Ubiquitin-associated

UBD Ubiquitin fold domain

UBP Ubiquitin specific protease

Ubx Ubiquitin regulatory X

Ufd Ubiquitin-fusion degradation

uhp1 Ubiquitinated histone-like protein

UIM Ubiquitin interacting motif

UPR Unfolded protein response

VCIP135 VCP interacting protein 135

VCP Valosin-containing-protein

VDAC1 Voltage-dependent anion-selective channel protein 1

VWFA von Willebrand Factor type A

W Tryptophan

XPC Xeroderma pigmentosum, complementation group C

YES Yeast extract with supplements

Chapter 1

Introduction

1.1 Ubiquitin

Ubiquitin is a small essential globular protein of just 76 amino acids (Figure 1.1), which is found throughout the eukaryotic lineage. The protein is highly conserved, and multiple copies are encoded in the genome, either as tandem repeats or fused to ribosomal proteins. In fission yeast, *Schizosaccharomyces pombe*, four single copies of ubiquitin are encoded as fusions at the N-terminus of ribosomal proteins: on two copies of L40, and on S46a and S46b. Further copies are fused head to tail as a single protein, expressed from *ubi4*$^+$ and induced on heatshock (Finley et al., 1987; Jain et al., 2009; The UniProt Consortium, 2010). Fused ubiquitin proteins are processed by post-translational cleavage to result in single ubiquitin moieties (See section 1.2).

The most striking characteristic of ubiquitin is its ability to be conjugated to substrate proteins via an isopeptide bond between the C-terminal di-glycine motif of the ubiquitin moiety, and an ϵ-amino group of a substrate lysine residue. Ubiquitin conjugation has also been observed to occur on the N-terminus of substrate proteins (Reviewed in Welchman et al., 2005). The reaction cascade involved in this process is discussed in more detail in section 1.2. Additionally, lysine residues within ubiquitin itself, highlighted in yellow in figure 1.1, are able to act as substrates for further ubiquitin conjugation, allowing for the formation of ubiquitin chains. The use of different residues in ubiquitin chain formation is an important mechanism in regulating its function (See section 1.3).

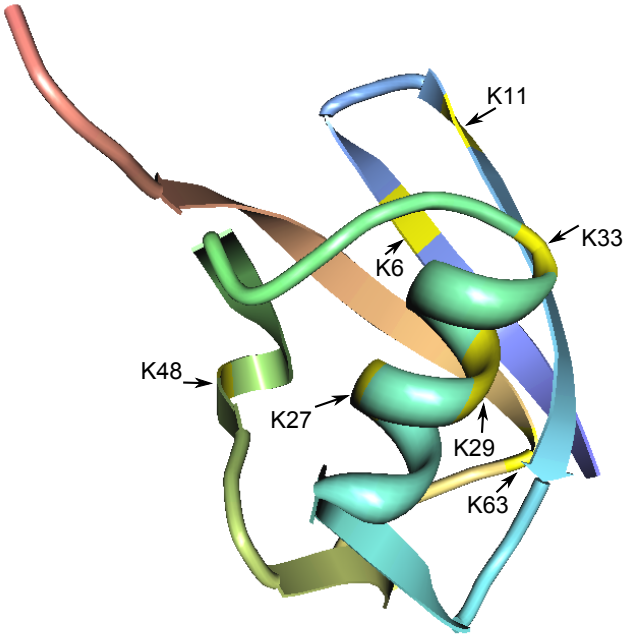

Figure 1.1: Ubiquitin structure as determined by X-ray crystallography (Vijay-Kumar et al., 1987). Lysine residues are highlighted in yellow and are indicated by arrows.

1.1.1 Ubiquitin-like Proteins

Ubiquitin is the defining member of a series of ubiquitin-like proteins, which show both structural and sequence homology to ubiquitin (Reviewed in Welchman et al., 2005). As with ubiquitin, many of these proteins share the C-terminal di-glycine motif, and may be conjugated to substrates in a similar manner to ubiquitin itself. In other cases, the ubiquitin-like moiety exists as a domain of a larger protein, known as a UBL domain, and as such lacks the residues necessary for conjugation.

Two of the most well characterised ubiquitin-like proteins are Nedd8/Rub1 and the SUMO proteins. Neither protein is a direct signal for ubiquitin degradation, although they often function in association with the ubiquitin system. For example, the conjugation of Nedd8 to cullins of the SCF complexes displaces the inhibitor Cand1, and is required for E3 ligase activity (Welchman et al., 2005). SUMOylation has been linked to a number of processes, including the import of Ran GTPase activating protein into the nucleus and regulation of NF-κB signalling. In the latter it appears to act as an antagonist to ubiquitin by blocking sites of ubiquitination on the IκB protein, preventing its ubiquitin mediated degradation. IκB inhibits the NF-κB transcription factor, and thus SUMO acts to down-regulate NF-κB activation (Hay, 2005; Welchman et al., 2005).

1.2 The Ubiquitination Cascade

Ubiquitination is an ATP dependent process governed by a series of enzymatic reactions known as the ubiquitin cascade (Figure 1.2). The variety of enzymes involved in the reaction diversifies as the cascade progresses, helping to provide specificity for a wide range of substrates and the regulated ubiquitination of each.

Prior to conjugation, ubiquitin moieties must be cleaved by an endopeptidase to reveal the active di-glycine motif. A variety of proteins demonstrate ubiquitin C-terminus peptidase activity, such as the UBP (ubiquitin-specific protease) family of proteins which contain a conserved ubiquitin peptidase repeat (Baker et al., 1992). UBP family proteins show a range of specificities, from different linear conjugations, both natural and artificial, to different ubiquitin chain linkages (Baker et al., 1992; Wilkinson et al., 1995; Tobias and Varshavsky, 1991). Together these enzymes are able to catalyse the processing of newly synthesised ubiquitin, as well as regenerating re-usable ubiquitin from ubiquitin chains (Hershko et al., 1983; Hershko and Ciechanover, 1998).

The first evidence of the ubiquitination cascade was presented by Hershko et al. (1983), and has been reviewed substantially since then (Hershko and Ciechanover, 1998; Miller and Gordon, 2005). The first step in the ubiquitination cascade is the activation of free ubiquitin. This process is catalysed by the ubiquitin activating enzyme, E1, which binds MgATP, followed by ubiquitin. The hydrolysis of ATP results in the release of PPi, and the formation of a ubiquitin-adenylate intermediate (Pickart, 2001). This is followed by the conjugation of ubiquitin via a C-terminal thioester linkage, to a cysteine residue on the E1 enzyme itself. Subsequently ubiquitin is transferred to a cysteine residue on the ubiquitin conjugating enzyme, E2. The final step of the reaction is the transfer of ubiquitin from the E2 enzyme, to an amino group on the substrate itself, most commonly an ϵ-amino group of a lysine residue. This final reaction is catalysed by a ubiquitin ligase, E3. At each stage of the reaction, the transfer of ubiquitin regenerates the site on the previous enzyme in the cascade, allowing for it to take part in another ubiquitination reaction (Pickart, 2001).

One characteristic of the ubiquitination cascade is an increasing diversification and specificity as the cascade progresses. Like most species, *S. pombe* contains just a single E1 enzyme, Uba1 (Ubiquitin activating enzyme), which is involved in the first step of all ubiquitination reactions. Unsurprisingly, as with ubiquitin, *uba1*$^+$ is essential for viability (Azad et al., 1997).

By contrast, there have been several E2 enzymes identified, with 11 proteins being flagged to show E2 activity in *S. pombe* (Colin Semple, personal communication).

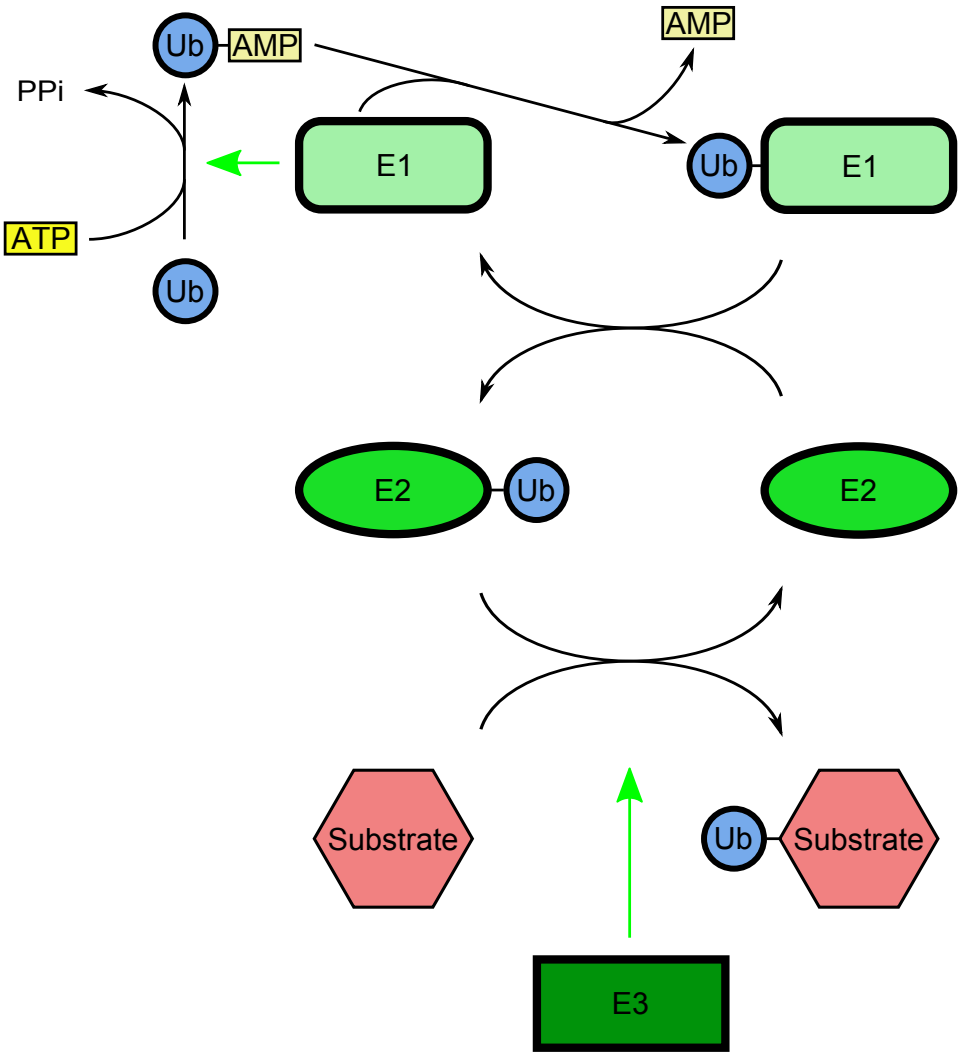

Figure 1.2: Diagram outlining the reactions involved in the ubiquitination cascade. Green arrows indicate reactions catalysed by an enzyme in which it is not involved directly. The outline shown best represents the behaviour of RING-domain E3 ligases; by contrast, ubiquitin is directly conjugated to HECT-domain E3 ligases before transfer to the substrate.

Known E2 enzymes share a conserved catalytic domain of approximately 150 amino acids. They show a range of specificities, from demonstrating cooperation with multiple E3 enzymes in several ubiquitination pathways, to more restricted and specified roles. Some E2 enzymes form stable complexes with specific E3s, such as the interaction between the *Saccharomyces cerevisiae* E2 Ubc2/Rad6 and the RING domain E3 Rad18 (Bailly et al., 1997). Ubc2 has also been shown to operate independently of Rad18, such as in the control of silencing at telomeres and the HMR locus in *S. cerevisiae* (Huang et al., 1997), and in the N-end rule pathway, in which it associates with the E3 ligase UBR1 to regulate the stability of proteins dependent on their N-terminal amino-acid (Dohmen et al., 1991). This illustrates the branching network of association between E2s and E3s.

The E3 enzymes are a wider group still, with variations in both sequence, and mechanism of action (Hershko and Ciechanover, 1998); they can be divided into two families on the basis of shared active site structures: RING (Really interesting new gene) finger, and HECT (Homologous to E6-AP) domain proteins (Reviewed in Pickart, 2001; Watson and Irwin, 2006). RING finger E3 ligases, such as Mdm2, are defined by conserved zinc finger structure (Watson and Irwin, 2006), and catalyse the direct transfer of ubiquitin from the E2 to the substrate. HECT domain E3s, such as E6-AP contain a conserved C-terminal domain of approximately 350 amino acids and form a thioester intermediate on a conserved cysteine during the reaction.

Enzymes also differ by how they coordinate their interaction with the target substrate, either binding directly, or via adapter proteins. In some cases, such as for E6-AP, the protein can interact directly or indirectly depending on the target substrate. This requirement for adaptor substrates can be particularly apparent in the E3 ligases that act as part of large multi-subunit protein complexes. SCF (Skp-Cullin-F-box) ligases containing the RING finger protein Rbx1 in complex with a cullin (Cul1/Cdc53) and Skp1, the latter protein is able to interact with a series of adaptor proteins, such as Cdc4p and Grr1p via their F-box domains, which in turn coordinate interaction with target substrates.

A subset of E3 ligases, sometimes termed E4 proteins, are responsible for extending ubiquitin chain lengths. One of the most well characterised E4 proteins is the protein Ufd2, which is necessary for forming extended chain lengths in the proteasome degradation pathway (Koegl et al., 1999). Ufd2 associates with proteins responsible for transporting proteins to the proteasome, such as Cdc48, Dsk2 and Rad23, and hence couples chain extension to proteasome delivery (Koegl et al., 1999; Kim et al., 2004; Richly et al., 2005; Hänzelmann et al., 2010).

1.3 Ubiquitin Signals

While the addition of ubiquitin to proteins is perhaps best associated with proteasomal degradation, the protein performs a wider range of functions. As mentioned above, lysine residues within ubiquitin are capable as acting as substrates for further ubiquitin conjugation, allowing the formation of ubiquitin chains. Variations in the residue used for chain formation, and in chain length, allow ubiquitin to perform distinctive roles within the cell. While all ubiquitin lysine residues are capable of supporting chain formation, only some have been determined to have physiological relevance (Reviewed in Miller and Gordon, 2005). Lysine-48, Lysine-11 and lysine-63 linked chains are the most numerous (Peng et al., 2003; Xu et al., 2009).

1.3.1 Mono- and Multi-Mono- Ubiquitination

Monoubiquitination describes the conjugation of a single ubiquitin to a lysine residue on the substrate; the conjugation of further single ubiquitin moieties to other suitable lysine residues on the same substrate, results in multi-monoubiquitination. In contrast to polyubiquitination (Section1.3.2) multi-monoubiquitination does not result in ubiquitin chain formation.

Monoubiquitination is involved in a wide variety of processes, such that it is difficult to identify it with a single particular function. Examples of events regulated by monoubiquitination include DNA repair, histone regulation and endocytosis. For example, monoubiquitination of lysine-164 of PCNA (Proliferating cell nuclear antigen) by the E2 Rad6, and the E3 Rad18 allows for the association of translesion polymerases; ubiquitination of lysine-123 of histone H2B is linked to chromatin compaction and gene silencing (Welchman et al., 2005).

1.3.2 Polyubiquitination

Polyubiquitination describes the conjugation of chains of ubiquitin to a substrate, formed from the conjugation of further ubiquitin moieties to lysine residues within ubiquitin itself. The use of different ubiquitin lysine residues in chain formation allows for targeting the substrate to different pathways.

1.3.2.1 Lysine-48, Lysine-29, Lysine-11

The targeting of proteins to the ubiquitin proteasome system is one of the most studied consequences of substrate ubiquitination. In particular, the delivery of substrates to the proteasome appears to depend on the formation of ubiquitin chains of four or more residues through lysine-48, lysine-29 or lysine-11 (Xu et al., 2009). The recognition of these chains and their delivery to the proteasome is considered in more detail in section 1.5. All other chain linkages, apart from lysine-63, also show stabilization on proteasome inhibition, suggesting at least a partial role of the proteasome (Xu et al., 2009).

Delivery to the proteasome can occur either as part of the regulated destruction of a protein, in response to external stimuli or cell cycle progression, or as part of the cell's quality control system. The latter process describes the removal of poorly folded proteins, which are thought to result from approximately 30% of all translation events (Schubert et al., 2000).

1.3.2.2 Lysine-63, Lysine-27

Another linkage specifically identified as having physiological relevance is lysine-63. Chains formed by lysine-63 linkages are not involved in proteolytic pathways, but rather operate in a regulatory capacity. For example, the conjugation of lysine-63 chains to the E3 ubiquitin ligase PARKIN is necessary for its mitochondrial localization (Geisler et al., 2010). Additionally, lysine-63 chains are also associated with DNA replication and repair. The extension of lysine-164 monoubiquitination of PCNA by the E2 Ubc13-Mms2 and the E3 Rad5 forms lysine-63 chains and prompts template switching, allowing error free bypass of DNA lesions (Welchman et al., 2005).

Lysine-27 linked ubiquitin chains have also been identified in association with mitophagy pathways. Damaged or redundant mitochondria are eliminated by autophagy pathways know as mitophagy, in which mitochondria are engulfed and degraded by autophagosomes. On mitochondrial localization PARKIN promotes the conjugation of lysine-27 linked ubiquitin chains to its substrate, the outer mitochondrial membrane protein VDAC1. In turn this appears to result in the recruitment of the UBA domain containing protein p62, which helps coordinate mitophagy (Geisler et al., 2010).

1.4 The Proteasome

The 26S proteasome is a large multi-subunit complex of around 30 proteins which is capable of degrading proteasome directed ubiquitinated substrates in a regulated ATP dependent manner. The complex consists of a hollow barrel like structure, the 20S core particle, capped on either side by a 19S regulatory particle (Figure 1.3). Disruption of the proteasome in *S. pombe* results in metaphase arrest (Gordon et al., 1993, 1996), due to the stabilisation of substrates which regulate cell cycle progression, such as Securin (Reviewed in Miller and Gordon, 2005).

The core particle contains the main proteolytic activity of the proteasome. The complex consists of four heptameric ring complexes, two each of alpha and beta. Each ring is formed of seven distinct proteins, meaning that the core particle contains a total of fourteen different proteins. Peptidase activity is found on three subunits of the β ring, β1, β2 and β5, with the activity orientated towards the inside of the barrel. In vertebrates, cytokine induced variant peptidases can be incorporated, adjusting proteasome activity to produce short peptides which may be integrated in the MHC (Major histocompatibility complex) as part of an immune response (Miller and Gordon, 2005).

The 19S regulatory particle is responsible for controlling access to the proteolytic chamber of the 20S, and thus ensures that proteasome activity is specific. The 19S subcomplex can be split into two different complexes, the base and the lid. The base is a multi-protein complex, including six ATPase subunits, which contact the 20S subunit. Regulation occurs in an ATP dependent manner under the control of the AAA-ATPase Rpt2/Mts2/S4 (Hertz-Fowler et al., 2004), while other ATPases act as anti-chaperones, unfolding substrates for entry into the proteolytic chamber. Non-ATPase components of the base include Rpn1/Mts4 (Glickman et al., 1998), which aids in shuttle factor recruitment (Section 1.5). By contrast the lid is formed from 8 non-ATPases including a Zn^{2+} protease, Pad1/Rpn11/POH1 which cleaves ubiquitin on substrates (Yao and Cohen, 2002). This cleavage is coupled to substrate recognition and translocation, and is essential for unimpeded entry into the core particle. The regulatory particle also contains Rpn10/Pus1/S5a, a protein capable of binding ubiquitin; the role this plays in ubiquitin recognition by the proteasome is described in more detail in section 1.5.

1.5 Ubiquitin Recognition and Shuttle Factors

The previous sections have considered the processes of ubiquitination, which can mark proteins of for degradation, and the destruction of proteins by the catalytic activity of the proteasome. These processes are linked by the ability of the proteasome, and associated proteins, to bind to ubiquitin. The components which participate in this process are termed shuttle factors.

1.5.1 Pus1/Rpn10/S5a

A screen for proteasome subunits with ubiquitin binding activity provided the first physical link between ubiquitinated proteins and the proteasome. S5a, a subunit of the 19S regulatory particle was found to bind ubiquitin, with particular affinity for lysine-48 linked chains of four or more subunits (Deveraux et al., 1994). Homologs of S5a are found throughout the eukaryotes, the protein is known as Pus1 in *S. pombe* and Rpn10 in *S. cerevisiae* (Figure 1.4).

Ubiquitin binding activity was isolated to a conserved C-terminal alpha helix, which is duplicated in the human homolog (Fu et al., 1998; Young et al., 1998; Wilkinson et al., 2000). This sequence would later be used to define the ubiquitin interacting motif (UIM), a ubiquitin interacting domain of 20 amino-acids, found in a range of proteins (Hofmann and Falquet, 2001). Pus1 also includes an N-terminal VWFA (von Willebrand Factor type A) domain (Jain et al., 2009; The UniProt Consortium, 2010). An interaction between an N-terminal region of Pus1 and the 19S base subunit Rpn1/Mts4, results in the protein's association with the proteasome (Xie and Varshavsky, 2000; Wilkinson et al., 2000; Seeger et al., 2003); additional interactions are also seen between Pus1 and Mts3 (Wilkinson et al., 2000). As well as the proteasome associated fraction, Pus1 also exists as an unbound population within the cytosol (Wilkinson et al., 2000).

Both *pus1*$^+$ and *rpn10*$^+$ were found to be non-essential genes, which indicated the existence of other proteins responsible for recruiting ubiquitinated proteins to the proteasome (Fu et al., 1998; Wilkinson et al., 2000). Surprisingly, Rpn10 with an inactive UIM domain is able to rescue the canavanine sensitivity of Rpn10 deletions, indicating that the protein has a functional role at the proteasome independent of its ability to bind ubiquitin (Fu et al., 1998; Wilkinson et al., 2000). Conversely, deletion of the *Drosophila melanogaster* ortholog, *pros54* results in mitotic and morphological defects, increased larval mortality, and pupal inviability (Szlanka et al., 2003).

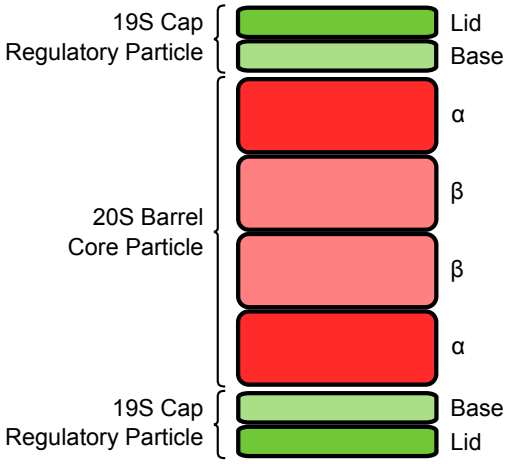

Figure 1.3: Structure of the 26S proteasome.

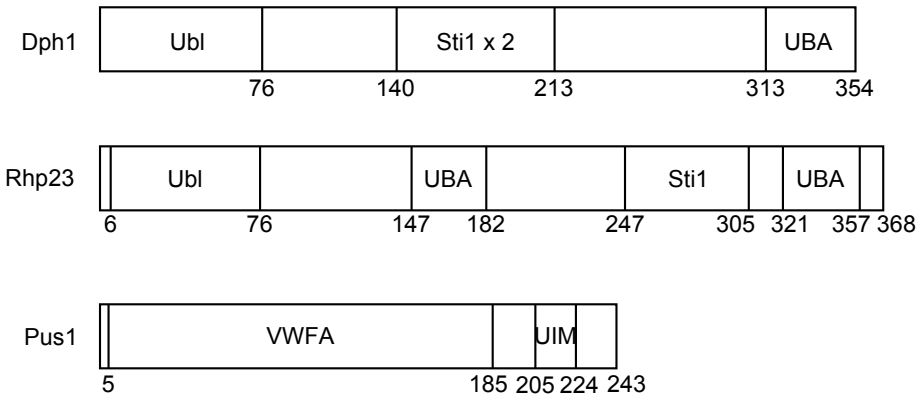

Figure 1.4: Domain structure of the proteasome shuttle factors Dph1, Rhp23 and Pus1 from *S. pombe*. (Schultz et al., 1998; Letunic et al., 2006, 2009; Jain et al., 2009)

1.5.2 Rhp23/Rad23/hHR23

The *S. pombe* Rhp23p and the Rad23 ortholog in *S. cerevisiae* (Figure 1.4) are capable of interacting both with polyubiquitin and with the proteasome. Interaction with tetra-ubiquitin chains is coordinated through two UBA domains (Wilkinson et al., 2001), one at the C-terminus, and one in the centre of the protein. The N-terminal UBL (Ubiquitin like) domain is homologous to ubiquitin and mimics its structure (Lowe et al., 2006); it associates with the proteasome via a central domain in the Mts4 subunit of the 19S regulatory particle (Wilkinson et al., 2001; Seeger et al., 2003). Additionally, the human orthologs of Rhp23, hHR23A and hHR23B, have both been shown to interact with S5a (Hiyama et al., 1999). As with *pus1*$^+$, *S. pombe* with deletions of the *rhp23*$^+$ gene are viable (Wilkinson et al., 2001; Elder et al., 2002).

As well as its role in the ubiquitin proteasome system, Rhp23/Rad23 is also associated with the repair of UV induced lesions (Reviewed in Dantuma et al., 2009). Briefly, Rad4/XPC (Xeroderma pigmentosum, complementation group C) in complex with Rad23 recognises and binds to lesions in the DNA. This complex is then able to recruit the proteins necessary for repair. The exact role of Rad23 in this process is unclear, although it is thought that its binding to Rad4 may help stabilise the protein. Additionally, a stimulatory effect of the UBL domain of Rad23, dependent on the presence of the 19S cap, suggests a possible role for the proteasome in DNA repair. However, as the UBL domain can be supplied *in trans* from the Sti1/XPC-binding domain the nature of its role is unclear (Dantuma et al., 2009). The *S. pombe* Rad23 homolog appears to have a similar role in nucleotide excision repair (Elder et al., 2002).

1.5.3 Dph1/Dsk2/hPLIC

Dph1 (Figure 1.4) acts in a similar manner to Rhp23, it contains a single C-terminal UBA domain for binding tetra-ubiquitin, and an N-terminal UBL domain for interacting with Mts4. Additionally, Dph1/Dsk2 appears to interact with free Pus1/Rpn10, inhibiting its interaction with the proteasome and suggesting that the shuttle factors may help regulate each other's activity (Matiuhin et al., 2008). Once more, *dph1* null mutants are viable, indicating that the shuttle factors have some partial redundancy.

In addition to its interaction with ubiquitinated substrates and the proteasome, the human Dph1 homolog, hPLIC, was found to interact with the human Hsp70 homolog Stch via its central pair of Sti1 domains (Stress inducible) (Kaye et al., 2000). Sti1 domains in other proteins have been demonstrated to coordinate interaction with both

Hsp70 and Hsp90 family proteins (Chang and Lindquist, 1994; Lässle et al., 1997). The exact function of the interaction between Dph1 and the Hsp70 and Hsp90 families is unknown, although other Sti1 domain containing proteins have been shown to act as co-factors (Chang et al., 1997). It is possible that the interaction of Dph1 with chaperones helps to couple the process of protein refolding to proteasome delivery; extended association with chaperone proteins is a likely indicator that a protein is terminally misfolded.

1.5.4 Genetic Interactions With and Among the Shuttle Factors

Deletion of any one of the shuttle factors results in viability in *S. pombe*, although there may be minor phenotypes. However deletion of multiple shuttle factors results in synthetic phenotypes, illustrating the degree of functional redundancy among the shuttle proteins. While Δ*dph1*Δ*pus1* strains grow at the same rate as wild-type cells, Δ*dph1*Δ*rhp23* show an elongated phenotype – average cell length is longer compared to wild-type – when grown at the elevated temperature of 36℃. Synthetic phenotypes are even more severe for the Δ*pus1*Δ*rhp23* strain which shows severe growth defects at 25 ℃, and metaphase arrest at 36℃. Knockout of all three shuttle factors is lethal; attempts to create spores with this genotype result in death within a couple of division after germination. Expression of Rhp23 lacking either the UBL or UBA domains is unable to rescue triple knock-outs, indicating that binding of both ubiquitin and the proteasome is important for its function. This indicates that the three proteins have overlapping functionality and together operate in an essential pathway (Wilkinson et al., 2001). Similar genetic interactions are seen in *S. cerevisiae* (Lambertson et al., 1999; Saeki, 2002; Peng et al., 2003; Díaz-Martínez et al., 2006), which contains an additional shuttle factor, Ddi1, which is redundant to Rpn10; the *S. pombe* homolog Mud1 does not appear to act in the same pathway (Welchman et al., 2005; Miller and Gordon, 2005).

Genetic screens identifying sensitivity to over-expression of proteins in a *S. cerevisiae* Δ*Dsk2*Δ*Rhp23* background identified substrates that were stabilized in a Δ*Dsk2* but not a Δ*Rhp23* background. Thus although the shuttle factors do show some redundancy, they still show distinct roles as part of the ubiquitin proteasome pathway (Liu et al., 2009).

Over expression studies revealed that all three shuttle factors result in an apparent stabilization of polyubiquitinated proteins on over expression (Funakoshi et al., 2002; Hartmann-Petersen, 2003). This behaviour may seem to be in contrast with their role in

protein degradation, however it is most likely a result of the protection of ubiquitinated proteins against the action of deubiquitination enzymes. It is dependent on the ability of the shuttle factors to bind ubiquitinated proteins, and is independent of their ability to bind the proteasome (Hartmann-Petersen, 2003). Additional suggestions that shuttle factor overexpression inhibits protein degradation by saturating the proteasome with empty shuttle factors, is complicated by findings that overexpression of the UBL domain alone is not sufficient to stabilize substrates (Ortolan et al., 2000; Funakoshi et al., 2002).

1.6 Cdc48

Cdc48, or p97/VCP, is a highly conserved, essential, 90.1kDa (Hertz-Fowler et al., 2004) AAA-ATPase (ATPases associated with a number of cellular activities) found throughout the eukaryotes. The degree of conservation, shown in table 1.1, is such that human p97 cDNA is able to rescue *S. pombe cdc48* mutants (Eric Chang, Personal communication). The protein forms a hexameric ring complex, which associates with a number of cofactors to form an active Cdc48 complex. The cofactors modify Cdc48 function to allow it to perform a variety of roles within the cell. Studies in mice (Müller et al., 1999) show that p97 bears a strong promoter which is able to drive expression in a wide range of adult tissues. However the intensity of p97 staining is not uniform, and its sub-cellular distribution can vary between cell-types. These patterns of expression suggest that in mammals p97 plays a diverse but regulated role in cellular processes.

1.6.1 Structure

Cdc48 subunits can be divided into three domains, joined by short linker regions (DeLaBarre and Brunger, 2003, 2005; Huyton et al., 2003). A globular N-terminal domain is able to coordinate binding to substrates and co-factors, as discussed in section 1.6.3. C-terminal to this are two type-II AAA-ATPase domains, defined as D1 and D2 (DeLaBarre and Brunger, 2003; Huyton et al., 2003). Each domain is able to associate with its counterpart in an adjacent Cdc48 subunit, allowing for the assembly of a two-tiered hexameric ring structure of 540kDa, shown in figure 1.5 (DeLaBarre and Brunger, 2003, 2005; Huyton et al., 2003). The D1 and D2 domains sit on top of each other in a head to tail fashion around a central 10Å pore containing a Zn^{2+} ion, the N-terminal domain associates with the D1 domain on the outside of the ring (DeLaBarre and Brunger, 2003; Huyton et al., 2003).

Species		% Identity
S. pombe	*Homo sapiens*	69%
	Xenopus laevis	68%
	Mus musculus	69%
	S. cerevisiae	75%
H. sapiens	*X. laevis*	96%
	M. musculus	99%
	S. cerevisiae	68%
X. laevis	*M. musculus*	96%
	S. cerevisiae	68%
M. musculus	*S. cerevisiae*	68%

Table 1.1: Table showing the sequence identity between cdc48/VCP/p97 homologs of different species (Moreland et al., 2005).

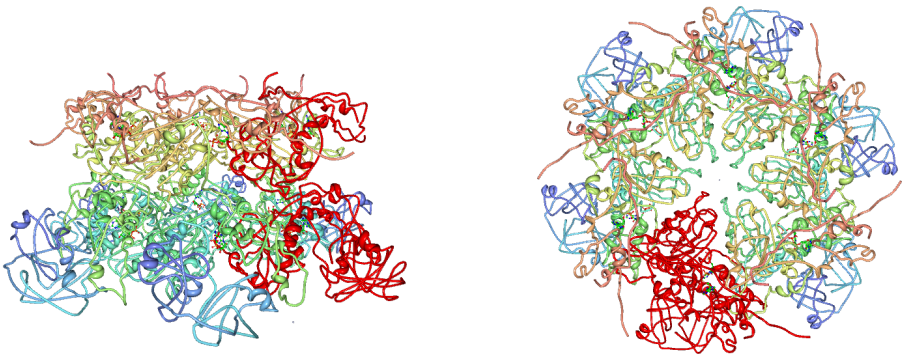

Figure 1.5: Crystal structure of the murine Cdc48 homolog p97/VCP. A single p97 monomer is indicated in red.(Huyton et al., 2003; Moreland et al., 2005)

Conformational changes induced on hydrolysis of ATP at the active sites result in a movement in the N-terminal domain. This may help mediate the protein's activity, possibly by imparting mechanical force on its substrates (DeLaBarre and Brunger, 2005). Cooperating interactions between each domain may coordinate to ensure orderly hydrolysis and controlled changes in Cdc48 conformation (DeLaBarre and Brunger, 2003, 2005; Ye et al., 2003).

1.6.2 AAA-ATPases

The AAA-ATPases are part of the AAA+ superfamily, a broad family of proteins associated with a range of processes. In addition to Cdc48/p97, AAA+ family proteins have been associated with the base of the proteasome regulatory particle (section 1.4), with mitochondrial proteases (section 1.7.1), with membrane fusion and other processes. According to the SMART database, *S. pombe* contains 78 proteins with a AAA-ATPase domain (Schultz et al., 1998; Letunic et al., 2009).

Despite their diverse functions, AAA+ proteins appear to share a conserved activity. The proteins use the hydrolysis of ATP to promote conformational changes, which help them exert mechanical force on their substrate. As a result, AAA-ATPase appear to function as anti-chaperones or unfoldases, and help promote the unfolding of proteins, their extraction from complexes, and other structural remodelling (Ogura and Wilkinson, 2001; Smith et al., 2006). For example, the AAA-ATPase components of the proteasome are responsible for unfolding proteasome substrates, and threading them in to the catalytic chamber.

In the case of Cdc48, the importance of residues surrounding the D2 pore suggest that unfolded proteins may be threaded through the pore, although the presence of a zinc ion at the junction between the D1 and D2 domains indicates that it is unlikely that proteins pass through the entire length of the protein (DeLaBarre et al., 2006).

1.6.3 Cdc48 Co-factors

Cdc48 interacts with a variety of cofactors, which help control its specificity and modulate its function. Most of these cofactors appear to interact via the N-domain, and in some cases do so in a mutually exclusive manner (Meyer et al., 2000; Ye et al., 2003).

1.6.3.1 Npl4 and Ufd1

One of the most well characterised Cdc48/p97 cofactors is the Npl4-Ufd1 dimer, which mediates the binding of Cdc48/p97 to polyubiquitinated proteins. One of its best characterised roles is in the ERAD pathway (section 1.6.4.5), however the complex is also involved in other Cdc48 regulated processes, such as signalling (section 1.6.4.2). First identified as a p97 cofactor in rat liver cytosol, the complex consists of a 67kDa Npl4 and 42kDa Ufd1 subunit (Meyer et al., 2000, 2002) (60.9kDa and 38.2kDa respectively in *S. pombe* (Hertz-Fowler et al., 2004)). The cofactors are found in two major pools within the cell: bound in the ternary complex with p97, and as a free Npl4-Ufd1 dimer. Interaction with the N-domain of p97 appears to be mediated through Ufd1 (Meyer et al., 2000; Ye et al., 2003; Meyer et al., 2002; Bruderer et al., 2004) and is strengthened in the presence of Npl4. This interaction is able to outcompete the binding between p97 and ubiquitin, suggesting that the two bind in a mutually exclusive manner (Meyer et al., 2000).

Ufd1 binds Cdc48/p97 and Npl4 via a disordered C-terminal domain; p97 binding is mediated by the BS1 domain – amino-acids 215 to 241 – whereas Npl4 binding is mediated by amino-acids 258 to 275 (Bruderer et al., 2004; Park et al., 2005). The N-terminus can be split into two sub-domains, Nn and Nc (Park et al., 2005) and is structurally similar to the N-domain of p97. It shows ubiquitin binding activity, specific to K48 linked chains and to monoubiquitin, in two separate non-overlapping domains (Park et al., 2005); the affinity for polyubiquitin is considerably higher than that for monoubiquitin.

The Npl4 protein contains a C-terminal zinc-finger ubiquitin binding domain, Npl4 zinc-finger (NZF), which is able to bind both K48 and K63 linked chains. The domain is absent in its homolog in *S. cerevisiae* (Meyer et al., 2000). Npl4 also contains a p97 binding site in its 89 most N-terminal amino-acids, which is activated upon the binding of Npl4 to Ufd1. The region appears to form a β-grasp fold, termed the ubiquitin fold domain (UBD), which is structurally homologous to ubiquitin and the Ubx domain; it appears to bind via a similar mechanism (Bruderer et al., 2004).

1.6.3.2 Ubx Proteins

The Ubx (Ubiquitin regulatory X) domain is a conserved domain of Cdc48 interaction. It shows structural, but only minor sequence, similarity to ubiquitin (Hartmann-Petersen et al., 2004)(Reviewed in Schuberth and Buchberger, 2008). It is commonly found at the C-terminus of proteins and coordinates interaction with the N-terminal

S. cerevisiae	*S. pombe*
Ubx1/Shp1	Ubx3
Ubx2, Ubx3	Ubx1
Ubx4	Ubx4
Ubx5	Ubx2
Ubx6	
Ubx7	
	Ubx5

Table 1.2: Table showing Ubx protein orthologs between *S. cerevisiae* and *S. pombe*.

domain of Cdc48. Ubx domain containing proteins are found throughout the eukaryotes, and have been identified in association with Cdc48 in a number of different pathways. A total of five Ubx containing proteins have been identified in *S. pombe* (Figure 1.6), and seven in *S. cerevisiae*. While some Ubx proteins show clear conservation between the two species, in other cases no direct ortholog is apparent (Figure 1.2). Additionally, the Ubx proteins have been named independently, and show no coordination between the two species. To avoid confusion, this discussion will prefix the names with sc or sp for the *S. cerevisiae* and *S. pombe* copies respectively.

1.6.3.3 *S. pombe* Ubx2

SpUbx2 was first identified in *S. pombe* although homologs exist in *S. cerevisiae* (scUbx5) and humans (UBXD7), its function is currently unknown. Interaction with Cdc48 is mediated through a C-terminal Ubx domain. The protein also contains two domains of ubiquitin interaction, an N-terminal UBA domain and a central UIM domain (Hartmann-Petersen et al., 2004). SpUbx2 also contains a central UAS domain, a thioredoxin-like fold of unknown function. Similar UAS domains are found in spUbx1, as well as in Ubx family proteins of other organisms (Hartmann-Petersen et al., 2004).

The knockout of spUbx2, or its over-expression, results in no immediate phenotype; levels of ubiquitinated substrates remain unperturbed (Hartmann-Petersen et al., 2004).

1.6.3.4 *S. pombe* Ubx1/Ucp10

SpUbx1 shows a similar domain composition to the spUbx2 protein, although it is unclear whether it retains a functional UIM domain. In addition, the protein is the only

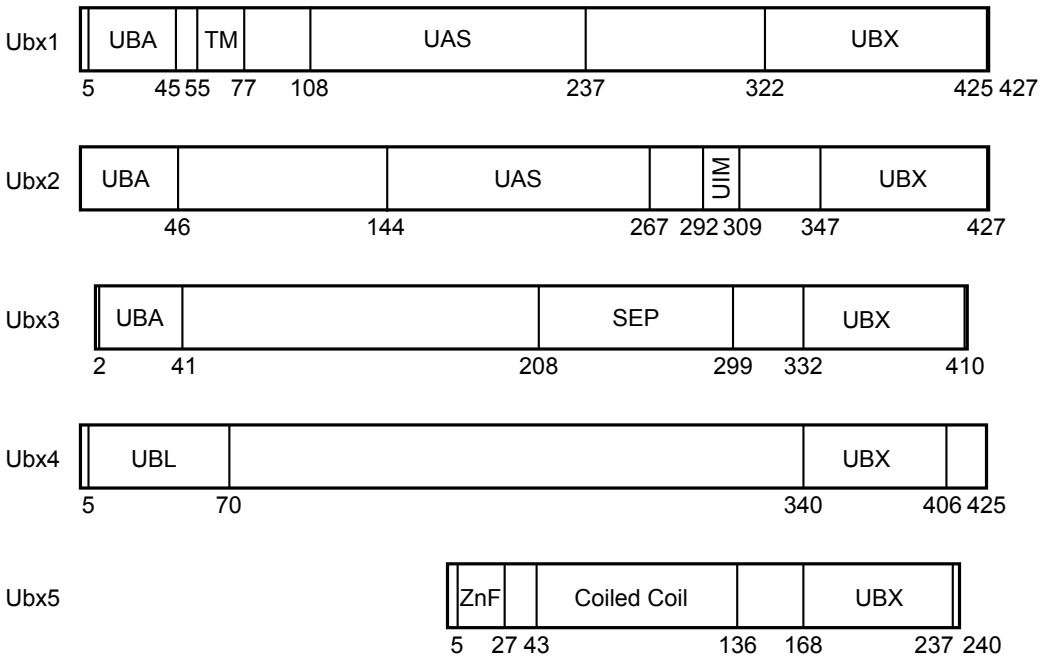

Figure 1.6: Domain structure of the *S. pombe* Ubx containing proteins. (Sonnhammer et al., 1997; Finn et al., 2010; Schultz et al., 1998; Letunic et al., 2009; Hulo et al., 2006; Murzin et al., 1995). Additional help with domain identification was provided by Philippe Gautier. Domains shown above have either significant homology to the reference sequences, or have been otherwise experimentally characterised (Hartmann-Petersen et al., 2004). Additional poorly conserved UIM domains were identified in in Ubx1 (286-298, E-val: 0.43), Ubx3 (45-62, E-val: 0.53), Ubx4 (364-384, E-val: 0.66) and Ubx5 (33-56, E-val: 0.05), however the small size of the UIM domain and high E-values means these are unlikely to be genuine hits. Similarly a poorly conserved UBA domain was detected in Ubx4 (343-379, E-val: 0.38) and Ubx5 (44-89, E-val: 0.06); in both cases the domain was of low significance and overlapped other potential domains.

S. pombe Ubx protein to contain a possible transmembrane helical region (Sonnhammer et al., 1998; Krogh et al., 2001).

1.6.3.5 *S. cerevisiae* Ubx2

The scUbx2 protein is discussed in more detail in section 1.6.4.5. The protein contains UBA and Ubx domains separated by two transmembrane domains which anchor the protein to the endoplasmic reticulum membrane, allowing it to function in ERAD (Schuberth and Buchberger, 2005; Neuber et al., 2005; Wilson et al., 2006). Another *S. cerevisiae* Ubx protein, scUbx3, is closely related to scUbx2; a single ortholog, spUbx1, exists in *S. pombe*.

1.6.3.6 p47/Shp1/SpUbx3

The cofactor p47 is responsible for coordinating the interaction of Cdc48/p97 with several targets, particularly in membrane fusion events (Kondo et al., 1997). A homolog in *S. pombe*, Ubx3, shows 28% identity to p47 (Hartmann-Petersen et al., 2004). Interaction between Cdc48/p97 and p47 occurs at a 6:3 ratio and is mediated through two independent binding sites on p47: a C-terminal Ubx domain and a more central BS1 domain (Hartmann-Petersen et al., 2004; Kondo et al., 1997; Uchiyama et al., 2002). Its association with p97/Cdc48 is mutually exclusive with Npl4-Ufd1, which appears to bind p97/Cdc48 with higher affinity (Meyer et al., 2002). Unlike Npl4-Ufd1, almost all the p47 within the cell is associated with p97.

The N-terminus of p47 contains a UBA domain, which is necessary and sufficient for its ubiquitin K48-linked chain binding activity, and is independent of its ability to bind p97 (Hartmann-Petersen et al., 2004; Meyer et al., 2002). Knockout of the UBA domain disrupts the Golgi assembly activity of $Cdc48^{p47}$, illustrating the vital role for the ubiquitin binding capability. In *S. pombe*, deletion of *ubx3* results in slow growing flocculent cells with canavanine and temperature sensitivity, and shows synthetic lethality with a *pus1* knockout. This indicates a potential role for $ubx3^{+}$ in protein degradation (Hartmann-Petersen et al., 2004).

1.6.3.7 Ubx4

S. pombe $ubx4^{+}$ is homologous to *S. cerevisiae* UBX4, which has been identified as having a Ubx dependent role in ERAD. Surprisingly, in budding yeast, the N-terminal UBL domain is not required for this function, despite being also found in the *S. pombe*

homolog (Alberts et al., 2009). It remains to be demonstrated whether spUbx4 also has a role in ERAD, and what the importance of the UBL domain may be. In other proteins, the UBL domain is responsible for proteasome recruitment, or binding to free Pus1.

1.6.3.8 *S. pombe* Ubx5

SpUbx5 (SPAC17C9.11c) is substantially shorter than the other *S. pombe* Ubx proteins and bears no immediate homolog in *S. cerevisiae*. The N-terminal zinc finger and coiled coil domains are likely to be important in coordinating protein function. Although such domains are unique to Ubx5 in *S. pombe*, zinc-finger domains are found in association with Ubx domains in other organisms; for example the protein Ubxn-1 in *Caenorhabditis elegans* contains a zinc-finger domain (Altschul et al., 1990).

1.6.3.9 Other Ubx proteins

Pux1, identified in *Arabidopsis thaliana*, appears to regulate the oligomeric status of Cdc48 (Park et al., 2007). The interaction occurs between the N-domain of Cdc48 and a centrally localised Ubx domain in Pux1. In turn this mediates the disassembly of the Cdc48 complex. While the interaction with Cdc48 is independent of its nucleotide status its disruption is dependent on its ATPase activity.

p37 is a 37kDa protein which interacts with p97 in a similar manner to p47, however the protein lacks the nuclear localisation signal and UBA domain of the larger p47. Like p47, three p37 proteins associate with each p97 hexamer in a manner which excludes other cofactors, including p47 (Uchiyama et al., 2006).

1.6.3.10 Lub1/Ufd3/Zzz4p/Doa1p

The gene *lub1*$^+$ in *S. pombe* is conserved across a variety of eukaryotes. It encodes a 78.6kDa Cdc48 cofactor (Ogiso et al., 2004; Hertz-Fowler et al., 2004). Cells in Δ*lub1* strains show increased sensitivity to a number of cellular stresses including UV, temperature, hydrogen peroxide and ethanol. The gene is non-essential under non-stressed conditions (Ogiso et al., 2004).

The Δ*lub1* phenotype may be rescued by over-expression of ubiquitin. Δ*lub1* strains show vastly depleted levels of both free and conjugated ubiquitin as a result of reduced ubiquitin stability, in turn this results in increased stability of targets of ubiquitination. This indicates a role for Lub1 in maintaining the stability of ubiquitin. It is unclear if

this action is directly dependent on its association with ubiquitin, which is mediated through the non-essential N-terminal WD domain.

1.6.3.11 Other cofactors

UFD-2 and CHN-1 are both ubiquitin E3 ligases which interact with CDC-48 in *C. elegans*. UFD-2 directly interacts with the C-terminus of CDC-48.1 and CDC-48.2. CHN-1 binds at a different binding site on UFD-2, and the two proteins may associate at the same time. As discussed in section 1.2, the association of E3 ligases with other elements of the ubiquitin system help to couple chain extension and substrate delivery.

Thus Cdc48/p97 has a substantial range of co-factor proteins, which generally bind through the N-terminal domain. Many of them show mutually exclusive binding, directing Cdc48 into performing distinct and separate functions, while in other cases co-factors may co-operate, working in concert in a single pathway. Co-factors can act both as adaptors, or moderators, either recruiting Cdc48 to specific targets, such as in the case of Npl4-Ufd1, or moderating the function of Cdc48 more directly, such as in the case of Pux1.

1.6.4 Target Interactions and Function

The range of co-factors introduced in the previous section allow Cdc48 to function in a wide range of pathways in a controlled and regulated manner; how Cdc48 acts in some of these pathways, and the roles the co-factors play in this, is the subject of this section.

1.6.4.1 Securin Stability

Separase, Cut1, is required to cleave the Scc1/Rad21 subunit of cohesin in *S. pombe*, allowing for sister chromatid separation at mitosis; the protein securin, Cut2, binds and sequesters separase in order to regulate its activity. An association between Cdc48 and the securin/separase system was found in a genetic screen in *S. pombe* (Yuasa et al., 2004; Ikai and Yanagida, 2006). Genetic interactions were shown when temperature sensitive mutants of *cdc48* could be rescued by over-expression of $cut1^{+}$, or be compromised by over-expression of $cut2^{+}$. Crosses revealed synthetic lethality of the temperature sensitive *cdc48* with *cut1* mutants at the permissive temperature.

Further analysis of *cdc48* mutants reveals a marked reduction in levels of Cut1 during mitosis in a transcription and proteasome independent manner, both at the permissive

and restrictive temperatures; this drop was concurrent with the drop in viability seen at the shift to the restrictive temperature. These observations indicate that Cdc48 appears to be required to protect the stability of separase following the destruction of securin.

1.6.4.2 Mga2p and Spt23p

Mga2p and Spt23p are two highly homologous membrane bound transcription factors found in *S. cerevisiae*. The two proteins form homodimers of 120kDa transmembrane proteins, each consisting of a globular N-terminal IPT domain attached to a C-terminal transmembrane domain. Subsequently, ubiquitination of one of the subunits results in the degradation of its transmembrane domain by proteasome processing to leave the 90kDa IPT domain, which remains tethered to the membrane via its 120kDa partner (Shcherbik and Haines, 2007).

On polyubiquitination of the 120kDa subunit by the E3 ubiquitin ligase Rsp5p, the dimer is bound by the $Cdc48^{Ufd1-Npl4}$ ternary complex. Cdc48 is then able to catalyse the release of the 90kDa protein from its membrane anchor to the cytosol in an ATP dependent manner. This allows the IPT domain to translocate to the nucleus, where it acts as a transcription factor (Shcherbik and Haines, 2007). *S. pombe* has a single uncharacterised homolog, which is likely to behave in a similar manner.

1.6.4.3 Spindle Disassembly

Controversial work (Cao et al., 2003) in *X. laevis* egg extracts and in *S. cerevisiae* has indicate a possible role for p97 in spindle disassembly. The work demonstrated that $p97^{Ufd1-Npl4}$ appears to be required for spindle disassembly at mitotic exit and the return to the interphase microtubule array. It was further shown that p97 interacts with several spindle assembly factors, XMAP215, TPX2 and Plx1, on mitotic exit, and appears to promote their dissociation from the spindle. However, more recent work (Heubes and Stemmann, 2007) has failed to reproduce these results, despite using very similar approaches and has thus called the findings into dispute.

1.6.4.4 Membrane Fusion

Membrane fusion events are not coordinated by a single shared mechanism, a fact which is hardly surprising given the targeted and directional fusion events required within the cell. Two AAA-ATPases appear to be responsible for coordinating two fusion pathways

within the cell, NSF and Cdc48 (Uchiyama et al., 2002; Rabouille et al., 1995; Acharya et al., 1995; Latterich et al., 1995).

Cdc48 has been identified in association with both Golgi and endoplasmic reticulum membrane fusion (Rabouille et al., 1995; Acharya et al., 1995; Latterich et al., 1995). In the former, p97 appears to act downstream of NSF Acharya et al. (1995), where in concert with the co-factor p47, p97 acts on the Golgi associated SNARE protein, Syntaxin5 (Kondo et al., 1997; Rabouille et al., 1998). This complex is later dissociated by a second Cdc48 co-factor VCIP135, which displaces p47 binding. Knockout of VCIP135 only appears to affect the reassembly of Golgi following mitosis, suggesting that another mechanism is at play during interphase. Additionally the p47 like co-factor p37 appears to contribute to Golgi maintenance (Uchiyama et al., 2006), indicating that Cdc48 plays multiple roles in regulating membrane fusion, coordinated by its different co-factors.

1.6.4.5 ERAD

In order for misfolded proteins in the endoplasmic reticulum (ER) to be degraded by the proteasome they must first be transported from the lumen or membrane of the ER to the cytosol. The pathway by which this occurs is known as endoplasmic reticulum associated degradation or ERAD; Cdc48/p97 appears to be an important component of this pathway. The process has been reviewed in detail on several occasions (Nakatsukasa and Brodsky, 2008; Raasi and Wolf, 2007; Määttänen et al., 2010; Xie and Ng, 2010).

ERAD is a multi-factorial pathway capable of promoting the ubiquitin-dependent degradation of proteins both in the ER lumen and membrane. Multiple misfolded protein recognition pathways feed into a single downstream pathway which coordinates protein extraction from the ER and transfer to the cytosolic ubiquitin proteasome system. These downstream recognition pathways appear to make use of adaptor factors associated with the core ERAD complex, which increase the range of substrates it can act upon (Carvalho et al., 2006; Kanehara et al., 2010). The process has been best characterised in *S. cerevisiae*.

The ERAD-C and ERAD-M pathways describe the detection and removal of ER membrane substrates with and without substantial cytoplasmic domains respectively. In the case of ERAD-C, misfolded proteins are recognised by cytosolic chaperones and protein ubiquitination is conducted by a membrane associated E3-ligase, Doa10 in budding yeast, which also ubiquitinates nuclear and cytoplasmic proteins (Nakatsukasa

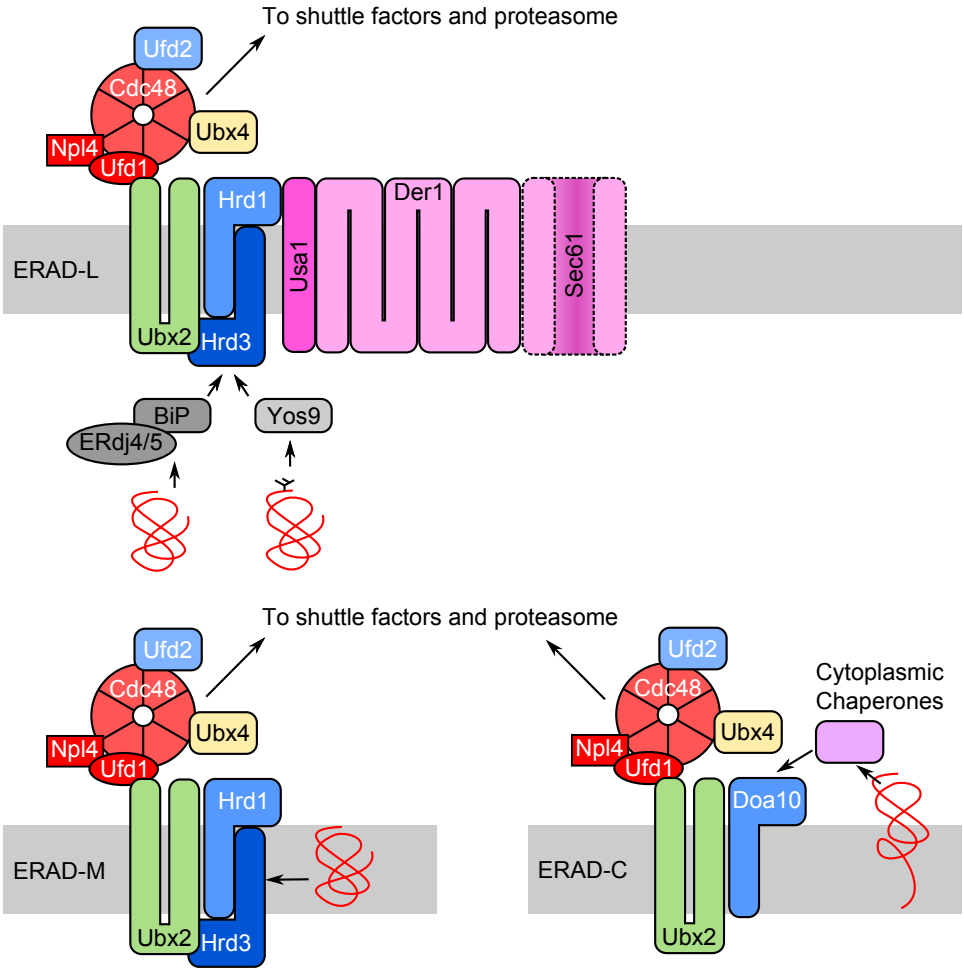

Figure 1.7: Summary of many of the important proteins involved in the ERAD pathway, and the requirements for different substrates. Other proteins involved are the accompanying E2s, as well as many chaperones in the ER lumen which aid folding and misfolded substrate detection. In addition, there is still considerable debate on the nature of the translocation pore, and it is possible that further elements remain to be identified.

and Brodsky, 2008; Deng and Hochstrasser, 2006; Xie and Ng, 2010). The ERAD-M pathway is more closely related to that of misfolded luminal proteins, ERAD-L, and ubiquitination occurs via the Hrd1-Hrd3 complex. Hrd1 is thought to recognise misfolded membrane proteins directly (Nakatsukasa and Brodsky, 2008; Xie and Ng, 2010).

The ERAD-L pathway is more complicated, and may consist of two semi-redundant pathways, a glycoprotein and non-glycoprotein pathway (Kanehara et al., 2010). The ER contains a series of chaperone proteins, including Hsp70 and Hsp90 family proteins, as well as the lectins Calnexin and Calreticulin, which bind glycosylated proteins. These chaperones help coordinate the correct folding of ER proteins, subsequently enabling their transport to other cellular compartments as necessary. Proteins targeted for secretion are glycosylated on import, and are tagged with an N-linked oligosaccharide, NAc-Gln_2-Man_9-Glc_3, which is quickly processed to remove two glucose residues and allow the binding of Calnexin and Calreticulin (Nakatsukasa and Brodsky, 2008; Määttänen et al., 2010). Additional processing enzymes work to ensure that correctly folded proteins are able to leave the ER, whereas misfolded proteins are retained by Calnexin and Calreticulin. Proteins that are retained for folding in the ER for an extended period eventually become processed by slow acting mannosidase enzymes, which remove a mannose residue. This modification flags up proteins experiencing difficulty binding, and prompts the association of the lectin Yos9. In turn, Yos9 recruits the misfolded proteins to the Hrd1-Hrd3 complex via the Hrd3 luminal domain. Additionally, the factors Usa1 and Der1 are required in association with Hrd1-Hrd3 for the removal of ERAD-L substrates (Nakatsukasa and Brodsky, 2008; Määttänen et al., 2010). Non-glycoprotein luminal substrates are processed in a similar manner, independent of Yos9, and instead relying of chaperones such as BiP and its cofactors. Glycan independent degradation appears to be promoted by sequences embedded in the substrate, which are presumably sequestered on correct folding (Kanehara et al., 2010; Määttänen et al., 2010). The system appears to have diversified in the metazoa, and a greater range of E3 ligases have been implicated in ERAD (Määttänen et al., 2010).

In *S. cerevisiae* the E3 ligases are linked to downstream elements of the ERAD pathway by the actions of the Cdc48 co-factor scUbx2 (Schuberth and Buchberger, 2005; Neuber et al., 2005; Wilson et al., 2006). ScUbx2 contains cytosolic Ubx and UBA domains, linked via two transmembrane domains, which anchor the protein to the ER membrane. ScUbx2 is able to interact with both $Cdc48^{Npl4-Ufd1}$ and with the E3 ligases, Doa10 and Hrd1. Importantly sc*UBX2* knockouts, and mutants lacking the Ubx domain, show

reduced degradation kinetics, particularly under stress conditions. The protein has been detected in association with both membrane and luminal ERAD substrates, and thus appears to link multiple pathways into a single downstream process (Schuberth and Buchberger, 2005; Neuber et al., 2005; Wilson et al., 2006). Interestingly, despite not being homologous, the human protein UBXD2, or Erasin, appears to be functionally similar to Ubx2. It is an ER membrane anchored Ubx protein which promotes ERAD and associates with both p97 and E3 ligases (Liang et al., 2006). It is possible that UBXD2 functions in place of Ubx2 in mammals, or else is a requirement of the diversification of the ERAD associated E3 ligases. The *S. pombe* protein most closely related to scUbx2, is the ER localized protein spUbx1, which is the only *S. pombe* to bear a transmembrane domain. SpUbx1 also contains the UBA and Ubx domains seen in scUbx2 (Sonnhammer et al., 1998; Krogh et al., 2001; Matsuyama et al., 2006). If spUbx1 can be demonstrated to have similar activity to scUbx2, it will be a prime candidate for further study of ERAD in *S. pombe*.

The $Cdc48^{Npl4-Ufd1}$ complex has been implicated in the destruction of membrane bound and luminal ER substrates in a range of organisms including *S. cerevisiae* and *M. musculus* (Rabinovich et al., 2002; Bays et al., 2001). Not only has the protein been shown to interact with ERAD substrates, but the disruption of complex function results in the stabilization of ERAD substrates, and the accumulation of ubiquitinated proteins at the ER membrane. Both substrate binding and AAA-ATPase activity appear to be required to mediate Cdc48 function (DeLaBarre et al., 2006). Cdc48 is thought to help to either extract proteins from the surface of the ER membrane, or else promote retrotranslocation. The ER import pore complex Sec61 and the putative pore protein Der1 have both been implicated in forming the pore necessary for retrotranslocation (Nakatsukasa and Brodsky, 2008). Work in mammals has suggested that some substrates may be processed in a p97 independent manner, suggesting that downstream pathways may have diversified in a similar way to the upstream substrate recognition pathways (Lass et al., 2007; Nakatsukasa and Brodsky, 2008).

Downstream of extraction from the ER membrane, the Cdc48 co-factor Ubx4 appears to be important for correct $Cdc48^{Npl4-Ufd1}$ behaviour, *S. cerevisiae* strains lacking Ubx4 show an accumulation of ubiquitinated substrates bound to Cdc48 (Alberts et al., 2009). Additionally, the action of the E4 ubiquitin ligase Ufd2 is necessary for the extension of ubiquitin chain length on Cdc48 substrates, allowing their subsequent proteasomal delivery by Dsk2 and Rad23 (Koegl et al., 1999; Medicherla et al., 2004; Raasi and Wolf, 2007; Richly et al., 2005).

1.6.4.6 Cdc48 and Disease

IBMPFD is a rare autosomal dominant disease that compromises inclusion body myopathy, Paget's disease and frontotemporal dementia. Several missense mutations in p97 have been identified which are linked to all three symptoms, as well as possible liver disorders (Guyant-Marechal et al., 2006; Haubenberger et al., 2005). Close studies of the neuronal phenotypes in several patients revealed the presence of large perinuclear vacuoles and a build up of ubiquitinated substrates. While no obvious plaques were observed an activation of apoptotic pathways was noted (Guyant-Marechal et al., 2006). Penetrance for each symptom varied between the different mutations, indicating possible subtle differences in mechanism behind the variety of problems, or alternatively reflecting the different genetic backgrounds in which the mutants were found. Investigation of the co-factor binding characteristics of Cdc48 mutations suggest that they result in changes in the structure of the N-terminal domain, and in turn alter the ratio of co-factors bound to Cdc48 (Fernández-Sáiz and Buchberger, 2010).

The understanding of the molecular basis behind the myopathy phenotype has been aided by studies in *C. elegans* (Janiesch et al., 2007). CDC-48 appears to form a complex with the E3 ligases UFD-2 and CHN-1 which in turn regulate the stability of the myosin chaperone protein UNC-45 via ubiquitination. UNC-45 helps maintain striated muscle; excess or insufficient UNC-45 can lead to muscle defects. Temperature sensitive *unc-45* mutants show paralysis due to sarcoma disorganisation, this is suppressed in *cdc48.1*, *ufd-2* and *chn-1* mutants, indicating genetic interaction. Conversely, *cdc48.1* is unable to rescue mutations in myosin itself, suggesting that the rescue is indeed mediated through *unc-45* and not a downstream process. Importantly, while *unc-45* over-expression alone has no appreciable phenotype, it results in an uncoordinated phenotype in *cdc-48.1*, *ufd-2* and *chn-1* mutants. The expression of wild-type human p97, but not the mutant form from IBMPFD patients, is able to rescue this phenotype, supporting the validity of the *C. elegans* model. This suggests that CDC-48 is responsible for controlling levels of UNC-45, and is probably involved in turnover; p97 from IBMPFD patients is defective in this activity.

1.7 Mitochondria and Mitochondrial Protein Degradation

During the course of the experiments described in this thesis, the mitochondria were found to have links with the proteasome shuttle factors. To understand the potential purpose of this interaction, it is necessary to understand mitochondrial protein

misfolding and associated proteolytic activity.

The mitochondrial environment is one rich in oxidative species, which have the potential to damage proteins, resulting in misfolding, aggregate formation and ultimately mitochondrial damage and cell death. Additionally, the assembly of the multi protein complexes of the electron transport chain requires a careful balance of protein levels to allow correct complex assembly. Clearly protein quality control is as important in the mitochondria as it is in the rest of the cell, and evidence suggests that there are several levels of control present. As mitochondria exist as membrane bound organelles, many of their proteins, especially those in the mitochondrial matrix, are isolated from the proteolytic systems in the cytosol; as a result mitochondria require additional mechanisms of protein degradation. If these processes go wrong, or are insufficient, a mitochondrial autophagy pathway, mitophagy, is able to remove damaged or superfluous mitochondria. Defects in the process are often associated with neuro and muscular degenerative diseases, such as Parkinson's disease and hereditary spastic paraplegia (Reviewed in Koppen and Langer, 2007; Germain, 2008).

1.7.1 Mitochondrial Proteases

Some mitochondrial protein destruction is mediated by a family of mitochondrially localised ATP dependent proteases (Reviewed in Langer et al., 2001; Koppen and Langer, 2007; Germain, 2008). This overview of the mitochondrial proteolytic system is concerned only with those proteases associated with protein quality control, and does not consider proteases involved in post-import processing.

Multi-protein AAA-ATPase complexes span the inner mitochondrial-membrane (Rapo port et al., 1982), and orientate their catalytic sites to face either the mitochondrial matrix, or the inter-membrane space. The proteins bind unfolded or unassembled membrane proteins and catalyse their removal from the membrane, followed by their proteolysis via the enzyme's metallopeptidase activity. The proteins also appear to help coordinate the post-import processing of mitochondrial proteins (Koppen et al., 2009). Additional ATP dependent proteases, Lon/PIM and ClpXP, can be found in the mitochondrial matrix. Lon is a homo-heptameric complex involved in the recognition and breakdown of oxidised substrates. ClpXP is a heteromeric complex of a protease and a AAA-ATPase, which is associated with the activity of the chaperone Hsp60 and the mitochondrial unfolded protein response (UPR^{mito}) in mammals and a variety of other eukaryotes (Yu and Houry, 2007; Koppen et al., 2009). The ClpP protease appears to be derived from bacterial species, in which, in addition to ClpX, it also interacts

with another AAA-ATPase, ClpA. Some bacterial species contain further ClpA like proteins, which may also interact with ClpP (Yu and Houry, 2007). *S. cerevisiae* lacks a ClpP ortholog and only has an ortholog of the ATPase subunit (van Dyck et al., 1998), *S. pombe* appears to lack orthologs of both ClpX and ClpP proteins (Yu and Houry, 2007; Altschul et al., 1990). The membrane associated protease Oma1 has also been associated with protein quality control in *S. cerevisiae*, and various downstream oligopeptidases have been implicated in the breakdown of the peptide products of the AAA-ATPases (Koppen et al., 2009).

This system provides mitochondrial proteases in the mitochondrial matrix and inner membrane. Inter-membrane space proteins also have accesses to the appropriately orientated inner membrane AAA-ATPase, however analysis of the peptides released from mitochondrial peptidase activity suggests that degradation products of inter-membrane space proteins are under-represented (Germain, 2008).

1.7.2 Mitochondrial Associated Ubiquitin Mediated Degradation

Growing evidence suggests that the ubiquitin proteasome system may also be involved in processing mitochondrial proteins. Early work indicated that mitochondrial proteins in reticulocytes were ubiquitinated and subjected to ATP dependent degradation (Rapo port et al., 1985). The knock-down of the chaperone Hsp90 results in the accumulation of a dense mass of mitochondrial protein and an eventual induction of cell death in COLO205 cancer cell lines (Margineantu et al., 2007). Similar morphological changes are seen on inhibition of the proteasome, and a comparison of ubiquitin levels of cells expressing wild-type and knock-down levels of Hsp90 suggest that Hsp90 promotes ubiquitination of mitochondrial proteins. In particular the matrix subunit OSCP was found to be ubiquitinated in an Hsp90 dependent manner (Margineantu et al., 2007). Sub-fractionation of mitochondria found that ubiquitinated proteins accumulated on the outer membrane of the mitochondria on proteasomal inhibition, and revealed a retrograde pathway of export of mitochondrial proteins (Margineantu et al., 2007). Several potential substrates of a mitochondria associated degradation pathway have been identified, and are considered in more detail in section 6.3.

1.8 Msp1

Msp1p (mitochondrial sorting of protein) was first identified as a AAA-ATPase domain containing protein in *S. cerevisiae* (Nakai et al., 1993; Schnall et al., 1994). The protein

is localized to the outer mitochondrial membrane by virtue of a 16 amino acid N-terminal transmembrane domain. Overexpression of *MSP1* was sufficient to cause the mislocalisation of a protein artificially directed to the outer mitochondrial membrane via a fusion with the MAS70 localization signal. This indicates that Msp1p likely plays a role in localizing mitochondrial proteins (Nakai et al., 1993).

1.9 Obr1/Uhp1

Obr1 was first identified in a screen in which over expression appeared to promote brefeldin A resistance (Turi et al., 1994). Subsequent work has found that the gene encodes a histone-like protein which is targeted by ubiquitination, and regulates silencing of the mating-type cassette in *S. pombe* (Naresh et al., 2003).

1.10 This Work

This thesis begins by attempting to dissect the role of the Cdc48 co-factors spUbx4 and spUbx5, as a means of identifying further roles for Cdc48 within the cell. At the time of starting the project, little information was available regarding the function of either protein. The identification of distinct phenotypes associated with either protein, or proteins which interact with them, would provide important insights into the function of the co-factors, and by extension the activity of Cdc48.

The work then moves to consider targets of the proteasome shuttle factor Dph1, as a means of identifying novels links with the ubiquitin proteasome system. Such interactions potentially identify proteins involved in the detection, processing and removal of misfolded proteins and other proteasome substrates. In particular, a mitochondrially localised AAA-ATPase provides a potential link between the mitochondria and the ubiquitin proteasome system. This discovery is used as the basis of a series of experiments, which attempt to discover whether the association identified a potential mitochondria associated degradation pathway.

Chapter 2

Material and Methods

All chemicals were supplied by Sigma-Aldrich, except where stated otherwise. Molecular biology reagent suppliers are indicated in the text.

2.1 Strains

2.1.1 *S. pombe*

Wild-type *S. pombe* is a modified wild-type 972 *S. pombe* strain with mutations in *leu1*, *arg3*, *ura4*, *his3*, and *ade6* making it auxotrophic for histidine, uracil, leucine , adenine and arginine. All strains constructed in this work were created in this background.

The strain *cdc48-353* was originally isolated by, and kindly provided by Mitsuhiro Yanagida (Ikai and Yanagida, 2006; Yuasa et al., 2004). It bears a temperature sensitive mutation in *cdc48* as a result of at G338D missense mutation. The *cdc48-353* strain is identified as $cdc48^{ts}$ in the text.

The strain BG_0508 was supplied by Bioneer as a heterozygous diploid knockout of SPAC17C9.11c/*ubx5*. Its genotype was given as:
Δ*ubx5*::kanMX4/*ubx5* *ade6*-M210/*ade6*-M216 *ura4*-D18/*ura4*-D18
leu1-32/*leu1*-32 h+/h+.

The strain BG_4627D was supplied by Bioneer as a heterozygous diploid knockout of SPCC24B10.10c/*mlp1*. Its genotype was given as:
Δ*mlp1*::kanMX4/*mlp1* *ade6*-M210/*ade6*-M216 *ura4*-D18/*ura4*-D18
leu1-32/*leu1*-32 h+/h+.

All other *S. pombe* strains were from Gordon lab stocks.

2.1.2 *S. cerevisiae*

All *S. cerevisiae* work was conducted using the strain PJ69-4A (James et al., 1996). This strain contains the *HIS3*, *ADE2* and *lacZ* genes under the control of three different Gal4 inducible promoters. This set-up allows for more stringent selection, reducing the number of false positives. Genotype: *MAT*a *trp1-901 leu2-3,112 ura3-52 his3-200 gal4*Δ *gal80*Δ *LYS2::GAL1-HIS3 GAL2-ADE2 met2::GAL7-lacZ*

2.1.3 *Escherichia coli*

Cloning and other DNA manipulation was made in Subcloning Efficiency DH5α Competent Cells (Invitrogen). Genotype: F- ϕ80*lac*ZΔM15 Δ(*lac*ZY A-*arg*F)U169 *rec*A1 *end*A1 *hsd*R17(r_K^-,m_K^+) *pho*A *sup*E44 *thi*-1 *gyr*A96 *rel*A1 λ^-.

Protein expression was conducted in the strain BL21(DE3)pLysS (Studier and Moffatt, 1986) or M15[pREP4] (Qiagen,Hilden, Germany) as indicated. Genotype BL21(DE3)pLysS: FŰ *omp*T *hsd*S_B (r_BŰ m_BŰ) *dcm gal* λ(DE3) pLysS, Cm^r. No genotype is available for the M15[pREP4] strain.

2.2 Media

All media are autoclaved before use. Where possible, media were prepared by HGU technical services.

2.2.1 *S. pombe*

2.2.1.1 YES Media

1 litre media: 5 g yeast extract (Becton Dickinson), 30 g glucose (Fisher Scientific), 225 mg each of adenine, histidine, leucine, uracil and lysine hydrochloride. For solid media add 20 g Bacto agar (Becton Dickinson).

2.2.1.2 Malt Extract Media

1 litre media: 30 g Bacto-malt extract (Becton Dickinson), 20 g Bacto agar (Becton Dickinson), 225 mg each of adenine, histidine, leucine and uracil. Adjust to pH 5.5 with NaOH (Fisher Scientific).

2.2.1.3 PMG Media

1 litre media: 3 g phtalic acid, 2.2 g di-sodium orthophosphate (Fisher Scientific), 20 g glucose (Fisher Scientific), 1 ml vitamins 1000×, 0.1 ml Minerals 10,000×, 20 ml Salts 50×. For solid media add 20 g Bacto Agar (Becton Dickinson). Uracil, adenine, leucine, arginine and histidine are added at 225 mg l^{-1} as required.
1 litre Vitamins 1000×: 1 g pantothenic acid, 10 g nicotinic acid, 10 g inositol, 10 mg biotin.
1 litre Minerals 10,000×: 5 g boric acid, 4 g $MnSO_4$, 4 g $ZnSO_4.7H_2O$, 2 g $FeCl_2.6H_2O$, 0.4 g molybdic acid, 1 g potassium iodide, 0.4 g $CuSO_4.5H_2O$, 10 g citric acid.
1 litre Salts 50×: 52.5 g Magnesium Chloride, 0.735 g Calcium Chloride, 50 g Potassium Chloride, 2 g sodium sulphate.

2.2.2 *S. cerevisiae*

2.2.2.1 YPAD Media (Clonetech Laboratories, 2001)

1 litre media: 20 g Difco peptone (Becton Dickinson), 10 g yeast extract (Becton Dickinson), 20g glucose (Fisher Scientific), 0.003% adenine hemisulphate, pH 6.5. For solid media add 20 g Bacto Agar (Becton Dickinson).

2.2.2.2 SD Media (Clonetech Laboratories, 2001)

1 litre media: 6.7 g yeast nitrogen base without amino acids (Becton Dickinson), 20 g glucose (Fisher Scientific), 100 ml dropout solution 10×, pH5.8. For solid media add 20 g Difco Bacto Agar (Becton Dickinson). Supplements added to cooled media as required.
1 litre Dropout Solution 10×: 200 mg L-arginine HCl, 300 mg L-Isoleucine, 300 mg L-Lysine HCl, 200 mg L-Methionine, 500 mg L-phenylalanine, 2000 mg L-threonine, 300 mg L-tyrosine, 200 mg L-uracil, 1500 mg L-valine.
Other Supplements: Other supplements were prepared as 100× stock solutions, were filter sterilised, and were stored in the dark at 4 ℃ until required. Stock concentrations were: L-adenine hemisulfate 2 g l^{-1}, L-histidine HCl monohydrate 2 g l^{-1}, L-leucine 10 g l^{-1}, L-tryptophan 2 g l^{-1}.

Antibiotic	Stock	Concentration (mg ml^{-1})	Solvent
Ampicillin	2000×	100	dH_2O
Kanamycin	1000×	100	dH_2O
ClonNAT	2000×	200	dH_2O

Table 2.1: Usage of antibiotics. ClonNAT: Nourseothricin, supplied by Werner BioAgents, Jena Germany. Other antibiotics obtained internally.

2.2.3 *E. coli*

2.2.3.1 LB Media

1 litre media: 10 g tryptone, 5 g yeast extract (Becton Dickinson), 10 g Sodium chloride (VWR), 1 g glucose (Fisher Scientific). For enriched media optional addition of 2.5 g magnesium sulphate. For solid media add 15 g agar.

2.2.3.2 Antibiotics

See table 2.1 for composition of stock solutions.

2.3 *S. pombe* Growth and Phenotype Analysis

2.3.1 Growth Curves

10 ml of YES (Section 2.2.1.1) was inoculated with a loop of cells from a patch freshly growing on solid YES agar. Cultures were shaken at 25 ℃ for approximately two days to produce a confluent pre-culture. 50 ml YES in 100 ml conical flasks was inoculated with a range of pre-culture volumes and were shaken overnight at 25 ℃. Cultures with an OD_{600} of approximately 0.3 were selected, and where appropriate volumes were adjusted to obtain approximately equal starting densities. Immediately, growth was measured both by OD_{600} (Section 2.3.2) and by cell density (Section 2.3.3). Cultures were returned to the 25 ℃ orbital incubator and readings were repeated hourly for the duration of the time course.

2.3.2 Measuring Optical Density

Optical density was used to quickly measure the overall growth of cells in media where no accurate measure of cell number was required. Absorbance was measured at 600nm with a WPA Biowave CO8000 cell density meter (Biochrom, Cambridge, UK). Readings were taken in cuvettes with a 1cm path length and were zeroed against the growth media.

2.3.3 Measuring Cell Density

200 µl of culture was transferred into an accuvette containing 1.8 ml formyl saline solution (0.9% saline, 3.7% formaldehyde). Samples were mixed by gentle agitation and stored at 4 ℃ until needed.

18 ml isoton was added to each sample, which was subsequently mixed by inversion and sonicated for ten seconds at an amplitude of approximately 2 µm. Samples were mixed by inversion again and a Beckman Coulter Z2 Coulter particle count and size analyser was used to measure the cell density. Gates were set to count particles above 2.5 µm. Three readings were taken and used to calculate an average. Care was taken to ensure that the counter maintained a steady flow and the aperture remained unobstructed, and unsuitable readings were discarded and repeated. The apparatus was flushed once with isoton between each sample.

2.3.4 Sensitivity Assays

Solid YES media (Section 2.2.1.1) was prepared containing a variety of stress factors at the concentrations indicated in the results tables. Where possible, stress factors were added to YES media which had cooled below 50 ℃ after autoclaving. This was not possible for sorbitol or for concentrations of potassium chloride of 0.4 M or higher; in these circumstances the stress factors were added to the media prior to autoclaving. Plates containing labile stress factors were prepared the day before usage, and were stored at 4 ℃ overnight.

S. pombe strains were inoculated into 5 ml YES liquid media and were shaken at 25 ℃ overnight. The OD_{600} of each culture was determined and was adjusted to give an absorbance of 0.5. Cultures were mixed thoroughly by vortexing and 400 µl aliquots were prepared in microcentrifuge tubes. Aliquots were vortexed and 100 µl of culture was transferred into 400 µl of distilled water to create a five fold dilution. Vortexing

and dilutions were repeated a further four times, to result in a series of six serial five fold dilutions for each strain.

5 µl of each serial dilution was spotted onto the selective media in a grid fashion and aliquots were vortexed before each spotting. Spots were allowed to dry before plates were transferred to an appropriate temperature incubator. Standard stress factors were assayed at 25 ℃.

Control strains were as follows, 36 ℃: *mts3.1*, 20 ℃: Δ*wee1*, TBZ: Δ*pof3*, CHX: Δ*kin1*, EMS and HU: Δ*rad3*, brefeldin A: Δ*brf1*, latrunculin A: Δ*pka1*, MBC: Δ*mad2*. All strains were taken from Gordon lab stocks.

2.4 *S. pombe* Mating

Strains of opposite mating types were crossed on solid malt extract media (Section 2.2.1.2). Inoculating loops were used to transfer a small patch of each strain into 10 µl of sterile dH_2O spotted onto the plates. Crosses were incubated at 25 ℃. Crosses were checked for the formation of asci after two days incubation, to indicate successful mating.

2.4.1 Free-spore analysis

A small quantity of cells and asci from the patch of crossed cells was transferred into 1 ml of filter-sterilized dH_2O supplemented with 5 µl β-glucuronidase (Sigma Aldrich). Digests were incubated at 25 ℃ overnight. Spores were pelleted by centrifugation for 3 minutes at 5,000 rpm in a microcentifuge, and were washed twice with dH_2O. Spores were plated onto appropriate selective media and plates were incubated at 25 ℃ until visible colonies were present. Once grown, plates were replica plated to appropriate selective conditions as necessary.

2.4.2 Tetrad Analysis

A small quantity of cells and asci from the patch of crossed cells was transferred onto YES media, and a Singer MSM micro-manipulator was used to arrange intact asci into a grid pattern. Asci were incubated either overnight at 20 ℃, or for three hours at 30 ℃ to prompt busting. The micro-manipulator was used to separate the spores in an organised grid before germination, and plates were incubated at 25 ℃ until visible

colonies were present. Once grown, plates were replica plated to appropriate selective conditions as necessary.

2.4.3 Induction of Bioneer diploids

Diploid strains were transformed (see section 2.5.3.2) with pSPO, a plasmid containing the *S. pombe* mating cassette, were washed and plated onto media selecting for uracil prototrophs. The resultant colonies were replica plated onto two ME plates and were incubated overnight. Successful induction of mating was detected via iodine staining and was confirmed by observation under the microscope for the presence of asci. Colonies which produced tetrads were subject to tetrad analysis.

2.5 DNA Manipulation

All DNA quantification was conducted using a NanoDrop ND-1000 (Thermo Scientific) in accordance with the manufacturer's instructions.

2.5.1 Restriction Enzymes

All restriction enzymes and associated buffers were supplied by either NEB (New England Biolabs) or Roche.

2.5.2 Plasmid Extraction

2.5.2.1 *E. coli*

Plasmids were extracted using a Qiagen Miniprep kit in accordance with the manufacturer's protocols.

2.5.2.2 *S. cerevisiae*

Cultures were inoculated into SD-L media and were incubated at 30 ℃ for 24 hours. 1.5 ml of dense culture was harvested by centrifugation at 5000 rpm for 2 minutes. Cell pellets were resuspended in 120 µl P1 resuspension buffer containing RNase A (Qiagen Minipep Kit). Approximately 130 µl of acid washed beads (Sartorius) were added to each sample, and cells were broken by vortexting at maximum speed for two periods of one minute. Beads were sedimented and the supernatant was transferred

to a fresh tube. 120 µl of P2 lysis buffer (Qiagen Miniprep Kit) was added to each tube; samples were mixed by inversion and were incubated for 5 minutes at room temperature. 180 µl on N3 Neutralisation buffer (Qiagen Miniprep Kit) was used to precipitate DNA; samples were incubated on ice for 5 minutes and the precipitate was pelleted by centrifugation at 13,000 rpm for 15 minutes. The supernatant was applied to a Qiagen Miniprep Kit column, and samples were washed and eluted in accordance with the manufacturer's instructions.

2.5.3 Transformations

Transformation protocols used were standard Gordon lab protocols. The text below has been adapted from work previously submitted by the author as part of an Edinburgh University masters project.

2.5.3.1 Bacteria

50 µl of DH5α cells (Invitrogen) were thawed on ice and incubated with 5 µl plasmid DNA for 15 minutes. Cells were heat-shocked at 42 ℃ for 30 seconds and were returned to ice for two minutes. Cells were recovered in 1 ml LB + Mg^{2+} shaking at 37 ℃ for 1 hour. Selection was conducted on L-Agar with appropriate antibiotic selection overnight at 37 ℃. Where other bacterial strains have been specified, they were transformed using an identical protocol.

When transformed with plasmids extracted from *S. cerevisiae*, cells were simultaneously transformed with a 1:100 dilution of the plasmid extract in water.

2.5.3.2 *S. pombe*

100 ml of YES in a conical flask was inoculated with between 0.25 ml and 2.0 ml of stationary-phase pre-culture. Cultures were incubated overnight in an orbital incubator at 25 ℃. At an OD_{600} of between 0.4 and 0.9 cells were transferred to 50 ml tubes and spun at 2000 g for 3 minutes and were washed once in dH_2O and once in 100 mM Lithium Acetate pH 4.9. Cells from the same culture were pooled before centrifugation after the second wash and the resultant pellet was resuspended in 100 mM Lithium Acetate pH 4.9 to a volume of 100 µl per 0.1 OD_{600} of the original culture.

Resuspended cells were split into 100 µl aliquots in sterile microfuge tubes. To each was added 5 µl tRNA (Sigma) and 5 µl purified plasmid DNA (approximately 1 µg), one aliquot was used as a no DNA control. Cells were thoroughly mixed with 370 µl PEG

3350 by vortexing and were incubated at 25 ℃ for 50 minutes, followed by heat-shock at 46 ℃ for 15minutes. Cells were then spun at 3,000 rpm in a microcentrifuge for two minutes, the supernatant was discarded and the cells were resuspended in YES and were recovered for three hours at 25 ℃. 200 µl of suspended cells were plated onto appropriate selective media.

2.5.3.3 *S. cerevisiae*

One on One: 10 ml YPAD was inoculated with PJ69-4a cells and was incubated at 30 ℃ overnight in an orbital incubator. The OD_{600} of each culture was determined, and the equivalent of 8.5 ml of $OD_{600} = 1$ culture was taken, spun at 1700 g for 5 minutes and resuspended in 50 ml YPAD. Resuspended cells were incubated at 30 ℃ until they reached an OD_{600} of between 0.5 and 0.6. Cells were harvested by centrifugation at 1700 g for 5 minutes and were washed once in 25 ml dH_2O before being resuspended in 1 ml of 0.1 M lithium acetate, pH7.5. Samples were transferred to microfuge tubes and cells were pelleted at 2000g for five minutes. The supernatant was removed, 50µl pre-boiled 10 mg ml^{-1} salmon sperm DNA was added to the cell pellet, sample volume was brought to 1 ml with the 0.1M lithium acetate and samples were vortexed. For each transformation 2.5 µl of each plasmid, bait and prey, were mixed in a separate microfuge tube and to this mix was added 95µl of the competent cells mixture prepared above. The cells were mixed and 500 µl PEG solution (8:2 PEG 50% : 0.5 M LiAc) was added to each transformation, which was then vortexed. Cells were incubated for 30 minutes at 30 ℃ before heatshock in a waterbath at 42 ℃ for 25 minutes, with gentle mixing every five minutes. Cells were spun out at 3000g and were resuspended in 300 µl of sterile dH_2O. Cells were kept in suspension by regular vortexing and 10 µl was spotted onto appropriate selective media, or 50 µl of cells were spread across selective media to produce single colonies. **Library Transformations:** PJ69-41 cells containing the bait vector were transformed with 10 µg of library DNA in accordance with the ×10 TRAFO protocol (Agatep et al., 1998).

2.5.4 PCR protocols

2.5.4.1 Taq

All diagnostic PCRs were conducted with Taq (Roche).

Per 20 µl reaction: 2 µl 10× Taq Buffer, 1 µl $MgCl^{2+}$ buffer, 0.16 µl dNTPs (25 nM each stock, Fisher Scientific), 2 µl primer A (10 µM stock), 2 µl primer B (10 µM stock),

0.4 µl Taq, 11.44 µl dH_2O, 1 µl template (100 ng μl^{-1} genomic, or approximately 30 ng μl^{-1} plasmid).

In the case of bacterial colony PCRs, the template is replaced with dH_2O, and a pipette tip is used to transfer a small proportion of a bacterial colony to the PCR mix; the same tip is used to establish a new colony on a fresh LB+Amp plate.

S. pombe colony PCR involved the replacement of the DNA component with a crude *S. pombe* DNA extract. Crude extracts were prepared by the transfer of a 2 mm diameter amount of *S. pombe* into 10 µl of SPZ digestion buffer. Digests were incubated for 15 min at 37 ℃ to lyse the cells, and 2 µl of digest was used in place of DNA in the PCR reaction. SPZ digestion buffer: 2 mg ml^{-1} Zymolyase-100T (MP Biomedicals), 1.2 M Sorbitol, 0.1 M sodium phosphate (VWR), pH 7.4.

The PCR protocol used was as follows; 1. 94 ℃ 3 min; 2. 94 ℃ 30 s; 3. 56 ℃ 40 s; 4. 72 ℃ 1 min; 5. Go to 2×29; 6. 72 ℃ 5 min. Annealing temperatures and elongation times were adjusted for individual PCRs if necessary.

2.5.4.2 Phusion

Phusion PCR reactions were conducted with Finnzymes High-Fidelity Phusion Master Mix with HF buffer (F-531, NEB). Unless otherwise stated, reactions were conducted in 50µl aliquots as follows: 15 µl dH_2O, 2.5 µl Primer A (10 µM stock), 2.5 µl Primer B (10 µM stock), 5 µl template (100 ng μl^{-1} genomic DNA), 25 µl 2× Phusion HF Master Mix. Samples were mixed gently, before being cycled under the following conditions; 1. 98 ℃ 30 s; 2. 98 ℃ 10 s; 3. x ℃ 10 s; 4. 72 ℃ 30s kb^{-1}; 5. Go to 2×29; 6. 72 ℃ 10 m. Temperature x is the annealing temperature and was adjusted as appropriate for each set of primers.

2.5.5 *S. pombe ubx4* Knockout Protocol

Gene knockout protocols were conducted as described in Gregan et al. (2006), slight modifications to the protocol were made to adapt it to a low-throughput approach. Primers for knockout of the desired gene were designed and ordered as detailed in the database established by Gregan et al. (2006).

Five 50 µl Phusion PCR reactions (section 2.5.4.2) were conducted to produce upstream and downstream homology arms. Downstream homology arms used primers JG21do and JG21di; upstream arms used JG21uo and JG21ui. The five reactions for each arm were pooled, were ethanol precipitated, and samples were separated on a 1% agarose

gel. Bands corresponding to the homology arms were visualised and purified by gel extraction (Qiagen) in 30 µl.

Homology arms were pooled into a single 60 µl sample, to which was added 7 µl NEB Buffer 2, 2 µl XbaI and 1 µl dH_2O. Digests were incubated at 37 ℃ for 2 hours and were subject to PCR purification (Qiagen) into 30 µl in accordance with the manufacturer's protocols. Homology arms were ligated together using an NEB quick ligation kit; 30 µl 2× Quick Ligation Reaction Buffer and 3 µl Quick T4 DNA Ligase were added to the sample, which was incubated at room temperature for five minutes. The ligated sample was separated by gel electrophoresis on a 1% agarsoe gel, and a band corresponding to ligation of upstream and downstream homology arms – as indicated by Gregan et al. (2006) – was purified by gel extraction (Qiagen) into 30 µl.

The vector pCloneNat1, and the purified homology cassette were digested with SalI and BglII in NEB buffer 3 supplemented with BSA, in accordance with guidelines provided by NEB. Samples were digested at 37 ℃ for 2 hours, and were purified on a PCR purification kit (Qiagen). 50 ng of digested vector was mixed with a 3 fold molar excess of homology cassette in a total volume of 10 µl. 10 µl 2× Quick Ligation Reaction Buffer and 1 µl Quick T4 DNA Ligase were added to the sample, which was mixed gently incubated at room temperature for five minutes. 5 µl of ligated mixture was transformed into DH5α (section 2.5.3.1) which was plated onto ampicillin selection.

Six bacterial colonies were tested by colony PCR (section 2.5.4.1) with the oligos upch_uni and dwch_uni; products were visualised on a 1% agarose gel. Colonies producing products of the expected size, as indicated by Gregan et al. (2006), were selected for the next stage. Positive colonies were grown up overnight in 5 ml YES media with ampicillin, and plasmids were extracted using a Miniprep plasmid extraction kit (Qiagen). Following plasmid extraction, Taq PCRs were repeated to confirm the colony PCR result.

Knockout plasmids were digested: 20 µl miniprep DNA, 3 µl NEB buffer 2, 1 µl XbaI, 6 µl dH_2O and were incubated at 37 ℃ overnight. Digestion was confirmed on a 1% agarose gel, and samples were purified with a PCR purifcation kit (Qiagen) into 30 µl. *S. pombe* were transformed with 5 µl of the linearised knockout vector and were plated onto YES media containing NAT selection.

Strains growing on the YES-NAT medium were positive for the insert. To confirm that it had integrated at the correct locus, possible positive strains were subject to *S. pombe* colony PCR. Dwch_uni2 and Dwch_ubx4 were used to detect correct downstream integration, Upch_uni2 and Upch_ubx4 upstream integration, and JG2A and JG2G

provided a positive control. PCR conditions were adjusted to; 1. 94 ℃ 3 min; 2. 94 ℃ 50 s; 3. 60 ℃ 60 s; 4. 72 ℃ 3 min; 5. Go to 2×36; 6. 72 ℃ 5 min.

Promising colonies were subject to DNA extraction, were retested by PCR analysis, and were confirmed by tetrad analysis of a cross to wild-type cells.

2.5.6 *S. pombe* Gene Tagging Protocol

Tagging procedures were heavily adapted from Bähler et al. (1998), based on protocols by Gregan et al. (2006) and Noguchi (2006).

Two 300-700bp cassettes were produced by PCR using the primers defined in table 2.2 and a genomic DNA template. For each cassette, three 50 µl Phusion PCR reactions (Section 2.5.4.2) were pooled and were ethanol precipitated (Section 2.5.6.1). Samples were separated on a 1% agarose gel, and the cassettes were purified by gel extraction (Qiagen) according to the manufacturer's protocol. DNA concentration was measured.

A second 50 µl Phusion PCR reaction was set up as follows: 25 ng template DNA (Plasmid pFA6a-GFP(S65T)), 25 ng each cassette A and cassette B, 25 µl 2× Phusion HF master mix, dH_2O to a total volume of 45 µl. The Phusion master mix was added last. Samples were mixed, and were subject to a two stage PCR protocol.

1. 98 ℃ 2 min; 2. 98 ℃ 10 s; 3. 40 ℃ 30 s; 4. 72 ℃ 1 min 30 s; 5. Go to 2 × 5; 6. Add 2.5 µl of each of the second stage primers (100 µM stock), mix gently; 6. 98 ℃ 10 s; 7. 55 ℃ 30 s; 8. 72 ℃ 1 min 30 s; 9. Go to 6 × 30; 10. 72 ℃ 10 min.

Samples were ethanol precipitated (Section 2.5.6.1), were separated on a 1% agarose gel, and the tagging cassettes were purified by gel extraction (Qiagen) according to the manufacturer's protocol. Gel extracts were eluted into 30 µl, and 5 µl was transformed into *S. pombe*. Transformed cells were recovered overnight, instead of for 3 hours, shaking in YES media at 25 ℃. Transformed cells were plated directly onto YES media containing G418 and were incubated at 25 ℃ until colony formation.

2.5.6.1 Ethanol Precipitation

For each 100 µl of sample: 10 µl of 3M NaOAc was added and samples were mixed, DNA was precipitated by the addition of 200 µl 100% ice cold ethanol, samples were incubated on ice for 30 minutes and were spun at 13,000 rmp for 15 minutes in a microcentrifuge rotor chilled to 4 ℃. Supernatant was removed and pellets were washed in chilled 70% ethanol. Samples were air dried and resuspended in 30 µl dH_2O.

Gene	Cassette A Primers	Cassette B Primers	Second Stage Primers
Mlp1	Mlp1_AF_B, Mlp1_AR_B	Mlp1_BF_B, Mlp1_BR_B	Mlp1_AF_B, Mlp1_BR_B
Dph1	Dph1_AF, Dph1_AR	Dph1_BF, Dph1_BR	Dph1_AF, Dph1_BR

Table 2.2: Primers used for gene tagging

2.6 β-galactosidase Assays

Strains to be assayed were streaked onto SD−WL media in an organised grid like fashion. Plates were incubated at 30 ℃ until colonies were formed. For each 15 cm plate, 10 mg X-gal was dissolved in 100 µl dimethylformamide, this was subsequently added to 10 ml Z-buffer supplemented with 60 µl β-mercaptoethanol. Two 15 cm diameter discs of filter paper were placed in the bottom of a petri-dish and were soaked in the X-gal containing solution. Air bubbles were removed. A third 15 cm diameter disc of filter paper was applied to the colonies and was pressed down to transfer the cells onto the filter paper. Filter papers were removed with foreceps and were immersed in liquid nitrogen for 30 seconds. As the paper defrosted it was applied colony side up to the X-gal soaked discs. Plates were incubated at 37 ℃ for an hour and interaction strength was assayed by eye based on the intensity of the blue pigment, indicating X-gal hydrolysis. Plates were incubated at 37 ℃ for a further 24 hours and were assayed at a number of points to allow the identification of weaker interactions.

1 litre Z-buffer: 16.1 g $Na_2HPO_4.7H_2O$ (Fisher Scientific), 5.5 g $NaH_2PO_4.H_2O$ (VWR), 0.75 g KCl, 0.246 g $MgSO_4.7H_2O$, dH_2O to 1 litre, pH 7.0. Filter sterilise before use.

2.7 Mitochondria Preparation

S. pombe were grown in 1 l YES media to mid-log phase as judged by an an OD_{600} of between 0.4 and 0.6. Cultures were centrifuged for 10 minutes at 2000 g. Supernatant was discarded, and cells were washed once in 200 ml distilled water then in 50 ml 10 mM EDTA (VWR). The mass of the pellet determined. Pellets were resuspended in 3 ml digestion buffer M per gram of cells. 0.5 mg ml^{-1} zymolyase-100T (MP Biomedicals) and 1 mg ml^{-1} *Trichoderma harzianum* lytic enzyme (Sigma Aldrich) were added and the cells were incubated at 37 ℃ for 1 hour under gentle shaking. Tubes were transferred to 4 ℃ and all subsequent steps were performed on ice or at 4 ℃ with chilled buffers. Cells were centrifuged for 15 minutes at 2000 g, the supernatant was removed, and retained if cloudy. The pellet was resuspended in 20 ml lysis buffer M, and protoplasts were broken with 20 strokes of a tight homogenizer, before incubation for 15 minutes on ice. 200 µl of preparation was retained to form the cell lysate fraction. Retained supernatant was pooled with the homogenized cells and samples were spun twice for 15 minutes at 2500 g, the supernatant was transferred to a fresh tube after each spin, taking care not to disturb the pellet. The pellets contained

cell debris, nuclei and unbroken cells; they were discarded. 200 µl of preparation was retained to form the post nuclear fraction. Samples were spun for 15 minutes at 12000 g and 200 µl of supernatant was retained for the post mitochondrial faction, the remained was discarded. Samples were subject to three rounds of the following: resuspension in 2ml lysis buffer M supplemented with 0.01% (w/v) BSA (New England Biolabs), centrifugation for 2 minutes at 800g, transfer of the supernatant to a fresh microcentrifuge tube, centifugation for 15 minutes at 12000g and removal of the supernatant and floating lipids. The final pellet was resuspended in 100µl lysis buffer M and protein concentrations were determined (Chiron et al., 2007).

2.7.1 Buffers

2.7.1.1 Digestion Buffer M

1.2 M sorbitol, 10 mM sodium citrate, 0.2 mM EDTA (VWR), pH5.8.

2.7.1.2 Lysis Buffer M

0.6 M sorbitol, 10 mM imidazol-HCl, 2 mM EDTA (VWR), 1 mM PMSF, Complete protease inhibitor cocktail tablets (Roche) 1 tablet 50 ml^{-1}, pH6.4. β-mercaptoethanol added to 0.3% (v/v) immediately prior to use.

2.8 Protein Pulldowns

2.8.1 Induction Conditions

Induction conditions were optimized separately for each construct. Table 2.3 shows the strains, temperatures and incubation time used for each construct.

Expression vectors were transformed into the appropriate bacterial strain, using the protocol in section 2.5.3.1. Transformed bacterial cell lines were inoculated into 10 ml LB with the appropriate antibiotic and were grown overnight at 37 ℃ in an orbital incubator. Subsequently 4 ml of confluent media was used to inoculate 200 ml of fresh LB media, with appropriate antibiotic selection, and the resultant cultures were shaken at 37 ℃ until they reached an OD_{600} of approximately 0.6. Protein expression was induced through the addition of IPTG to a final concentration of 100µg ml^{-1}. Cultures were shifted to the induction temperature, and were incubated for the length of time indicated in table 2.3. Following inductions, cultures were spun at 3900 g for

Protein	Expression Vector	Strain	Temperature	Time
GST	pGexKG	BL21 pLyseS	25 ℃	4 hours
GST-Mlp1	pGexKG	BL21 pLyseS	25 ℃	4 hours
GST-Pus11	pGexKG	BL21 pLyseS	25 ℃	4 hours
His	pQE32	M15	36 ℃	4 hours
His-Dph1	pQE32	M15	36 ℃	4 hours

Table 2.3: Induction conditions

10 minutes, the supernatant was discarded, and pellets were frozen at -20 ℃ until use.

2.8.2 GST binding

Bacterial pellets were resuspended in 10 ml GST binding buffer and were sonicated on ice in three bursts of 10 seconds at 2.5 microns. Following sonication, the suspension was rotated for 30 minutes at 4 ℃. Debris was pelleted through centrifugation at 12,000 rpm in a chilled Beckman-Coulter JA-20 rotor, at 4 ℃. The supernatant was transferred to a fresh tube and was incubated with 200 µl glutathione sepharose 4B (GE Healthcare) beads on a roller at 4 ℃ for 1 hour. Beads were harvested by centrifugation at 3000 rpm in a microcentrifuge for 2 minutes, and were washed three times in 1 ml GST binding buffer.

2.8.2.1 GST Binding Buffer

50 mM Tris-HCl pH 7.5 (VWR), 100 mM NaCl (VWR), 10% Glycerol, 1% Triton, Complete protease inhibitor cocktail tablets (Roche) 1 tablet 50 ml^{-1} added prior to use.

2.8.3 His binding

Bacterial pellets were resuspended in 4 ml His binding buffer and were sonicated on ice in three bursts of 10 seconds at 2.5 microns. Following sonication, the suspension was rotated for 30 minutes at 4 ℃. Debris was pelleted through centrifugation at 12,000 rpm in a chilled Beckman-Coulter JA-20 rotor, at 4 ℃. The supernatant was filtered with a syringe and 0.22 µM membrane filter and transferred to a fresh tube. 200 µl lysate was mixed with 50 µl GST protein bound beads prepared above and samples were agitated

gently at 4 ℃ for 2 hours. Beads were harvested by centrifugation at 3000 rpm in a microcentrifuge for 2 minutes, and were washed five times in 1 ml His binding buffer.

2.8.3.1 His Binding Buffer

50 mM Tris-HCl pH 7.5 (VWR), 400mM NaCl (VWR), 10% Glycerol, Complete protease inhibitor cocktail tablets (Roche) 1 tablet 50 ml^{-1} added prior to use.

2.9 Protein Manipulation

2.9.1 Western Blots

Protein preparations were suspended in SDS loading buffer to 1× and was boiled at 100 ℃ for 5 minutes. Approximately 30 µg of protein was loaded into each well of a 10% polyacryamide gel and loading was adjusted to ensure equal ammounts of protein loaded in each well. A protein size marker (NEB broadrange 65-175 kDa prestained markers) was run in an availible well. Gels were cast in Biorad Protein III kits. Stacking gel was cast on top of the resolving gel to a depth of approximately 2 cm, including wells. Gels were run at 180 V for one hour.

Western blotting used a wet blotting protocol onto PVDF (Hybond-P, GE Healthcare) membrane in blotting buffer. Blots were blocked in an appropriate blocking buffer for one hour at room temperature or overnight at 4 ℃. Primary antibody and secondary antibody incubations were both done for an hour at room temperature using the dilutions, buffers and secondary antibodies shown in table 2.4. Following each antibody incubation, blots underwent 3 ten minute washes in PBST. Anti-rabbit and anti-mouse secondary antibodies were provided by GE Healthcare, anti-sheep antibody was provided by Dako (P0163). Dph1 antibodies were purified from sera on a PD-10 Desalting column (Amersham Biosciences) followed by binding to GST-Dph1 on a GST Orientation Kit (Thermo Scientific); kits were used according to the manufacturer's instructions.

Antibody staining was visualised using an ECL Plus western blotting detection system (GE Healthcare) in accordance with the manufacturer's protocol. Exposure times on Amersham Hyperfilm (GE Healthcare) were adjusted to give the clearest image.

Antibody	Supplier	Dilution	Buffer	Secondary
Anti-Cdc48	Gordon Lab Supplies	1:50,000	Milk	ECL anti-rabbit antibody
Anti-Dph1	Gordon Lab Supplies	1:20,000	Milk	ECL anti-sheep antibody
Anti-Ubiquitin	Dako (Z0458)	1:5,000	BSA	ECL anti-rabbit antibody
Anti-6×His	Qiagen (34610)	1:2,000	BSA	ECL anti-mouse antibody
Anti-Hsp60	Sigma Aldrich (H3524)	1:10,000	Milk	ECL anti-mouse antibody
Anti-Actin	AbCam (8224)	1:10,000	Milk	ECL anti-mouse antibody
Secondary Antibodies	1:5,000	Milk		

Table 2.4: Usage of antibodies.

Reagent	10% Resolving Gel	Stacking Gel
dH_2O	4 ml	2.1 ml
30% Acrylamine/Bis solution (Biorad)	3.3 ml	0.5 ml
1.5 M Tris pH 8.8 (VWR)	2.5 ml	
1 M Tris pH 6.8 (VWR)		380 µl
10% SDS (Fisher Scientific)	100 µl	30 µl
10% APS (Sigma)	100 µl	30 µl
TEMED (Sigma)	4 µl	3 µl

Table 2.5: Composition of polyacrylamide gels.

2.9.1.1 2× SDS Gel-loading Buffer

100 mM Tris-Cl pH 6.8 (VWR), 4% (w/v) SDS (Fisher Scientific), 0.2% (w/v) bromophenol blue, 20% (w/v) glycerol, 200 mM β-mercaptoethanol.

2.9.1.2 Polyacrylamide Gels

Composition of polyacrylamide gels used is shown in table 2.5.

2.9.1.3 Tris-glycine Electrophoresis Buffer

25 mM Tris (VWR), 250 mM glycine, 0.1% (w/v) SDS (Fisher Scientific)

2.9.1.4 Immersion Blotting Buffer

48 mM Tris base (VWR), 39 mM glycine, 20% methanol, 0.0375% SDS (Fisher Scientific)

2.9.1.5 PBST

PBS (Unipath, Oxoid), 0.1% Tween

2.9.1.6 Milk Blocking buffer

PBS (Unipath, Oxoid), 0.1% Tween, 10% Milk (Sainsbury's, skimmed instant dried milk.)

2.9.1.7 BSA Blocking buffer

PBS (Unipath, Oxoid), 0.1% Tween, 3% BSA (Melford)

2.10 Plasmids

Table 2.6 lists the plasmids mentioned in this thesis derived from commercial sources or previous bodies of work.

Plasmids pI2, pACT-Arp3, pACT-Obr1, pACT-Mlp1 and pACT-SPAPB24D3.07c were all pulled out of the exponential growth library as part of either this work, or the preliminary work on which it was based.

Table 2.7 lists the plasmids made as part of this work. For each plasmid, 50 µl Phusion reactions were conducted using the indicated primers, and successful PCR was confirmed on a 1% agarose gel. Where necessary due to low yields multiple reactions were conducted in parallel, and the reactions were pooled. PCRs were purified with a Qiagen PCR purification kit in accordance with the manufacturer's instructions. PCR products, and the destination vector were subject to restriction enzyme digest using the indicated enzymes. Digest conditions were as indicated by the enzyme manufacture, and where simultaneous digests were not possible, sequential digests were conducted. Digested vectors were treated with antartic phosphatase (NEB) in accordance with manufacturer's protocols, and both vector and insert were purified by PCR purification (Qiagen). 50 ng of digested vector was mixed with a 3 fold molar excess of insert in a total volume of 10 µl. 10 µl 2× Quick Ligation Reaction Buffer and 1 µl Quick T4 DNA Ligase were added to the sample, which was mixed gently incubated at room temperature for five minutes. 5 µl of ligated mixture was transformed into DH5α (section 2.5.3.1) which was plated onto appropriate selection.

pGBT9-Cdc48 was cloned with KOD HiFi polymerase, in place of Phusion. 4×50 µl reactions: 28.6 µl dH_2O, 5 µl 10×buffer#2 for KOD HiFi DNA polymerase, 5 µl dNTPs to concentration 0.2 µM, 2 µl $MgCl_2$ to concentration 1 mM, 1 µl template DNA (from 30 ng μl^{-1} stock), 4 µl primer A to concentration 0.4 µM, 4 µl primer A to concentration 0.4 µM, 0.4 µl KOD HiFi DNA Polymerase. PCR cycles as follows: 1. 95 ℃ 15 s; 2. 55 ℃ 30 s; 3. 72 ℃ 60 s; 4. Go to 1×29. Reactions were purified from a 1% agarose gel with a Qiagen gel extraction kit, instead of by PCR purification.

Plasmid	Description	Supplier	GenBank Accession
pGex-KG	Bacterial GST expression vector	Guan and Dixon (1991)	
pQE32	Bacterial 6×His expression vector	Qiagen	
pGBT9	Yeast two-hybrid bait vector	Clonetech Laboratories	U07646
pGAD424	Yeast two-hybrid prey vector	Clonetech Laboratories	U07647
pAS	Yeast two-hybrid bait vector	Clonetech Laboratories	U30496
pACT	Yeast two-hybrid prey vector	Clonetech Laboratories	AF264723
pFA6a-GFP(S65T)-kanMX6	GFP tagging cassette	Bähler et al. (1998)	
pCloneNat1	Knockout cassette	Gregan et al. (2006)	EF101285
pAS-SNF1	SNF1 Yeast two-hybrid bait control	Gordon Lab Stocks	
pACT-SNF4	SNF4 Yeast two-hybrid prey control	Gordon Lab Stocks	
pGBT9-Dph1	Dph1 Yeast two-hybrid bait	Gordon Lab Stocks (Jayne Miller)	
pACT-Rhp23	Rhp23 Yeast two-hybrid prey	Gordon Lab Stocks (Jayne Miller)	
pACT-Pus1	Pus1 Yeast two-hybrid prey	Gordon Lab Stocks (Jayne Miller)	
pAS-Ubx1	Ubx1 Yeast two-hybrid bait	Gordon Lab Stocks	
pAS-Ubx2	Ubx2 Yeast two-hybrid bait	Gordon Lab Stocks	
pGBT9-Ubx3	Ubx3 Yeast two-hybrid bait	Gordon Lab Stocks (Ingo Amn)	
pQE32-Dph1	His tagged Dph1	Gordon Lab Stocks (Katalin Fullop)	
pGEXKG-Dph1	GST tagged Dph1	Gordon Lab Stocks (Katalin Fullop)	
pCRTOPO-Cdc48	Cdc48 cDNA template	Gordon Lab Stocks (Rasmus Hartmann-Petersen)	

Table 2.6: Table of plasmids

Plasmid	Template	Vector	Primers	Restriction Enzymes
pGBT9-Ubx4	Genomic DNA	pGBT9	JG25F, JG25R	BamHI, SalI
pGBT9-Ubx5	Genomic DNA	pGBT9	JG26F, JG26R	BamHI, SalI
pGBT9-Cdc48	pCRTOPO-Cdc48	pGBT9	JG1L, JG1R	BamHI, SalI
pGBT9-Dph1-fr1	Genomic DNA	pGBT9	Dph1_5'_BamHI, Dph1_3Š_XhoI	BamHI, XhoI
pGBT9-Dph1-fr2	Genomic DNA	pGBT9	Dph1_5'_BamHI, Dph1_dSTI_XhoI	BamHI, XhoI
pGBT9-Dph1-fr3	Genomic DNA	pGBT9	Dph1_5'_BamHI, Dph1_dUBA_XhoI	BamHI, XhoI
pGBT9-Dph1-fr4	Genomic DNA	pGBT9	Dph1_dUBL_BamHI, Dph1_3'_XhoI	BamHI, XhoI
pGBT9-Dph1-fr5	Genomic DNA	pGBT9	Dph1_dSTI_BamHI, Dph1_3'_XhoI	BamHI, XhoI
pGBT9-Dph1-fr6	Genomic DNA	pGBT9	Dph1_sti_Fw, Dph1_sti_Rv	EcoRI, SalI
pGAD424-Mlp1-fr1	Genomic DNA	pGAD424	MSP3'F, MSP5'R	BamHI, SalI
pGAD424-Mlp1-fr2	Genomic DNA	pGAD424	MSP3'F, MSP_NT5'R	BamHI, SalI
pGAD424-Mlp1-fr3	Genomic DNA	pGAD424	MSP3'F, MSP_AAAE5'	BamHI, SalI
pGAD424-Mlp1-fr4	Genomic DNA	pGAD424	MSP_AAA3'F, MSP5'R	BamHI, SalI
pGAD424-Mlp1-fr5	Genomic DNA	pGAD424	MSP_CT3'F, MSP5'R	BamHI, SalI
pGAD424-Mlp1-fr6	Genomic DNA	pGAD424	MSP_AAA3'F, MSP_AAAE5'	BamHI, SalI
pGAD424-Mlp1-fr7	Genomic DNA	pGAD424	MSP_AAA3'F, MSP_AAA5'R	BamHI, SalI
pGexKG-Mlp1	Genomic DNA	pGexKG	MSP3'F2, MSP5'R	EcoRI, SalI
pQE32-Mlp1	Genomic DNA	pQE32	MSP3'F, MSP5'R	BamHI, SalI

Table 2.7: Table of plasmids

2.11 Primers and Other Oligonucleotides

Table A.1 in appendix A lists the sequence of all the primers mentioned in this thesis. Primers were supplied by Sigma Aldrich.

2.12 Microscopy

2.12.1 Co-localization

The imaging system comprises a Coolsnap HQ CCD camera (Photometrics Ltd., Tuscon, AZ) Zeiss Axioplan II fluorescence microscope with Plan-neofluor objectives, a 100W Hg source (Carl Zeiss, Welwyn Garden City, UK) and Chroma #83000 triple band pass filter set and Chroma #83700 emission filters (Chroma Technology Corp., Rockingham, VT). The single excitation and emission filters are installed in motorised filter wheels (Prior Scientific Instruments, Cambridge, UK). Image capture and analysis were performed using in-house scripts written for IPLab Spectrum (Scanalytics Corp., Fairfax, VA). (Description of imaging system written and supplied by Paul Perry)

2.12.2 Mitochondrial Staining

S. pombe were grown up in 10 ml YES pre-cultures in an orbital incubator at 25 ℃ until cultures were confluent. Approximately 100 µl of culture was transferred into 10 ml fully supplemented PMG media and was grown in an orbital incubator at 25 ℃ until an OD_{600} of approximately 0.6. 1 ml of culture was harvested at 5000 rpm for 2 minutes. The cell pellet was resuspended in 1ml fully supplemented PMG media containing 50 nM MitoTracker Red CMXRos (Invitrogen), and was incubated for 15 minutes at 25 ℃. Cells were harvested, washed once in fully supplemented PMG and then resuspended in fully supplemented PMG containing molten 0.5% low melting point agarose. Molten media was allowed to cool to 37 ℃ before being added to the cell pellet. 5 µl of cell suspension was spotted onto non-coated glass slides and was gently covered with a glass coverslip.

2.12.3 Deconvolution

The imaging system comprises a Hamamatsu Orca AG CCD camera (Hamamatsu Photonics (UK) Ltd., Welwyn Garden City, UK), Zeiss Axioskop fluorescence microscope with Plan-apochromat objectives, a Lumen 200W metal halide light source (Prior

Scientific Instruments, Cambridge, UK) and Chroma #83000 triple band pass filter set (Chroma Technology Corp., Rockingham, VT) with the excitation filters installed in a Prior motorised filter wheel. A pizoelectrically driven objective mount (PIFOC model P-721, Physik Instrumente GmbH & Co, Karlsruhe) was used to control movement in the z dimension. Hardware control, image capture and analysis were performed using in-house scripts written for IPLab Spectrum (Scanalytics Corp, Fairfax, VA). (Description of imaging system written and supplied by Paul Perry)

Deconvolution of images was conducted using the iterative restoration function of the software Volocity (Improvision, Waltham, MA). Individual Z-plane images were separated by 0.2 µm and 21 images were taken per stack.

2.13 Bioinformatics

Alignments were generated using ClustalW using the default settings (Larkin et al., 2007). The resultant alignment files were exported and were typeset using the package Texshade (Beitz, 2000), which was used to highlight conserved and similar residues. The conserved and similar residues highlighted by Texshade were used to calculate the percentage identity and similarity. Both identity and similarity were calculated as a percentage of the longest protein.

Chapter 3

Characterisation of the Ubx4 and Ubx5 genes

3.1 Ubx4 and Ubx5

Ubx4 (SPBC21C3.11, Section 1.6.3.7) and Ubx5 (SPAC17C9.11c, Section 1.6.3.8) are two members of a series of Cdc48 co-factors defined by the presence of the Ubx domain (Section 1.6.3.2); the structure of the proteins is represented in figure 3.1. In addition to a C-terminal Ubx domain, Ubx4 also contains an N-terminal TUG family UBL domain (Schultz et al., 1998; Letunic et al., 2009; Finn et al., 2010; Sonnhammer et al., 1997), also found in the *S. cerevisiae* homologue. Ubx5 contains an N-terminal predicted Zinc-finger domain, followed by a coiled coil, which may act together to form a nucleoside triosephosphate hydrolase motif (Schultz et al., 1998; Letunic et al., 2009; Finn et al., 2010; Sonnhammer et al., 1997; The UniProt Consortium, 2010; Jain et al., 2009). Both proteins show widespread distribution throughout the cell, and may be found in both the cytosol and the nucleus (Matsuyama et al., 2006).

The first step in attempting to characterise the role of the Cdc48 cofactors Ubx4 and Ubx5 was to obtain a knockout of each gene. The viability of the knockouts would help reveal whether the *ubx4*$^+$ and *ubx5*$^+$ genes are essential, and subsequent analysis of the resulting phenotypes would be important in helping to determine the function of each protein.

3.2 Knockouts of *ubx4* and *ubx5* Are Viable

3.2.1 *ubx4* Knockouts

The *ubx4*$^+$ gene was knocked out with natMX4, a resistance cassette for the clonNAT (nourseothricin) antibiotic (Gregan et al., 2006). Briefly, extended regions both upstream and downstream of the *ubx4*$^+$ gene were amplified by PCR (Figure 3.2). XbaI restriction sites within the outermost primers were used to ligate the two fragments together, and the resultant product was integrated into the pCloneNat1 vector. This vector was linearised at the XbaI site, and was transformed into wild-type haploid *S. pombe*. The PCR products acted as regions of extended homology, directing the cassette to the *ubx4* site via homologous recombination. Colonies were selected for ClonNAT resistance (Gregan et al., 2006).

Colonies growing on the selective media were crossed to wild-type lines and were subject to tetrad analysis. The clonNAT resistance marker segregated 2:2, indicating that the marker had successfully integrated (Figure 3.3a). Primers within the knockout cassette and flanking the *ubx4* gene were used in PCR analysis (Figure 3.4). This confirmed that the cassette had correctly integrated at the *ubx4* locus, knocking out the gene. Furthermore, this result also indicated that the gene *ubx4*$^+$ is not essential for basic viability.

3.2.2 *ubx5* Knockouts

Heterozygous diploid *ubx5* knockouts were available from Bioneer; the strain BG_0508 was obtained and meiosis was induced with the pSpo plasmid, bearing the mating cassette. Three induced diploid colonies were subject to tetrad analysis. Tetrads were replica plated onto media containing G418, which was selective for the cassette used to knockout *ubx5*. Surprisingly, not all colonies showed 2:2 segregation of the G418 resistance cassette: some consistently produced only G418 resistant spores (Data not shown). This suggested that some of the diploids were homozygous knockouts, an observation confirmed by PCR analysis (Figure 3.5). One of the resulting haploid colonies confirmed to contain the knockout cassette was selected for confirmation. The strain was back-crossed to wild-type and the G418 resistance markers were confirmed to segregate 2:2 (Figure 3.3). The confirmed strain was used for further study. The successful isolation of a haploid Δ*ubx5*::G418 strain indicates that *ubx5*$^+$ is not essential for basic viability.

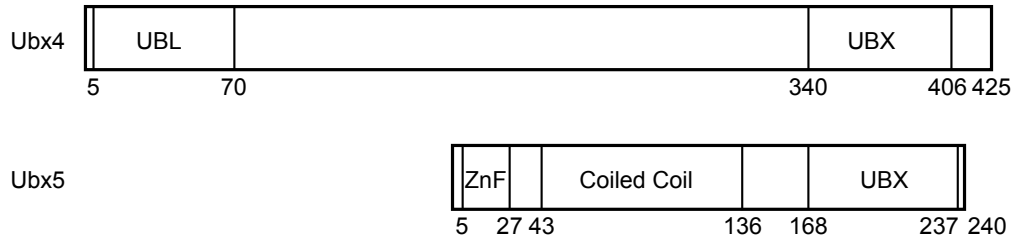

Figure 3.1: Domain structure of Ubx4 and Ubx5. ZnF indicates a putative zinc finger domain. (Schultz et al., 1998; Letunic et al., 2009; Finn et al., 2010; Sonnhammer et al., 1997; The UniProt Consortium, 2010; Jain et al., 2009)

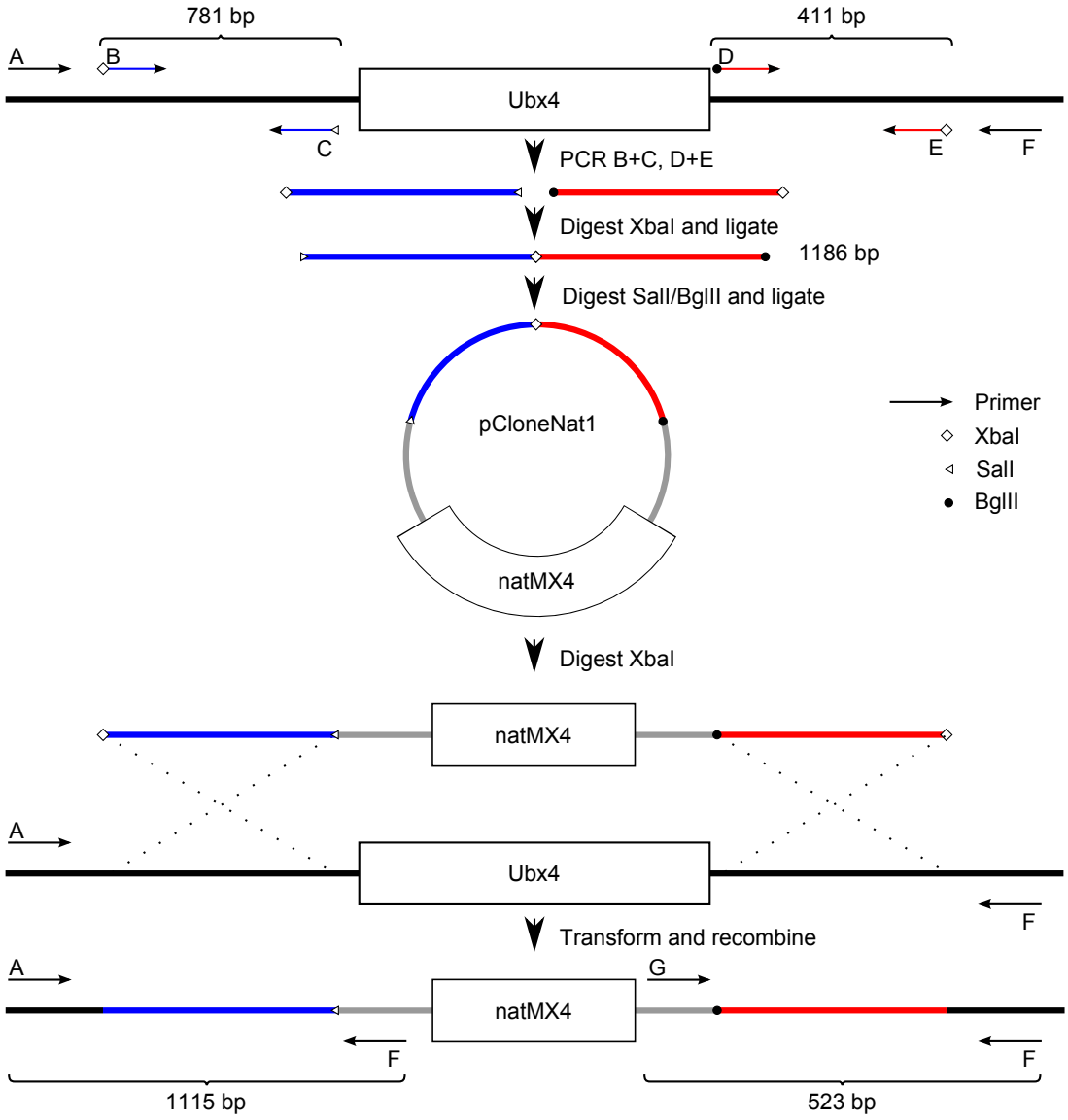

Figure 3.2: Diagram illustrating the knockout protocol. Primers indicated by A–G. (A) Upch-ubx4 (B) JG21uo (C) JG21ui (D) JG21di (E)JG21do (F) Dwch-ubx4 (G) Upch-uni2 (H) Dwch-uni2. Figure not to scale. Adapted from Gregan et al. (2006).

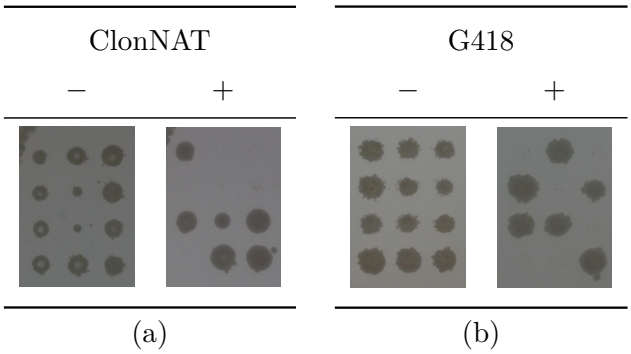

Figure 3.3: Example tetrads from a (a) Δ*ubx4* and (b) Δ*ubx5* cross to wild-type. Growth is shown on both selective and non-selective media. For the Δ*ubx4* stain, 56 separate tetrads were studied, of which 24 had four viable spores germinate. All 24 usable tetrads showed a 2:2 segregation of the clonNAT marker, confirming integration. For the Δ*ubx5* stain, 56 separate tetrads were studied. All usable tetrads showed a 2:2 segregation of the G418 marker, confirming integration.

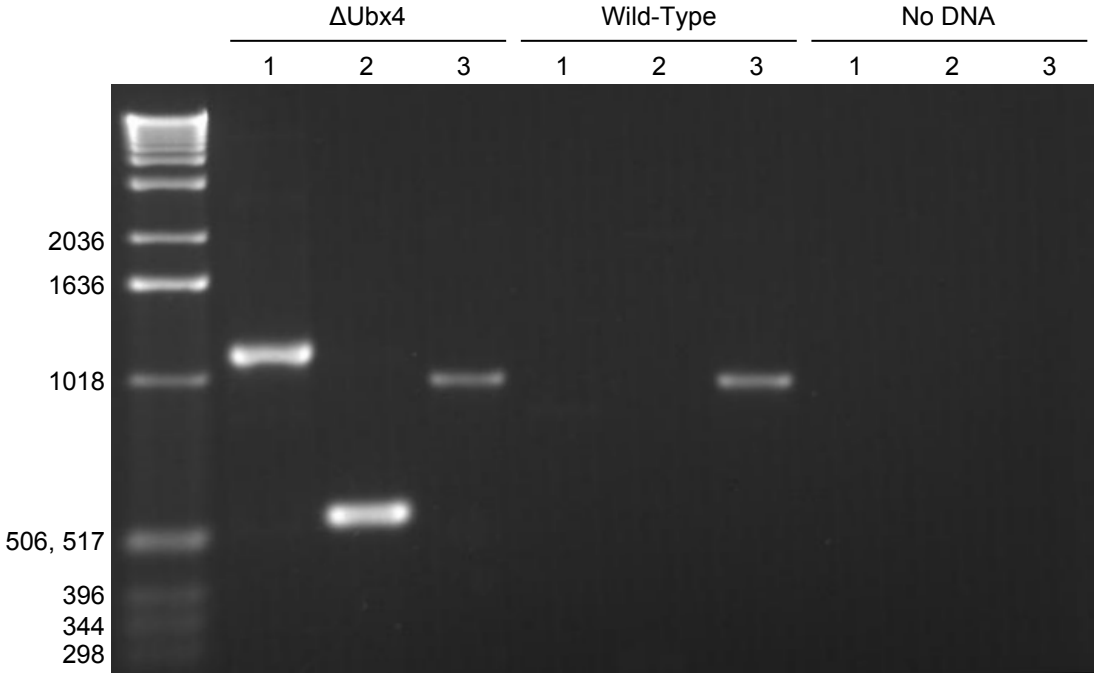

Figure 3.4: PCR analysis of DNA extracted from a putative Δ*ubx4*::natMX4 and a wild-type strain. Primers (1)Upch_ ubx4/Upch_ uni2 and (2)Dwch_ ubx4/Dwch_ uni2 were used to detect upstream and downstream integration respectively. Primers (3)JG2A/JG2G provide a positive control, and amplify a region located within *cdc48*. Samples were run on a 1% agarose gel and were stained and visualised with ethidium bromide. PCR of the putative Δ*ubx4*::natMX4 produces bands of the expected size for both the upstream (1115 bp) and downstream (523 bp) integration sites, which are absent from the wild-type DNA, indicating an insertion of the natMX4 cassette at the *ubx4* locus.

3.3 *Ubx4* and *Ubx5* Do Not Affect the Growth Rate

The discovery that Δ*ubx4* and Δ*ubx5* strains were viable raised questions as to whether their loss had a significant impact on the phenotype of the cells. One way of assessing this was to measure the growth rate of the knockout strains compared to the wild-type. Growth of Δ*ubx4*, Δ*ubx5* and wild-type strains was measured over the course of seven hours at 25 ℃ (Figure 3.6). No appreciable difference in growth rate can be observed between the three strains, indicating that the loss of neither $ubx4^+$ nor $ubx5^+$ has any notable effect on the growth rate under standard conditions at 25 ℃.

3.4 Study of Stress Factor Sensitivity

In order to better deduce the role of Ubx4 and Ubx5, including their interaction with Cdc48, a series of sensitivity assays were conducted. A range of different stress factors (Bimbó et al., 2005) were used to screen for a variety of cell processes which may be disrupted by the knockout. This information is summarised in table 3.1; the raw data is presented in the appendices, section B.2.

Stress factors act to disrupt the activity of selected pathways, and *S. pombe* with defects in these pathways may be particularly sensitive to the associated stressors. Defects in the microtubule network, including processes linked to spindle formation, can be explored with the microtubule poisons MBC and TBZ. Similarly, latrunculin A provides insights regarding the actin cytoskeleton. DNA replication can be inhibited with hydroxyurea treatment, whereas DNA damage can be induced by EMS, providing means of stressing the DNA replication and repair pathways. Similarly, the oxidative stresses, such as hydrogen peroxide, can result in DNA damage. Proteins may also be damaged through oxidative stress; similarly inhibition of protein synthesis with cycloheximide, and elevated or reduced temperatures, also lead to an accumulation of misfolded proteins and partially assembled complexes. This provides a means of stressing systems involved in the detection and removal of misfolded proteins, including the ubiquitin proteasome system. Secretory pathway proteins may be identified using the secretory pathway inhibitor Brefeldin A. More general stress responses, such as to salt (potassium chloride) and other osmotic stressors (sorbitol) can identify defects in the relevant stress response system, as well as homeostatic mechanisms. Finally, cell wall integrity can be assessed with the detergent SDS.

	Strain								
Stress	$\Delta ubx4$ $ubx5^+$ $cdc48^+$	$ubx4^+$ $\Delta ubx5^+$ $cdc48^+$	$\Delta ubx4$ $\Delta ubx5$ $cdc48^+$	$ubx4^+$ $ubx5^+$ $cdc48^{ts}$	$\Delta ubx4$ $ubx5^+$ $cdc48^{ts}$	$ubx4^+$ $\Delta ubx5$ $cdc48^{ts}$	$\Delta ubx4$ $\Delta ubx5$ $cdc48^{ts}$	wt	Control
None	+	+	+	-	-	-	-	+	
MBC	+	++	+	+	-	+	-	+	- - -
TBZ	+	+	+	-	-	-	-	+	-
Latrunculin A	+	+	+	- - -	- - -/- -	- - -	- - -	+	- - -
Hydroxyurea	-	-	-	-	-	-	-	+	- - -
EMS	+	+	+	+	+	+	+	+	- - -
H_2O_2	+	+	+	-	+	+	+	+	
Cycloheximide	+	+	+	- -	- - -	- - -	- - -	+	- - -
36°C	- -	+	+	- - -	- - -	- - -	- - -	+	- - -
20°C	+	+	-	-	-	-	-	+	- - -
Brefeldin A	+/-	+	+	-	-	-/+	-	+	-
KCl	+	+	+	- -	- -	- -	- -	+	
SDS	+	+	+	-	-	-	-	+	

Table 3.1: Sensitivity of the knock-out strains to a variety of stress factors. + indicates wild-type growth, -, - - and - - -, growth retarded by one, two and three or greater dilution factors respectively, when compared to wild-type. Where notable contrast existed between different concentrations of stress factor, the two responses have been separated by a forward slash. Photographs of the spot assays in appendix B.2.

3.4.1 Δ*ubx4* and Δ*ubx5* Strains Shows Minor Stress Sensitivity Phenotypes

Δ*ubx4* strains have a restricted range of phenotypes and growth on non-selective conditions is comparable to that on wild-type. At 36 ℃, the Δ*ubx4* strain shows a reduced viability compared to wild-type, a phenotype absent from the dual Δ*ubx4* Δ*ubx5* strain. Similarly, the mild sensitivity to high concentrations of Brefeldin A, a secretory pathway inhibitor, seen in the Δ*ubx4* strain is absent in the double knockout. The loss of Ubx4 also appears to partially rescue the sensitivity to high concentrations of latrunculin A seen in the *cdc*48^{ts} strain.

The loss of Ubx5 alone results in mild resistance to the microtubule poison MBC, although sensitivity to TBZ is unaffected. This effect is not seen in the absence of Ubx4, or in the presence of the *cdc*48^{ts} mutation. MBC and TBZ both inhibit microtubule polymerization, with MBC generally showing stronger effects than TBZ at comparable concentrations. Additionally, TBZ appears to disrupt cortical actin and results in a disruption of cell polarity (Quinlan et al., 1980; Sawin and Nurse, 1998; Sawin and Snaith, 2004). Both proteins achieve this result by binding to β-tubulin and in the case of MBC this has been shown to inhibit the binding of GTP, stabilizing the monomeric form, inhibiting its polymerisation into microtubules, resulting in a loss of the microtubule network through dynamic instability (Davidse and Flach, 1978; Winder et al., 2001). Disruption of the microtubule network can be particularly significant at mitosis, where it can result in chromosome non-disjunction and lead to aneuploidy (Wood, 1982).

Surprisingly, the loss of either *ubx4*$^{+}$ or *ubx5*$^{+}$ results in near wild-type growth of the *cdc*48^{ts} strain on hydrogen peroxide containing media, despite having no effect on the reduced viability of the *cdc*48^{ts} strain on YES media alone.

3.4.2 *cdc48*^{ts} Shows Overall Reduced Growth and Multiple Sensitivities

Unsurprisingly, the *cdc48*^{ts} mutants show significantly impaired growth at 36 ℃; the strain was originally isolated in a screen for temperature sensitive mutants generated by random mutagenesis (Yuasa et al., 2004). The strain also shows minor growth retardation compared to wild-type in the absence of added stress factors, indicating that the strain is impacted by the *cdc48*^{ts} mutation at the permissive temperature under standard conditions. It is likely that the similar minor growth retardation under other stress factors, such as TBZ and SDS, is a result of the general growth phenotype. This wide ranging growth retardation of *cdc48*^{ts} mutants is not seen on MBC containing

media, although this appears to be dependent on the presence of Ubx4.

The *cdc48*^{ts} strain shows strong growth inhibition on cycloheximide and latrunculin A compared to wild-type, as well as an increased impairment under high concentrations of potassium chloride. Cycloheximide is an inhibitor of protein biosynthesis and is likely to disrupt a broad range of cellular processes, however the depletion of ubiquitin is one of the key elements behind its toxicity. Thus elements in the ubiquitin-proteasome pathway are likely to be particularly affected by the presence of cycloheximide (Hanna et al., 2003). More surprising is the sensitivity to potassium chloride and latrunculin A, an osmotic salt stressor and actin cytoskeleton poison (Coué et al., 1987) respectively, as these stresses have no direct correlation to known Cdc48 functions.

3.5 Yeast Two-Hybrid Screens to Identify Novel Interactors

In the absence of any striking phenotype in either the Δ*ubx4* or Δ*ubx5* strain, it is especially important to provide an alternative approach for identifying the role of the proteins. To attempt to dissect the role of the Ubx4 and Ubx5 further, it was resolved to conduct a yeast two-hybrid library screen using the two proteins as bait. Yeast two-hybrid screens exploit the modular nature of the transcription factor GAL4 to detect protein-protein interactions in a *S. cerevisiae* expression system (Figure 3.7). Briefly, the binding domain of GAL4 is expressed as a fusion construct with the protein of interest, the bait, in this case Ubx4 or Ubx5. *S. cerevisiae* expressing this construct are co-transformed with a vector expressing a fusion between the GAL4 activation domain, and a candidate interactor, the prey. The bait is recruited to the promoter of the selectable marker via the fused GAL4 DNA binding domain; the absence of an appropriate activation domain means that it is unable to drive transcription. In the event of an interaction between the bait and prey however, the GAL4 activation domain is recruited to the promoter via the fused prey protein; once there it is able to drive expression of the selectable marker, allowing for identification of interacting proteins. The use of a cDNA library fused to the activation domain allows for rapid screening of a large number of proteins for interaction, and identification of possible candidates by the isolation of colonies expressing the selectable marker.

Firstly the Ubx4 and Ubx5 bait vectors were assayed for their interaction with Cdc48 (Table 3.2). Ubx4 was confirmed to interact strongly with Cdc48 and showed no auto-activation; the interaction between Ubx5 and Cdc48 was weaker, but still specific. Thus both proteins are expressed correctly in the yeast two-hybrid system and are suitable for conducting a library screen.

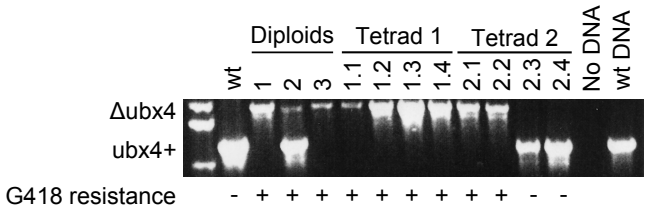

Figure 3.5: PCR analysis of DNA extracted from Bioneer supplied Δ*ubx5*::G418 and a wild-type strain. Three diploid colonies were subject to PCR analysis using the primers JG27N and JG27C which flank the *ubx5* gene. Colonies 1 and 3 both appear to be homozygous knockouts, colony 2 is a heterozygote. Colonies 1 and 2 were both subject to tetrad analysis showing 4:0 and 2:2 segregation of G418 resistance respectively. PCR analysis of the resultant haploids confirmed that the G418 resistance cassette segregated with the larger PCR product.

Binding Domain	Activation Domain	-WL	-WHL	-WHLA
pGBT9	pACT			
pGBT9-ubx4	pACT			
pGBT9-ubx5	pACT			
pGBT9-ubx4	pGAD424-cdc48			
pGBT9-ubx5	pGAD424-cdc48			
pGBT9	pGAD424-cdc48			
pGBT9-ubx5	pI2			
pGBT9	pI2			
pAS-SNF1	pACT-SNF4			
None	None			

Table 3.2: Confirmation of Ubx4 and Ubx5 vectors. *S. cerevisiae* was co-transformed with the binding domain and activation domain plasmids and was spotted onto selective media (Section 2.2.2.2). Column headings indicate the supplements missing from the SD media, tryptophan (W), leucine (L), histidine (H) and adenine (A).

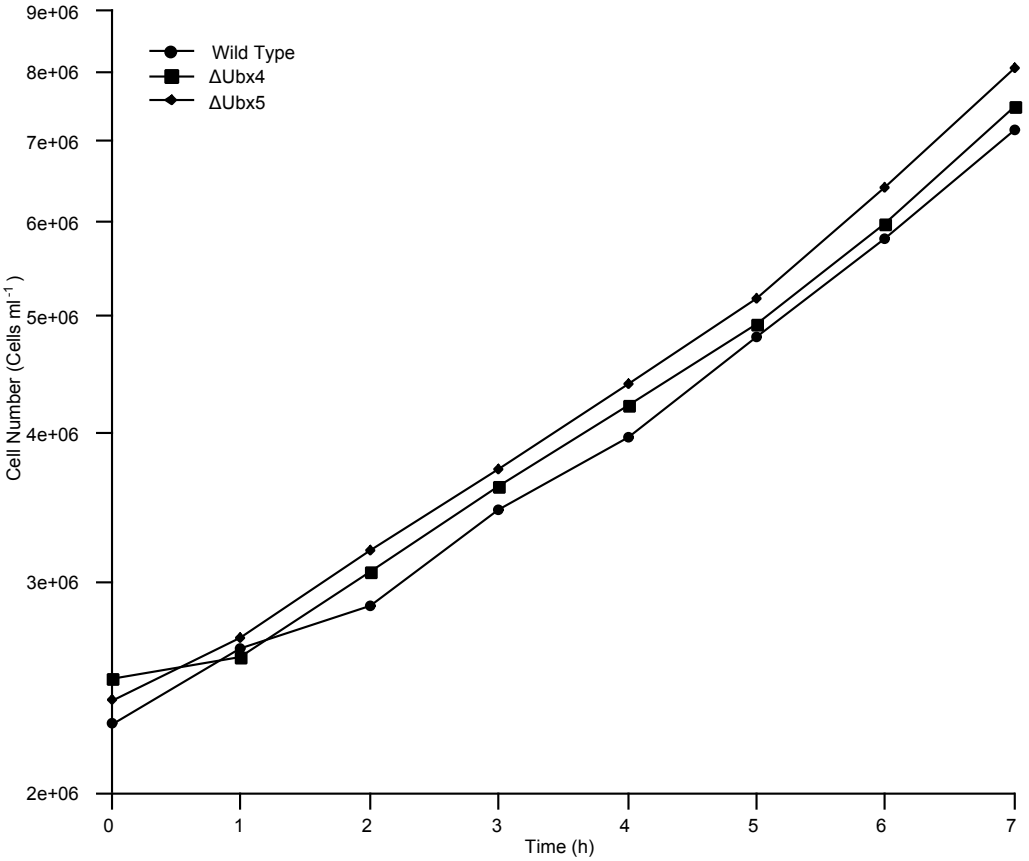

Figure 3.6: Representative growth of Δ*ubx4*, Δ*ubx5* and wild-type strains over a period of seven hours at 25 °C. Growth is assayed by measuring cell density and is plotted on a logarithmic scale. The difference between the growth curves is largely a result of the slightly differing starting concentrations; the parallel nature of the lines indicates that the growth rates of the strains do not differ appreciably. The growth curves were repeated three times, showing the same result; graphs showing further repeats of the assay, as well as measurements of OD_{600}, can be found in figure B.1 in appendix B.

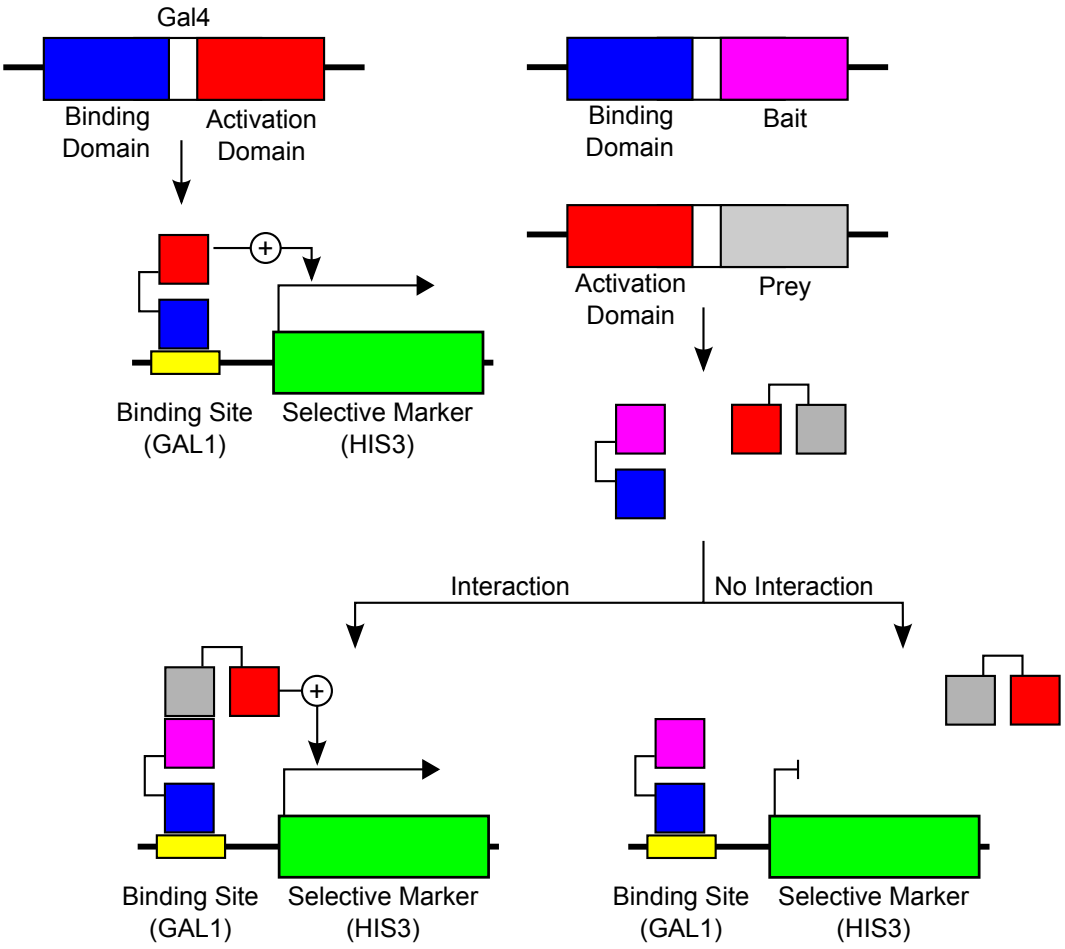

Figure 3.7: Diagram showing the concept behind the yeast two-hybrid assay. Only one selective marker has been shown for illustration. In practice the system can also be used to drive expression of *ADE2* and *lacZ*, under control of the *GAL2* and *GAL7* promoters respectively (James et al., 1996). On the left is an illustration of the action of the intact GAL4 transcription factor. On the right the binding and activation domains are shown fused to two proteins of interest; interaction between them is sufficient to drive expression from the *GAL1* promoter.

PJ69-4A strains containing *ubx4*$^+$ or *ubx5*$^+$ baits were transformed with a *S. pombe* cDNA library prepared from exponentially growing cells, and were plated onto selective media (See section 2.5.3.3), approximately 1×10^6 transformants were screened for each bait. The same library used in this screen had previously been used to successfully screen other bait proteins, including Cdc48. Positive colonies were selected and streaked onto both stringent and less stringent selection and growth was scored. Colonies were subject to β-galactosidase assays and the approximate level of expression was categorised by eye. The results of each assay were used to score the strength of the interactions, allowing for the strongest interactions to be identified. The results of this approach are presented in figure C.1 in appendix C. A summary of the library screening and analysis process is presented in figure 3.8.

A process was begun to isolate and identify the prey vectors found within the positive strains. Plasmid extraction was achieved as described in section 2.5.2.2 and *E. coli* containing the correct plasmid were identified by PCR with primers specific to the activation domain plasmid. In addition to this, sequencing was performed directly on PCRs from the activation domain plasmid isolated from *S. cerevisiae*, as plasmid isolation had low efficiency and specificity. PCRs using primers specific to prey plasmids containing *cdc48*, or *his5*, were also used to help quickly exclude the respective elements.

Early efforts identified an interaction between Cdc48 and Ubx4 as being responsible for the nine strongest interactions identified. Unfortunately, the initial analysis revealed that many of the other sequences identified were unpromising. Other candidates included empty prey vectors and intergenic regions, which were unlikely to be genuine interactors. Furthermore, attempts to re-test successfully isolated plasmids revealed that they either failed to re-test, or otherwise demonstrated auto-activation in the presence of the binding domain alone (See pI2 example in table 3.2). Thus, although the library screen was able to confirm the known interaction between Ubx4 and Cdc48, it failed to provide any further candidate interactors for further study. As a result of these early results, it was resolved to abandon the work on the Ubx4 and Ubx5 proteins, the discussion in section 3.6, describes the reasoning behind this decision in more detail.

3.6 Discussion

As discussed in section 1.6, the protein Cdc48 is involved in a diverse range of processes within the cell, and it is likely that it has other roles that have yet to be identified. To coordinate these functions, Cdc48 makes use of a series of co-factors, which change its specificity and modulate its function. These co-factors provide ideal targets for study,

as they allow for different roles of Cdc48 to be studied in isolation. Furthermore, several known co-factors, such as Npl4-Ufd1 and Ubx3/p47, act as adaptor proteins, coordinating the binding of Cdc48 to its targets. Finding binding partners of co-factors could help identify possible targets of the Cdc48 complex, including those which may not be bound by Cdc48 itself.

The Ubx proteins in particular provide good candidates for study, as the Ubx domain provides a conserved site of Cdc48 interaction (Hartmann-Petersen et al., 2004; Buchberger et al., 2001). This allows for easy identification of previously uncharacterised co-factors, which may then be subject to further study. On starting the project, *ubx4*$^+$ and *ubx5*$^+$ were largely uncharacterised, both in *S. pombe* and in other organisms. As a result, they provided ideal candidates for identifying novel functions for Cdc48, or for providing further mechanistic details regarding known roles. Recently, other work has revealed more information regarding the role of Ubx4 in particular, and some of the findings here will also be considered in that context.

3.6.1 Growth and Viability

The viability and wild-type growth rates of the Δ*ubx4* and Δ*ubx5* strains indicate that neither protein is essential for standard growth. The double knockout strain is also viable, indicating that the two proteins are not simply functionally redundant; this does not exclude the possibility that redundancy in other proteins is responsible for maintaining the viability of the knockouts.

3.6.2 Stress Sensitivity

Stress sensitivity assays identified a slight sensitivity to a few stress factors, particularly in the Δ*ubx4* lines. The most notable of these is the temperature sensitivity of the Δ*ubx4* strain. This is in line with similar sensitivity observed in *S. cerevisiae* by Alberts et al. (2009), possibly indicating a conserved role for Ubx4 between *S. cerevisiae* and *S. pombe*. Surprisingly the loss of Ubx5 is able to rescue this temperature sensitive phenotype. Alberts et al. (2009) found that Ubx4 was required for the release of ubiquitinated substrates from Cdc48 and that Δ*ubx4* mutants had reduced levels of free cytoplasmic Cdc48. The loss of Ubx5 may prevent it sequestering Cdc48, resulting in an increase in the levels of free Cdc48 within the cell. This would suggest that the levels of free Cdc48 may be as important as the degradation of its targets in causing temperature sensitivity in the Δ*ubx4* strains. If this were the case, over-expression of Cdc48 in Δ*ubx4* strains would be expected to relieve the temperature sensitive

phenotype. The suggestion that Cdc48/p97 associated phenotypes may be a result of changes in the dynamics of co-factor competition, is supported by recent work by Fernández-Sáiz and Buchberger (2010). It was found that disease causing mutations in p97 are associated with shifts in the relative binding affinity for the various co-factors, which would be predicted to result in a corresponding redistribution of p97 activity.

Conversely, the cycloheximide sensitivity observed by Alberts et al. (2009), was not replicated in this study. This difference could be a result of the different species used in the two studies, or of the CPY* expression used by Alberts et al. (2009), which may have a resulted in an increased sensitivity. Interestingly in a $cdc48^{ts}$ background, the loss of either *ubx4* or *ubx5* increases sensitivity of cycloheximide.

The mild sensitivity to high concentrations of the secretory pathway inhibitor, brefeldin A, seen in the $\Delta ubx4$ strain is surprising given its purported role in the ERAD pathway (Section 1.6.3.7). While it is possible that this sensitivity is a side effect of defects in the ERAD pathway, or a result of differences between *S. cerevisiae* and *S. pombe*, it is also possible that the secretory pathway is another target of Ubx4. Alberts et al., found that the UBL domain of Ubx4 was not required for its association with Cdc48, or for its role in the breakdown of the ERAD substrate CPY*. This suggested that Ubx4 may participation in other processes, in addition to the ERAD pathway. The study of brefeldin A sensitivity in strains lacking the Ubx4 UBL domain could be help further dissect this possibility.

Curiously, slight resistances were also noted, such as an increased resistance to MBC in the $\Delta ubx5$ strain and a resistance to hydrogen peroxide in both strains. While it is possible that these phenotypes are a direct result of the loss of the proteins in question, indicating roles with the microtubule network, or oxidative stress response respectively, it is also possible that the phenotypes are a side effect of Cdc48 function. As the activity of Cdc48 is regulated by its co-factors, which may bind in mutually exclusive manners (Section 1.6.3), the depletion of one co-factor would reduce competition for free Cdc48, potentially allowing the efficiency of other co-factors to increase. However, as the MBC resistance of $\Delta ubx5$ appears to be dependent on the presence of $ubx4^{+}$, and yet the $\Delta ubx4$ are not MBC sensitive themselves, it suggests that this relationship between co-factors and sensitivity may be quite complicated.

While the sensitivity assays have provided hints regarding the role of Ubx4 and Ubx5, it is not possible to draw any firm conclusions from the sensitivity data alone. The lack of any striking sensitivity phenotypes, such as complete inviability in the presence of specific stress factors is disappointing, as such a phenotype would be very useful in future diagnostic screens. Further data regarding binding partners of Ubx4 and

Ubx5 would be useful for tying phenotypic observations to mechanistic information, and would provide suitable candidate hypothesis for further study.

3.6.3 Ubx4 and Ubx5 Interactors

The yeast two-hybrid screen to identify Ubx4 and Ubx5 interactors only managed to identify the known interaction between Ubx4 and Cdc48. The similar interaction between Ubx5 and Cdc48 was not detected, possibly a result of the weaker interaction between the two proteins (Table 3.2). Of the remaining weaker interactions isolated and re-tested, all were found to be false positives, indicating that the screen has a high background at lower stringencies.

The inability to identify additional binding partners of the Ubx4 and Ubx5 proteins is likely to be due to limitations of the yeast two-hybrid screening system. A cDNA library is produced through reverse transcription of RNA preparations. The inefficiency of this process over extended transcripts means that large proteins can be under represented, or be expressed as truncated constructs lacking the N-terminus. This reduces the likelihood of identifying large binding partners, particularly those which interact through domains near the N-terminus. Similarly, the amplification of the cDNA library results in further under representation of transcripts with low expression levels, which are already under-represented in the initial library. Although large, Cdc48 is a highly abundant protein, which can expect to be strongly represented in the library.

Other limitations are likely to occur at the protein level. The interaction of other Cdc48 co-factors with their targets is often dependent on target ubiquitination, which relies on the presence of the correct E2 and E3 enzymes. As the yeast two-hybrid system takes place in *S. cerevisiae* rather than *S. pombe*, the *S. cerevisiae* native E2 and E3 enzymes may not be sufficient for correct ubiquitination of the target proteins. Similar issues may arise if the proteins only interact as part of a complex, of which further elements may either be absent from *S. cerevisiae*, or insufficiently conserved. Further restrictions arise from the requirement for both binding and activation domains to be correctly localised to the nucleus, which may not be possible for membrane localized proteins. Finally, interactions which are particularly transient may drive insufficient expression from the promoter to allow for reliable identification of positive colonies.

Other difficulties with the screen were the high incidence of false positives. In some cases these appeared to be result of co-transformation with multiple library plasmids, as PCR with flanking oligos resulted in two or more defined bands (Data not shown). In other cases expression of proteins such as His5, the *S. pombe* homolog of the His3 selectable

marker, bypassed the selective process indirectly. The use of more stringent selection, particularly for adenine auxotrophy, helps eliminate some of these false positives and use of the library at lower concentrations would reduce the number of dual transformants. Under the recommendation of members of the lab who had previous experience with the PJ69-4A strain 3-amino-1,2,4-triazole (3-AT) was not used in the initial screen. However, guidance from James et al. (1996) suggests that the concentration required may vary between bait plasmids, and recommends concentrations of between 0 and 2 mM. The use of higher levels of 3-AT could reduce the background on less-stringent media, while still allowing weaker interactions, such as that between Ubx5 and Cdc48 to grow. 3-AT functions by inhibiting the histidine biosynthesis enzyme, imidazole glycerol phosphate dehydratase, encoded by the *HIS3* selective marker. This effectively suppresses histidine biosythesis at low levels of *HIS3* expression, preventing leaky expression from the uninduced *GAL1* promoter supporting growth on media lacking histidine; high levels of *HIS3* expression in the presence of an interaction are able to overcome this inhibition (Hilton et al., 1965; Klopotowski and Wiater, 1965). Alternatively, more recent recommendations from James (Personal communication) suggest that initial transformations be plated onto less stringent selection before replica plating onto more stringent selection after a period of 14 to 20 days. This two stage selection process will eliminate a lot of the false positive colonies, while recovering the weaker genuine interactions.

In addition to the yeast two-hybrid screen, other mass throughput screens could also be useful for identifying genes which interact with $ubx4^+$ and $ubx5^+$. All the *S. pombe* open reading frames have been systematically disrupted, and a knockout library is available from Bioneer (Daejeon, South Korea) and could be used as the basis for a screen for synthetic lethality with the $\Delta ubx4$ and $\Delta ubx5$ strains. Synthetic lethality describes the situation in which two genes show genetic interaction, such that the loss of both is lethal, whereas either single mutant is viable. Such screens have been used extensively in *S. cerevisiae* in which it has been possible to assay genetic interactions of a range of intensities, allowing the identification of genes which act in the same or opposing pathways, and make predictions regarding the function of uncharacterised genes (Reviewed in Boone et al., 2007). Recent improved techniques in manipulating the genetics of *S. pombe* make similar approaches now available for fission yeast. Previously, a significant background level of diploids would remain following a cross, making screens difficult. However, the creation of recessive cycloheximide resistance mutations in the ribosomal gene Rpl42 allow for the specific selection of haploid strains following genetic crosses, and multiple approaches have been developed to select for a single mating type. This approach has already been shown to be useful for identifying

elements of the RNAi pathway and nuclear function (Roguev et al., 2007, 2008). Further screens for genetic interactions can also be conducted using overexpression libraries, in which *S. pombe* are screened for inviability when candidates are overexpressed in the mutant background. Liu et al. (2009) found that strains lacking in Dsk2 and Rad23 showed growth defects when some of their substrates were overexpressed.

A more direct approach can be made by the expression of tagged Ubx4 and Ubx5 proteins in *S. pombe*, which may subsequently be purified on an appropriate column, allowing for the isolation of any bound proteins. Bound proteins should be visible as bands on a polyacrylamide gel, and can be identified via mass spectroscopy.

3.6.4 Summary

The identification of the Ubx4-Cdc48 interaction indicated that the screen was functional in principal. However the high level of unrepeatable interactions and false positives in the remaining candidates indicated that it would be unproductive to continue processing the remaining candidates. The majority of the remaining candidates showed markedly weaker interactions than clearly identified false positives, and were unlikely to yield genuine interactions. Any further work on Ubx4 or 5 would require a solid base for further study, and continued work using the yeast two-hybrid system could not be guaranteed to provide one. In addition, time constraints applied by the PhD program meant that attempts to address the limitations of the current screening protocol would be unlikely to leave sufficient time to pursue the role of any candidates identified. Other work with Ubx4 and Ubx5 had similarly been unable to provide a solid base for further work, although did offer hints as to possible function. As a result of these limitations, and with time considerations in mind, it was decided that further work on Ubx4 and Ubx5 would be unproductive. Other work, looking at targets of the proteasome shuttle factor Dph1, provided a clear starting point for further investigation, and early work provided a promising hypothesis for further testing. It was decided to focus the remainder of the thesis on this area.

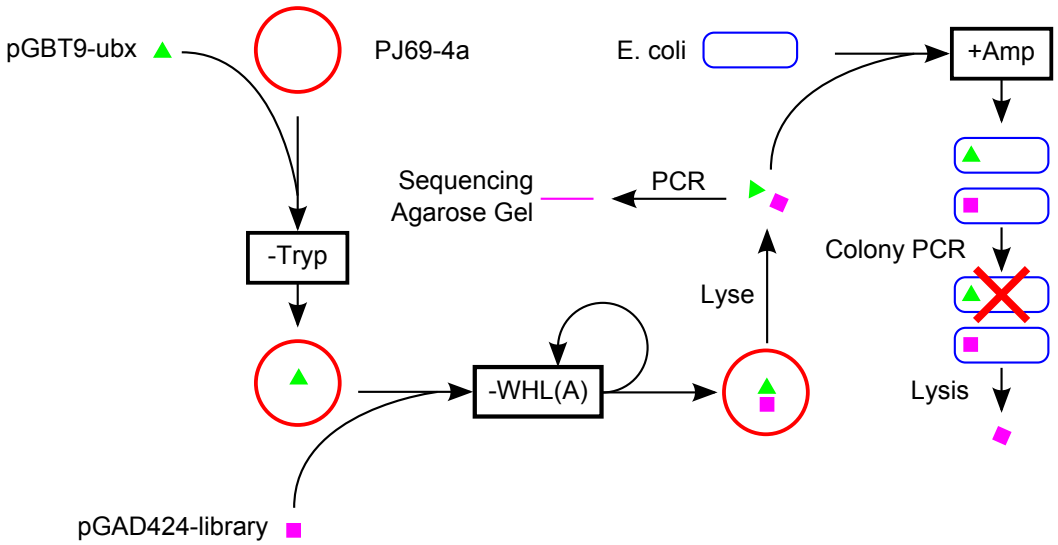

Figure 3.8: Summary of the screening and identification process.

Chapter 4

Identification of Novel Dph1 Interactions

4.1 The Shuttle Factor Dph1 Shows Novel Interactions

Prior work in the lab, conducted by Ingo Amn, identified possible novel interactors with the Dph1 proteasome shuttle factor (See section 1.5.3, domain structure shown in figure 4.1). A yeast two hybrid screen with a Dph1 bait, both full-length and lacking the ubiquitin interacting UBA domain, identified several possible targets, summarized in table 4.1. The four candidates which were identified with the highest frequency were selected for further verification to provide proteins for further study.

4.1.1 The Candidates

Of the four candidates identified at the highest frequency in the original screen, two had been previously characterised in *S. pombe*. The gene *obr1* (overexpressed in brefeldin A resistant strains), also known as *apt1* (AP-1 target gene) or *uhp1* (ubiquitinated histone-like protein), encodes a histone like protein which appears to be involved in mating cassette silencing (Naresh et al., 2003). The protein is discussed in more detail in section 1.9. The gene *arp3* encodes an actin like protein, involved in polarized cell growth, cytoskeletal reorganization and contractile ring formation (McCollum et al., 1996). SPCC24B10.10c has been previously uncharacterised in *S. pombe*, but shows homology to the *S. cerevisiae* gene *MSP*1 (Hertz-Fowler et al., 2004), with 41.4% protein sequence identity and 56.1% similarity (Figure 4.2). This gene will be named *mlp1*, for 'Msp1 like protein,' throughout the remainder of this thesis. SPAPB24D3.07c is

	Frequency of Interaction	
Candidate	Full-Length	ΔUBA
Obr1	10	6
SPCC24B10.10c (Mlp1)	5	2
Arp3	4	2
SPAPB24D3.07c	4	1
Ppa1	2	1
SPCC306.06c	1	1
Sod2	0	1
Ain1	0	1
Rps002	0	1
Ctf1	0	1
SPAC5D6.13	0	1
SPAC17G6.11c	0	1
SPCC757.05c	0	1
Mug84	0	1
SPBC14C8.04	0	1
Mud1	1	0
Pub1	1	0
Hob1	1	0
Act1	1	0
Trm112	1	0
Rps602	1	0
Cal1	1	0
SPCC11E10.07c	1	0
Car3	1	0
SPCC1281.06c	1	0
SPBC660.05	1	0
SPBC1539.03c	1	0

Table 4.1: Possible Dph1 interacting proteins and the frequency with which each candidate was identified in a yeast two-hybrid screen of a *S. pombe* mitotic library against full-length and ΔUBA forms of Dph1. Based on screen conducted by Ingo Amn.

an entirely uncharacterised gene, with no obvious orthologs (Hertz-Fowler et al., 2004; Altschul et al., 1990) in other organisms.

4.1.2 The Interaction Between Dph1 and the Four Candidates is Reproducible

To confirm the interaction between Dph1 and the candidates, yeast-two hybrid assays were repeated with the plasmids isolated from the original strains. Each plasmid was also tested against an empty pGBT9 vector, to ensure that it wasn't exhibiting auto-activation, or interaction with the binding domain itself. Table 4.2 shows the growth of the resultant transformants under the varying selective conditions used in each experiment. Tryptophan (*TRP*1) and leucine (*LEU*2) markers are located on the bait and prey plasmids respectively; the -WL media, lacking tryptophan and leucine selects for correct transformation only. A positive interaction between bait and prey allows for expression of histidine (*HIS*3) and adenine (*ADE*2) markers allowing for growth on stringent (-WHLA) and less stringent (-WHL) selection.

All four candidates reproduced the interaction observed in the original screen, and showed markedly increased growth relative to the binding domain only control. Similarly, transformants containing pGBT9-*dph1* and the empty activation domain vector pACT, were unable to grow under selection, indicating that growth was dependent on the presence of both Dph1 and a suitable candidate interactor. Of particular note are Obr1 and Mlp1 which both support strong growth on the stringent selection and minimal background growth with negative controls. As a result, Mlp1 and Obr1 were selected for further study, the domain structure of both proteins is shown in figure 4.1.

4.1.3 Obr1 and Mlp1 Interact With Dph1 Via Its Sti1 Domains

A series of *dph1* truncations, figure 4.3, were created to dissect the role of the various sub-domains in coordinating the interaction with the novel targets. These truncations were used as the basis of further yeast two-hybrid assays with both Mlp1 and Obr1, shown in table 4.3.

The UBL domain of Dph1 is not responsible for the interaction with both Mlp1 and Obr1; the fr2 truncation, consisting of the UBL domain alone, is unable to interact with either target. Furthermore, the loss of the UBL domain in fr4 has no notable effect on the strength of the interaction, as demonstrated by similar levels of growth on stringent

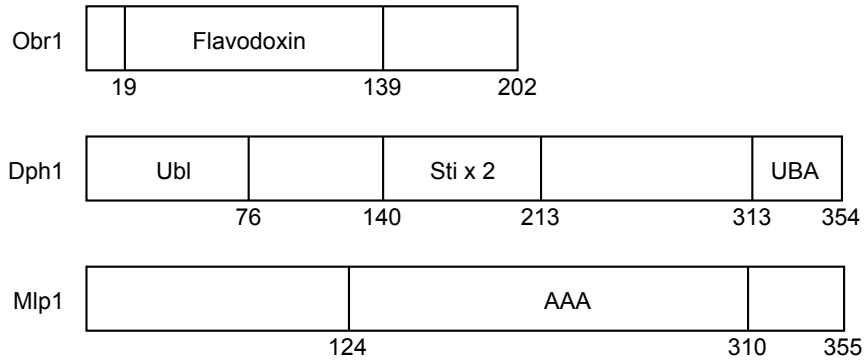

Figure 4.1: Domain structure of Dph1 and its interactors

Binding Domain	Activation Domain	-WL	-WHL	-WHLA
pGBT9	pACT			
pGBT9-dph1	pACT			
pAS	pACT			
pGBT9-dph1	pACT-arp3			
pGBT9	pACT-arp3			
pGBT9-dph1	pACT-obr1			
pGBT9	pACT-obr1			
pGBT9-dph1	pACT-mlp1			
pGBT9	pACT-mlp1			
pGBT9-dph1	pACT-SPAPB24D3.07c			
pGBT9	pACT-SPAPB24D3.07c			
pAS-SNF1	pACT-SNF4			
None	None			

Table 4.2: *S. cerevisiae* was co-transformed with the binding domain and activation domain plasmids and was spotted onto selective media (Section 2.2.2.2). Column headings indicate the supplements missing from the SD media, tryptophan (W), leucine (L), histidine (H) and adenine (A).

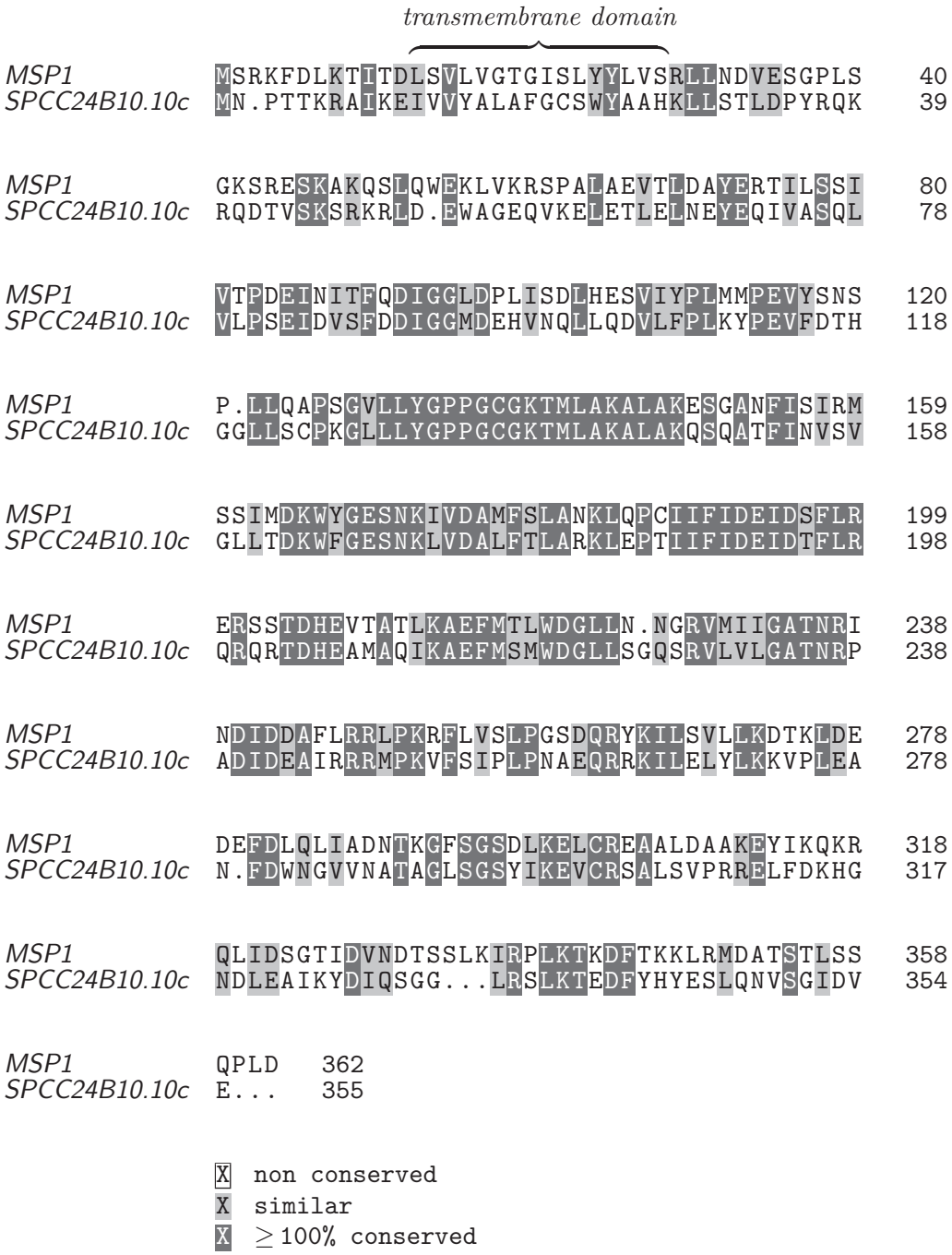

Figure 4.2: Comparative alignment of *S. cerevisiae* Msp1 with *S. pombe* SPCC24B10.10c (Larkin et al., 2007; Beitz, 2000). The Msp1 transmembrane region is indicated with the brace.

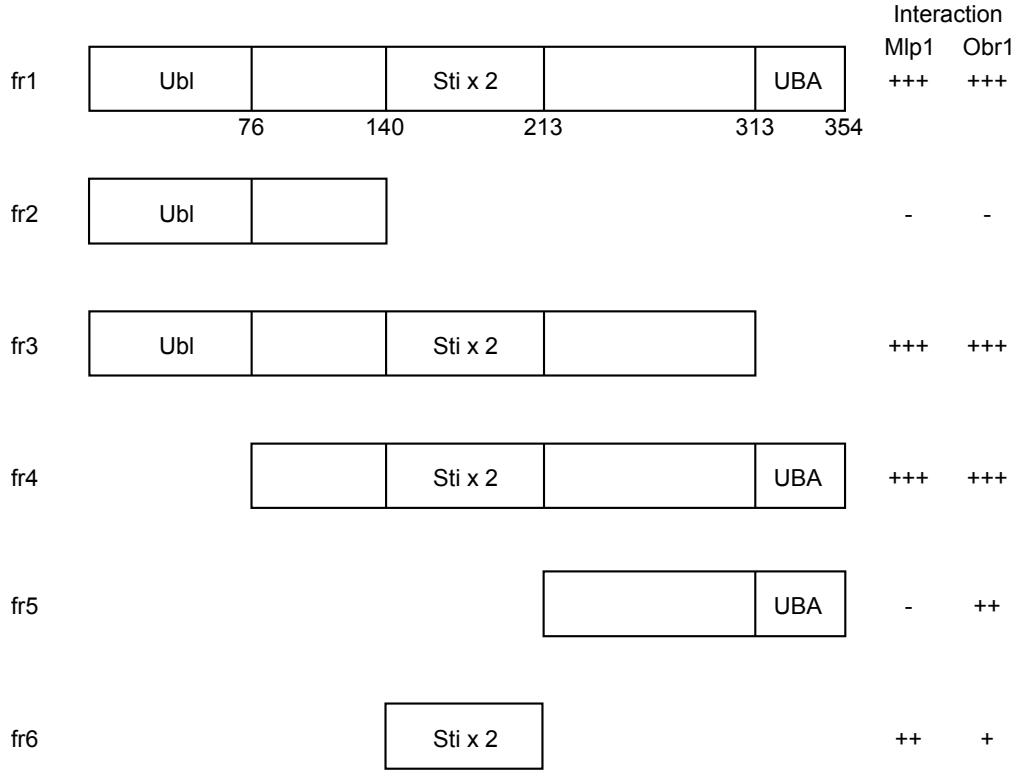

Figure 4.3: A series of Dph1 truncations, labelled fr1 to fr6, were developed to ascertain which domains were necessary for Mlp1 and Obr1 interaction. These truncations were closely based on a similar series of truncations created by Katalin Fullop, as this would allow for direct comparison with other Dph1 expression vectors already available in the lab.

Binding Domain	Activation Domain	-WL	-WHL	-WHLA
pGBT9-dph1-fr1	pACT-mlp1			
pGBT9-dph1-fr2	pACT-mlp1			
pGBT9-dph1-fr3	pACT-mlp1			
pGBT9-dph1-fr4	pACT-mlp1			
pGBT9-dph1-fr5	pACT-mlp1			
pGBT9-dph1-fr6	pACT-mlp1			
pGBT9-dph1-fr1	pACT-obr1			
pGBT9-dph1-fr2	pACT-obr1			
pGBT9-dph1-fr3	pACT-obr1			
pGBT9-dph1-fr4	pACT-obr1			
pGBT9-dph1-fr5	pACT-obr1			
pGBT9-dph1-fr6	pACT-obr1			
pGBT9-dph1-fr1	pACT			
pGBT9-dph1-fr2	pACT			
pGBT9-dph1-fr3	pACT			
pGBT9-dph1-fr4	pACT			
pGBT9-dph1-fr5	pACT			
pGBT9-dph1-fr6	pACT			
pGBT9	pACT			
pAS-SNF1	pACT-SNF4			
pGBT9	pACT-mlp1			
pGBT9	pACT-obr1			

Table 4.3: Domains of Dph1 interactions. *S. cerevisiae* was co-transformed with the binding domain and activation domain plasmids and was spotted onto selective media (Section 2.2.2.2). Column headings indicate the supplements missing from the SD media, tryptophan (W), leucine (L), histidine (H) and adenine (A).

selection as with the full-length protein. This is consistent with the ubiquitin-like nature of the UBL domain, as neither Mlp1 nor Obr1 have domains previously associated with ubiquitin binding activity.

The interaction between Dph1 and Mlp1 can be reconstituted with a truncated construct consisting solely of the Sti1 domains; fr6 interacts with sufficient affinity to allow growth on stringent selection. Furthermore, none of the constructs lacking the Sti1 domain are able to demonstrate any ability to interact with Mlp1. This suggests that the Sti1 domain is solely responsible for coordinating the interaction between Mlp1 and Dph1, and is both necessary and sufficient for this behaviour.

The Dph1 interaction with Obr1 is coordinated through multiple domains. Both fr5 and fr6 are able to interact with Obr1, although neither is sufficient to reconstitute the strength of interaction observed in the full-length protein, and support only minimal growth on stringent selection. This indicates that the Sti1 domains are also involved in the interaction with Obr1, with additional binding occurring through the C-terminal region. It appears that these separate interactions coordinate to result in the full strength binding, as evidenced in the truncation fr4, which supports growth comparable to that of the full-length protein.

4.1.4 Mlp1 Interacts With Dph1 Via Its N-terminus

Following the identification of the importance of the Dph1 Sti1 domains, it was decided to focus further study on the Mlp1 target. Mlp1 contains a single AAA-ATPase domain located in the C-terminal half of the protein. The exact region identified as belonging to the AAA-ATPase domain varies depending on the seed and parameters used (Schultz et al., 1998; Letunic et al., 2006; Finn et al., 2010; Sonnhammer et al., 1997). Truncations were created to isolate the roles of the N and C terminal regions flanking the AAA-ATPase domain, and the AAA-ATPase domain itself as identified by both models (Figure 4.4).

Yeast two-hybrid assays with the truncated Mlp1 constructs are shown in table 4.4. The truncation construct fr2 is able to interact with Dph1 to a similar degree as the full-length protein; none of the truncations lacking this region show the same binding activity. This indicates that the N-terminal region of Mlp1 is able to bind to Dph1, and suggests that it is solely responsible for this activity. Surprisingly, the fr3 construct does not show the same binding activity despite containing the N-terminal domain. This may be a result of structural or stability problems with this particular construct. Together with the results from section 4.1.3 this indicates that the Sti1 domains of

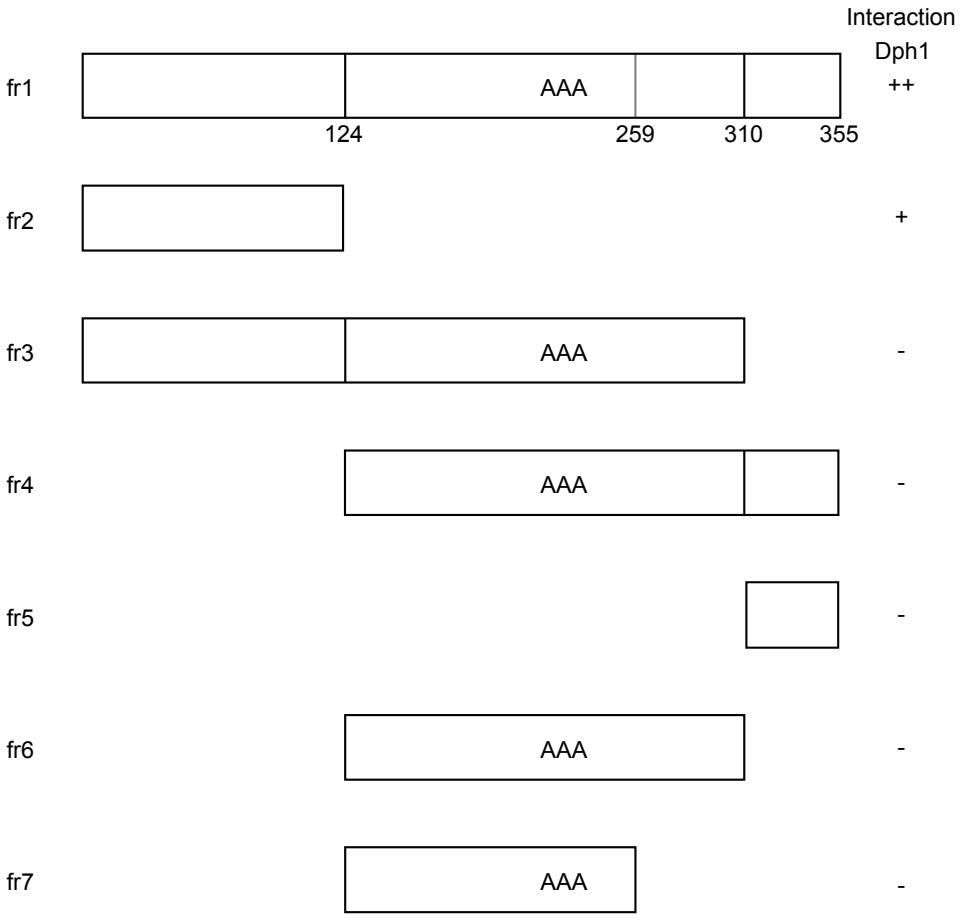

Figure 4.4: A series of Mlp1 truncations, labelled fr1 to fr7, were developed to ascertain which domains were necessary for Dph1 interaction.

Binding Domain	Activation Domain	-WL	-WHL	-WHLA
pGBT9-dph1	pGAD424-mlp1-fr1			
pGBT9	pGAD424-mlp1-fr1			
pGBT9-dph1	pGAD424-mlp1-fr2			
pGBT9	pGAD424-mlp1-fr2			
pGBT9-dph1	pGAD424-mlp1-fr3			
pGBT9	pGAD424-mlp1-fr3			
pGBT9-dph1	pGAD424-mlp1-fr4			
pGBT9	pGAD424-mlp1-fr4			
pGBT9-dph1	pGAD424-mlp1-fr5			
pGBT9	pGAD424-mlp1-fr5			
pGBT9-dph1	pGAD424-mlp1-fr6			
pGBT9	pGAD424-mlp1-fr6			
pGBT9-dph1	pGAD424-mlp1-fr7			
pGBT9	pGAD424-mlp1-fr7			
pGBT9-dph1	pGAD424			
pGBT9	pGAD424			
pAS-SNF4	pACT-SNF1			
none	none			

Table 4.4: Domains of Mlp1 interactions. *S. cerevisiae* was co-transformed with the binding domain and activation domain plasmids and was spotted onto selective media (Section 2.2.2.2). Column headings indicate the supplements missing from the SD media, tryptophan (W), leucine (L), histidine (H) and adenine (A).

Dph1 interact with an unidentified region in the N-terminus of Mlp1.

4.1.5 The Interaction With Mlp1 is Specific to Dph1

The Sti1 domains responsible for the interaction between Dph1 and Mlp1 are not exclusive to Dph1, but are found in a series of different proteins. The SMART database (Schultz et al., 1998; Letunic et al., 2006) identifies three such proteins in *S. pombe*, Dph1, the other shuttle factor Rhp23, and Sti1. An additional protein, Mud1 also contains a Sti1 domain (Chris Ponting, personal communication). Binding to Mlp1 may be a property of either Sti1 domains in general, or of the proteasome shuttle factors. To test this, Mlp1 binding to Rhp23 was assessed (Table 4.5). Neither Rhp23, nor Pus1 were able to interact with Mlp1. This indicates that the interaction is neither a general property of Sti1 domains, nor of shuttle factors, and instead appears to be a specific property of Dph1.

4.1.6 Mlp1 Interacts with a Specific Subset of Cdc48 Co-Factors

Mlp1 shares the AAA-ATPase domain with a large family of proteins, among which is the protein Cdc48, which is discussed in detail in section 1.6. The shared domain between the two proteins, and Mlp1's interaction with the ubiquitin proteasome system, in the form of the shuttle factors, raised the possibility that Mlp1 was acting in a similar manner to Cdc48 (Section 4.3). To help address this, the interaction of Cdc48 with the shuttle factors and the interaction of Mlp1 with a subset of the Cdc48 co-factors was tested (Table 4.5).

Unsurprisingly, Cdc48 did not show any interaction with the shuttle factors. However, Mlp1 did show a specific interaction with two of the Cdc48 cofactors, Ubx1 and Ubx2, with particularly strong affinity for Ubx2. The lack of an interaction with the remaining Ubx proteins indicates that this reaction is unlikely to be through the Ubx domain, and instead is likely to be found in a domain conserved between the two proteins.

4.2 Discussion

The role of the proteasome shuttle factors in the ubiquitin proteasome system has already been studied by several labs, as discussed in section 1.5. Loss of shuttle factors results in the stabilization of a subset of proteasome substrates; for example, substrates of the ERAD pathway are particularly stabilized. These findings suggest that the

Binding Domain	Activation Domain	-WL	-WHL	-WHLA
pGBT9-dph1	pGAD424-mlp1			
pGBT9-mlp1	pACT-rph23			
pGBT9-mlp1	pACT-pus1			
pGBT9-mlp1	pGAD424-cdc48			
pAS-ubx1	pGAD424-mlp1			
pAS-ubx2	pGAD424-mlp1			
pGBT9-ubx3	pGAD424-mlp1			
pGBT9-ubx4	pGAD424-mlp1			
pGBT9-ubx5	pGAD424-mlp1			
pGBT9-dph1	pGAD424-cdc48			
pGBT9-cdc48	pACT-rhp23			
pGBT9-cdc48	pACT-pus1			
pGBT9-mlp1	pGAD424-mlp1			
pGBT9-mlp1	pGAD424			
pGBT9-mlp1	pACT			
pGBT9-cdc48	pGAD424			
pGBT9-cdc48	pACT			
none	none			
pGBT9-ubx3	pGAD424			
pAS-SNF4	pACT-SNF1			

Table 4.5: Interaction of Mlp1 with other proteins. *S. cerevisiae* was co-tranformed with the binding domain and activation domain plasmids and was spotted onto selective media (Section 2.2.2.2). Column headings indicate the supplements missing from the SD media, tryptophan (W), leucine (L), histidine (H) and adenine (A).

shuttle factors provide an explicit link between upstream and downstream elements of protein degradation pathways (Medicherla et al., 2004; Richly et al., 2005). As a result, proteins that interact with the shuttle factors are implicated in this pathway. While the UBA domain is responsible for binding substrates of the ubiquitin proteasome system, proteins which interact with regions outside this domain will be more likely to play an active role in the ubiquitin proteasome system.

4.2.1 Interactors

4.2.1.1 SPAPB24D3.07c

Of the four candidates successfully retested, SPAPB24D3.07c provided the least insight into its function. The gene is predicted to encode an uncharacterised ER localised protein, and shows no obvious homology with proteins of other species (Hertz-Fowler et al., 2004). The lack of orthologs in other species, and the viability of the knockout strain (Kim et al., 2010) strongly suggest that the protein is unlikely to play a central role in the regulation of protein degradation. Furthermore, given its predicted localisation in the ER lumen, an interaction with the cytosolic Dph1 protein is surprising, and possibly indicates a non-specific interaction. Further study of this potential interaction would require confirmation of predicted sub-cellular localization and *in vivo* confirmation of the interaction.

4.2.1.2 Arp3

The interaction between Dph1 and Arp3 provides an intriguing link with the actin cytoskeleton, although the nature of this link is yet to be determined. Arp3 is an essential gene (McCollum et al., 1996; Kim et al., 2010) which encodes an actin-like protein. It is part of a multi-protein complex involved in the regulation of actin polymerisation (McCollum et al., 1996; Pelham and Chang, 2002). At the current time, it is not possible to tell if Dph1 is involved in regulating actin behaviour, or if interaction with the actin cytoskeleton aids or regulates Dph1 activity. Recent work on Dph1 has suggested that interaction with the actin cytoskeleton via myosin V, is important for its delivery of some substrates to the proteasome (Martín-García and Mulvihill, 2009). Unpublished work conducted in the lab by Ingo Amn, revealed a genetic interaction between *pus1* and the myosin type V genes *myo51* and *myo52*. Δ*myo51* Δ*myo52* strains showed a markedly reduced growth rate in a Δ*pus1* background, but not in wild-type or Δ*dph1* strains. This evidence provides another link between the actin

cytoskeleton and the ubiquitin proteasome system, and suggests that Pus1 provides an alternative redundant pathway that is able to compensate for the loss of the myosin V proteins. The lack of a similar phenotype between Δ*dph1* and Δ*myo51* Δ*myo52* is consistent with them acting in the same pathway.

4.2.1.3 Obr1

Obr1/Uhp1 has already been identified in association with the ubiquitin proteasome system, in that the protein undergoes regulated ubiquitination by Rhp6, a process essential for the regulation of mating-type silencing in *S. pombe* (Naresh et al., 2003). It is thought that Obr1 may help set up a meta-stable chromatin state during S-phase to help promote mating type switching.

The interaction of Dph1 with a proteasome substrate is unsurprising. However, Dph1 retains its Obr1 binding activity even in the absence of the UBA domain, indicating that binding is not solely a result of and interaction between conjugated ubiquitin and the UBA domain. Instead, Dph1 appears to contain two regions exhibiting Obr1 binding activity: the Sti1 domains, and a further site in the C-terminal portion of the protein, containing the UBA domain. A comparisons of the strength of interaction between full-length and truncated constructs suggests that the two domains co-operated to ensure maximum affinity. Furthermore, as this full strength binding can be recapitulated with the construct lacking the UBA domain, it suggests that the C-terminal site of interaction is likely to be in the undefined C-terminal region, rather than the UBA domain. Further study will be required to help localise the binding sites more precisely; a series of smaller deletions, followed by targeted mutagenesis would be helpful in achieving this.

The identification of Obr1 binding activity independent of the UBA domain, suggests that Dph1 may play a more complicated role than simply delivering ubiquitinated Obr1 to the proteasome. The behaviour of Obr1 has been shown to be tightly regulated in a cell cycle dependent manner (Naresh et al., 2003) and an association of Dph1 with the locus in a ubiquitin independent manner may be necessary for priming for a rapid response on ubiquitination. Alternatively, Obr1 may help recruit Dph1 to mating-cassettes to promote its activity on other components of the chromatin structure. Identifying genetic interactions between *dph1*, *obr1* and *rhp6* will be informative in identifying how the proteins cooperate, as will studying the effect the loss of Dph1 has on Obr1 stability and mating type switching. In particular, it will useful to repeat the experiments of Naresh et al. (2003) in a Δ*dph1* strain, to see if it reproduces the

switching dependent loss of mating cassette silencing seen in the Δ*obr1* and *rhp6*$^{-}$ strains; this will indicate that Dph1 acts in the same pathway as Obr1/Uhp1.

4.2.1.4 Mlp1

Mlp1 is a putative mitochondrially localised AAA-ATPase, homologous to the *S. cerevisiae* protein, Msp1. The role of Msp1 within *S. cerevisiae* is still largely uncharacterised, and its *S. pombe* homologue remains almost entirely unresearched. As a result, the reason for its interaction with the Dph1 shuttle factor is not readily apparent. However, the information that is available raises an interesting possibility.

While the mitochondria appear to have their own constitutive protease systems (Section 1.7.1), some experiments have also identified the possibility of ubiquitin mediated proteolysis of mitochondrial proteins by the proteasome (Section 1.7.2). As the proteasome is located in the cytosol, this process would require the existence of a pathway for the extraction of mitochondrial proteins to the cytosol, analogous to the ERAD pathway in the endoplasmic reticulum (Section 1.6.4.5).

Msp1 is located in the outer mitochondrial membrane, and over expression is sufficient to result in the mis-localization of mitochondrial outer membrane proteins (Nakai et al., 1993; Schnall et al., 1994). While the *S. pombe* homologue shows poor sequence conservation in the transmembrane region (Figure 4.2) it does contain a region characteristic of a short transmembrane helix (Figure 4.5), suggesting that the membrane localization is likely to be conserved. Similarly, high throughput localization screens suggest that Mlp1 retains the mitochondrial localization of its *S. cerevisiae* ortholog (Matsuyama et al., 2006). Furthermore, the AAA-ATPase domain of Mlp1 places it in the same family as the protein Cdc48, which is involved in, amongst other processes, the extraction of proteins from the endoplasmic reticulum as part of the ERAD pathway. Protein unfolding and structural remodelling is a common trait of AAA-ATPase containing proteins (section 1.6.2). This raises the possibility that Mlp1 may be performing a similar function, such as catalysing protein unfolding to aid membrane extraction or translocation. Taken together, these factors suggest a possible role of Mlp1 in the removal of ubiquitinated proteins from the mitochondria, and their transfer to the proteasome via the Dph1 shuttle factor.

In the scenario described above, the association of Dph1 with Mlp1 would help couple proteasome delivery to mitochondrial extraction, and would prevent the accumulation of ubiquitinated proteins, either on the surface of the mitochondrial outer membrane, or in the surrounding cytosol.

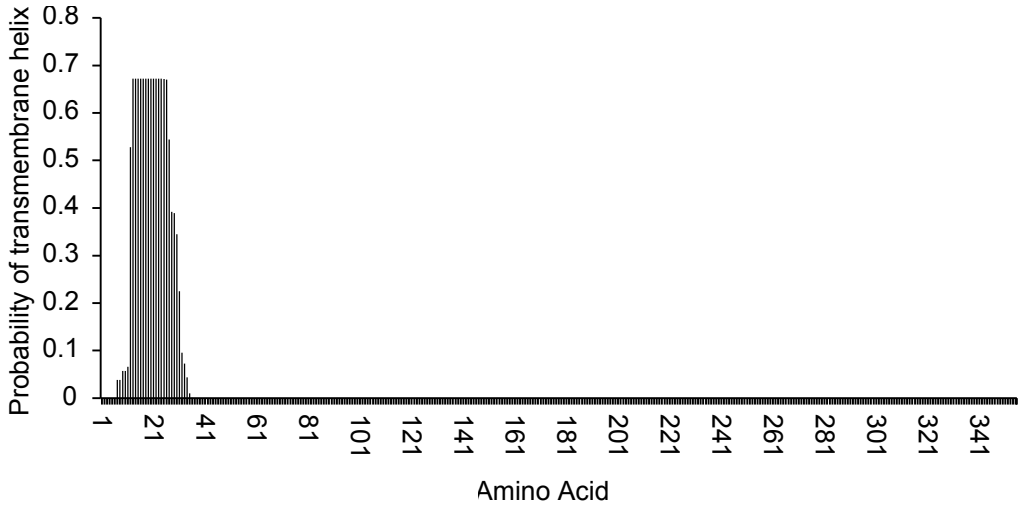

Figure 4.5: Probability of transmembrane helices across the length of the protein Mlp1. (Sonnhammer et al., 1998; Krogh et al., 2001)

4.2.2 The Sti1 Domain

Previously, Sti1 domains have only been demonstrated to be important for interaction with both Hsp70 and Hsp90 family proteins (Chang and Lindquist, 1994; Lässle et al., 1997). The novel interaction shown here with both Mlp1 and Obr1 is surprising, and indicates that the Sti1 domains of Dph1 at least, may be responsible for coordinating the interaction with a wider range of proteins. By contrast Rhp23, another Sti1 domain containing protein, was unable to demonstrate interaction with Mlp1, indicating that the property is specific to Dph1. The potential for the Sti1 domains to act as widespread means of shuttle factor recruitment is worthy of further investigation, and differences in binding affinity of the Dph1 and Rhp23 domains may be at least partly responsible for determining their specificities.

4.2.3 Mlp1 and Ubx proteins

A further link between Mlp1 and the ubiquitin proteasome system, was its association with the Cdc48 co-factors spUbx1 and spUbx2; the remaining Ubx proteins did not show the same interaction. Comparison of the binding and non-binding co-factors (Bioinformatics support provided by Philippe Gautier) identifies the thioredoxin like UAS domain – found in Ubx1 and Ubx2, but not the non-binding Ubx proteins – as a potential domain of interaction (Sonnhammer et al., 1997; Finn et al., 2010; Schultz et al., 1998; Letunic et al., 2009; Hulo et al., 2006; Murzin et al., 1995). Attempts to identify conserved motifs outside of the UAS domain failed to identify any conserved

motifs of significance (data not shown).

SpUbx1 shows close homology to both scUbx3 and scUbx2 (Figure 1.2), notably sharing the endoplasmic reticulum localization of the latter (Matsuyama et al., 2006). Interestingly, scUbx2 has been shown to have a role in ERAD, in which it appears to recruit Cdc48 to the ER membrane (Schuberth and Buchberger, 2005; Neuber et al., 2005; Wilson et al., 2006); it has yet to be shown whether spUbx1 acts in a similar manner. As spUbx1 appears to be localised to the endoplasmic reticulum its association with the mitochondrial Mlp1 is unlikely to be recapitulated *in vivo*. Instead, the interaction seen in the yeast two-hybrid assay is possibly an artifact. If the interaction between Mlp1 and spUbx2 is coordinated through the UAS domain, then the presence of a UAS domain in spUbx1 may be sufficient to allow non-specific binding in the yeast-two hybrid assay. In support of this possibility, Mlp1 interacts more strongly with spUbx2 than with spUbx1 in the yeast two-hybrid assays.

By contrast, spUbx2 shows widespread localisation throughout the nucleus and cytoplasm (Matsuyama et al., 2006). As with spUbx1, in addition to its central UAS domain, and C-terminal UBX domain, spUbx2 also includes an N-terminal UBA. Additional ubiquitin binding activity was also found to localise to a UIM domain, located between the UAS and UBX (Hartmann-Petersen et al., 2004); spUbx2 lacks the transmembrane domain present in spUbx1. It is tempting to speculate that spUbx2 acts to recruit Cdc48 to Mlp1 at the mitochondrial membrane, performing a similar function to scUbx2 at the endoplasmic reticulum. Though no association of Mlp1 with Cdc48 could be detected in the yeast two-hybrid assay; as this interaction will likely be dependent on the presence of the correct co-factors this is unsurprising. A further possibility is that spUbx2 is acting in a Cdc48 independent manner, and that it is being recruited to Mlp1 to act as a co-factor; this would be the first case of Cdc48 co-factors being able to assist the function of other AAA-ATPases. However, as Mlp1 binding activity is restricted to spUbx1 and spUbx2, and it shows no apparent homology with the N-terminus of Cdc48, it is unlikely that the mechanism of co-factor recruitment would be conserved between Mlp1 and Cdc48 (With thanks to Philippe Gautier for bioinformatics assistance).

The interaction between Mlp1 and the two Ubx proteins is an attractive target for further study. Immediate work should focus on confirming the domains of interaction, particularly with respect to the UAS domain shared between the two positive interactors. It will also be important to determine the involvement of Cdc48 in the interaction. Immunoprecipitation or *in vivo* pulldowns of Mlp1 could be used to identify which elements are present in the complex.

4.3 Summary

The Sti1 domains of Dph1 have been identified as having a novel interaction with the proteins Obr1 and Mlp1, a homologue of the *S. cerevisiae* Msp1. The interaction with Mlp1 occurs via its N-terminal region and is specific to Dph1, rather than a general property of Sti1 domains. Homology between Mlp1 and the *S. cerevisiae* protein Msp1, as well as its association with the shuttle factors of the ubiquitin proteasome system, lead to the idea that the protein may be involved in a mitochondrial associated degradation pathway, analogous to the ERAD pathway.

Chapter 5

Further Investigation of Mlp1-Dph1 Interaction

The results of the yeast-two hybrid experiment provided an interesting link between the proteasome shuttle factors and the mitochondrial protein Mlp1. In pursuing this further, it will be important to identify further lines of evidence which help confirm that this interaction is biologically relevant. Consideration will also be given to the functional importance of such an interaction, particularly with respect to stabilization of mitochondrial ubiquitin conjugates, and possible defects in mitochondrial morphology.

5.1 Interaction of Recombinant Protein

5.1.1 Recombinant Constructs Were Successfully Induced in Bacteria

Recombinant expression of proteins in bacteria can be used as another means of identifying protein interactions. The addition of tags to the N or C terminus of a protein can provide a residue for interaction with a column or antibody, allowing one to conduct a pulldown assay (Summarised in figure 5.1).

Previous work in the lab had created plasmids for expressing recombinant Dph1, tagged with either 6×Histidine or GST. To complement these constructs, Mlp1 was sub-cloned into pGEX-KG and pQE32, GST and 6×Histidine tagged expression vectors respectively. Plasmids were transformed into an appropriate expression strain (Section 2.8.1) and a range of induction conditions were tested. Due to difficulties in inducing expression from the pQE32-Mlp1 vector (results not shown), pGexKG-Mlp1 and pQE32-Dph1 were used as the basis of the assay. In addition, a vector expressing a

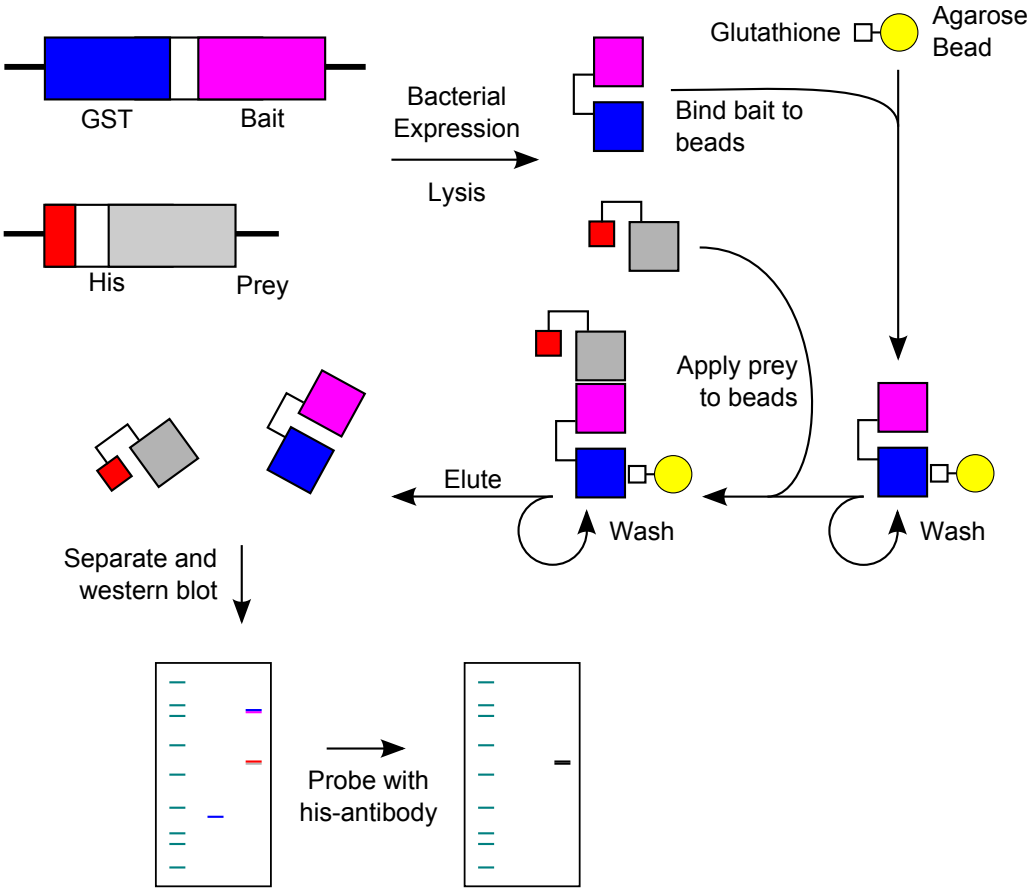

Figure 5.1: Bait and prey are expressed in *E. coli* as recombinant proteins fused to GST and 6×Histidine tags respectively. The bait protein is bound to glutathione-agarose beads via the interaction between glutathione and the GST tag, excess protein is removed by washing. Bacterial extract containing the 6×Histidine fused prey is applied to the column. The prey is retained in the event of the two proteins interacting. Non-binding proteins are washed off, and the remaining proteins are eluted, separated by SDS-PAGE and subject to western blotting. Antibodies against the 6×Histidine tag are used to probe the blot and detect any bound prey protein.

GST tagged form of Pus1 was used as a positive control for detecting Dph1 interaction, GST was induced from empty pGex-KG vector to act as a negative control. No positive control was available for Mlp1. Figure 5.2 shows the results of a range of induction conditions used to optimise expression of each construct. All constructs could be induced to produce a strong band of the expected size. Pus1-GST, Mlp1-GST and GST alone were all induced for 3 hours at 25 ℃; Dph1-His only showed faint induction at 25 ℃, but could be induced efficiently at 36 ℃ for 3 hours.

5.1.2 GST Pulldown Assays

Bait proteins Mlp1-GST or GST alone were bound to glutathione-agarose beads and binding was confirmed by SDS-PAGE (Figure 5.3). Bacterial lysates containing either induced Dph1-His or His were applied to the beads and were incubated to allow binding. Unbound proteins were removed by washing, and the remaining proteins were eluted by boiling in SDS-PAGE buffer. Proteins were separated by SDS-PAGE and were visualized by western blotting and probing with 6×Histidine antibodies (Figure 5.4). Dph1-His was confirmed to interact with Pus1-GST as expected, however it was not possible to reconstitute the interaction between Dph1 and Mlp1 seen in the yeast-two hybrid experiments.

5.2 Dph1 is Localized to Mitochondrial Fractions in an Mlp1 Independent Manner

To provide another avenue of evidence for a mitochondrial role for Dph1, mitochondrial purifications were tested for the presence of the protein. Both wild-type and Δ*mlp1* strains were studied to try and deduce the role Mlp1 might play in localizing Dph1 to the mitochondria. Δ*mlp1* strains were obtained from Bioneer (Daejeon, Korea) as heterozygous knockouts. Meiosis was induced (Section 2.4.3) and the G418 marker was confirmed to segregate 2:2 (data not shown); the knockout of *mlp1* was confirmed by PCR (data not shown). The successful isolation of a Δ*mlp1* strain indicated that it was non-essential.

Mitochondrial fractions were prepared and the proteins were separated by SDS-PAGE on a 10% gel. Samples were taken during the fractionation process to help monitor its progress. The levels of Dph1 protein in each sample were judged by western blotting; actin and Hsp60 antibodies were used to probe for cytoplasmic contamination and mitochondrial enrichment respectively (Figure 5.5).

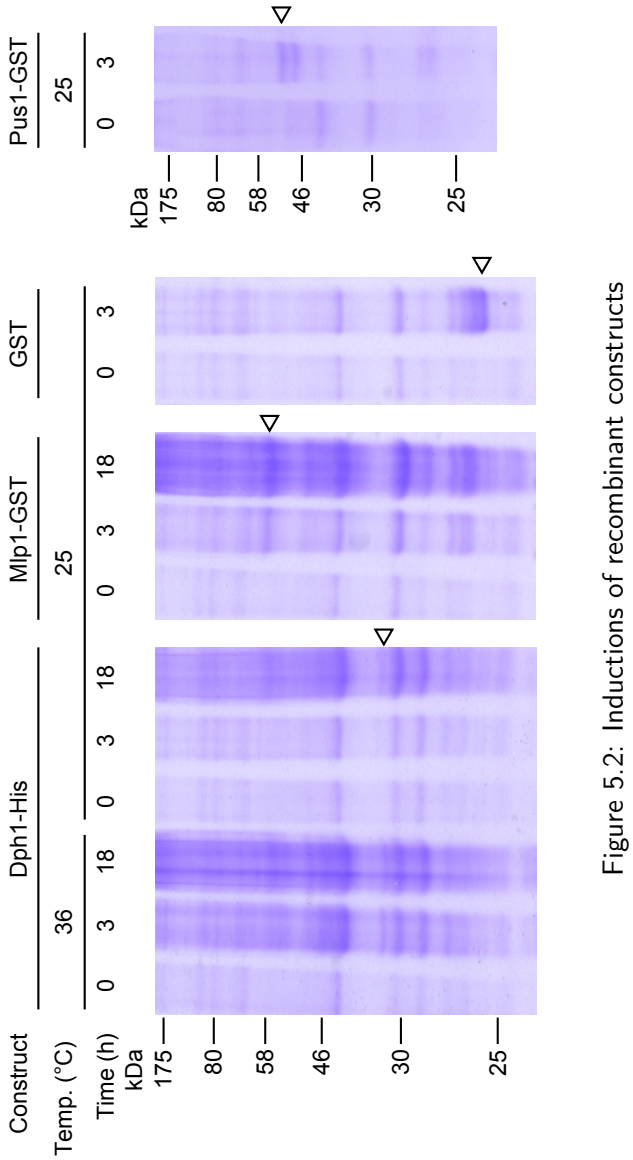

Figure 5.2: Inductions of recombinant constructs

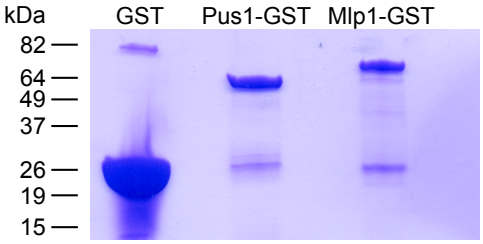

Figure 5.3: 5 µl prepared glutathione-agarose beads were boiled in SDS-PAGE loading buffer and were loaded onto a 10% SDS-PAGE gel and proteins were separated by electrophoresis. Gels were stained with commassie. All three columns contain a substantial band of the expected size, indicating that the bait proteins have correctly bound to the beads.

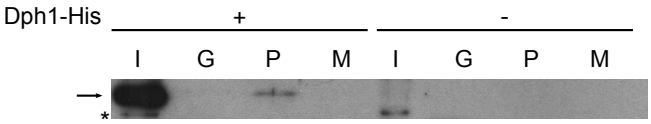

Figure 5.4: Protein lysates from bacteria expressing Dph1-His or His alone were applied to columns bound with (G) GST, (P) Pus1-GST and (M) Mlp1-GST. The bound proteins were eluted from the beads, separated by SDS-PAGE and visualised by western blotting and probing with 6×Histidine antibodies. The input lane (I) represents 1:250 of the total protein applied to the column. Dph1-His is indicated by the arrow, the asterisk indicates non-specific antibody binding. Dph1-His bound exclusively to Pus1-GST; no binding to Mlp1-GST was detectable.

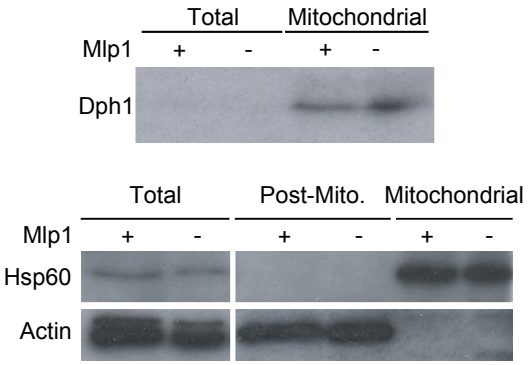

Figure 5.5: Mitochondrial purifications were made from both wild-type and Δ*mlp1 S. pombe*. Protein concentrations were measured and equal amounts were loaded in each lane. Total and post-mitochondria samples indicate fractions taken at various stages of the purification process. Protein samples were boiled in SDS-Page buffer for five minutes and were separated on a 10% polyacrylamide gel. Blots were probed with the indicated antibody. Actin and Hsp60 represent cytoplasmic and mitochondrial markers respectively. Specificity of the Dph1 antibody is illustrated in figure B.9 in appendix B.

Mitochondrial fractions were strongly enriched in Hsp60, and drastically depleted for actin, indicating that the purification process had been highly efficient. Dph1 was detected in both wild-type and Δ*mlp1* mitochondrial fractions, indicating that it is localized to the mitochondria in an Mlp1 independent manner. Dph1 was apparent in the total fraction on longer exposures (data not shown).

5.3 Mitochondrial Ubiquitin Levels Are Not Affected By the Loss of Mlp1

If Mlp1 is acting in a mitochondrial analogue of the ERAD pathway one would expect that cells lacking Mlp1 would show a corresponding defect in the degradation of mitochondrial associated ubiquitinated proteins. To begin to address this possibility, mitochondrial purifications were prepared from *S. pombe* and were subject to analysis by western blotting (Figure 5.6). Ubiquitin is clearly present in both mitochondrial and total fractions (Figure 5.6, upper gel), and the massive enrichment of Hsp60, and depletion of actin, suggest that this is unlikely to be a result of cytoplasmic contamination (Figure 5.6, lower gels). The loss of Mlp1 alone does not result in a gross increase in the levels of mitochondrial ubiquitin, as the level of ubiquitinated proteins appears to be consistent between the wild-type and Δ*mlp1* preparations.

5.4 Fluorescence Microscopy

5.4.1 Mlp1 is Mitochondrially Localized

The *S. cerevisiae* homolog of Mlp1, Msp1p, is mitochondrially localized (Nakai et al., 1993), and over-expression of a GFP tagged form of Mlp1 suggest that the same is true in *S. pombe* (Matsuyama et al., 2006). To confirm this, and to aid with further localization experiments, it was decided to tag the C-terminus of Mlp1 with GFP under its native promoter.

A GFP cassette was integrated at the C-terminus of Mlp1 (Figure 5.7) and correct integration was confirmed by PCR and tetrad analysis (Data not shown). Subsequently, the *mlp1-GFP:G418* strain was also crossed to *dph1-tomato:G418* (Martín-García and Mulvihill, 2009), a strain bearing *dph1* endogenously tagged with a red GFP variant.

Mlp1-GFP cells were grown and mitochondria were stained with mitotracker-red, a mitochondrial marker. Live cells were embedded in agarose and were visualised by

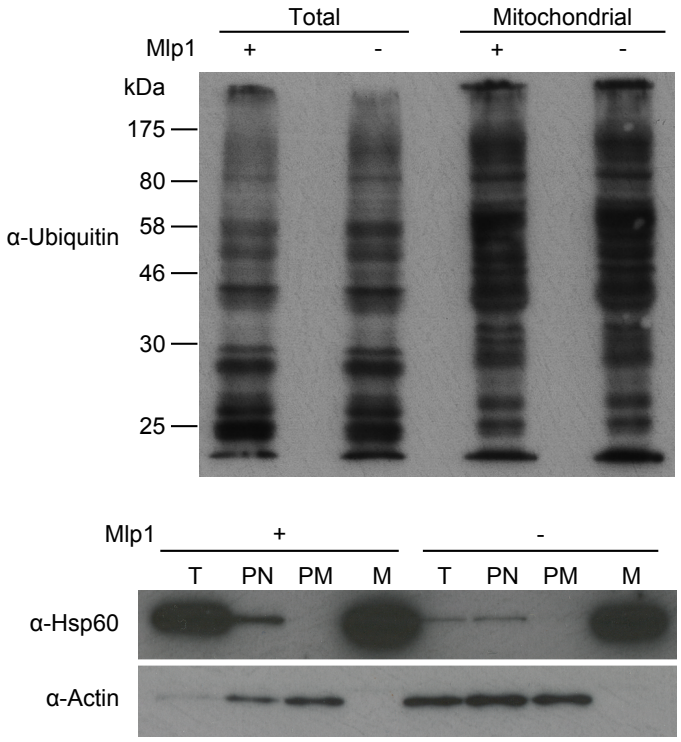

Figure 5.6: Mitochondrial purifications were made from both wild-type and Δ*mlp1 S. pombe*. (T) Total, (PN) post-nuclear, and (PM) post-mitochondria samples indicate fractions taken at various stages of the purification process. Protein samples were boiled in SDS-Page buffer for five minutes and were separated on a 10% polyacrylamide gel. Blots were probed with the indicated antibody. Actin and Hsp60 represent cytoplasmic and mitochondrial markers respectively.

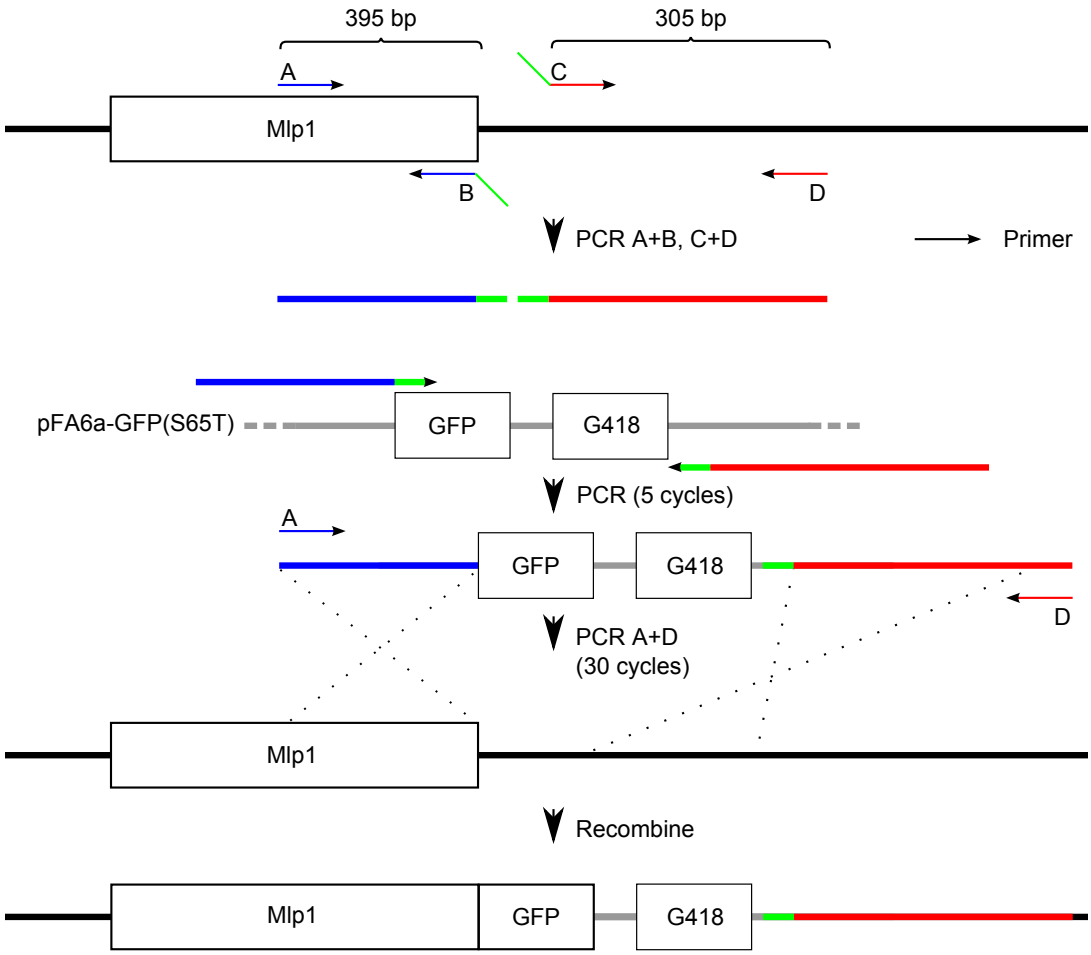

Figure 5.7: Diagram showing the procedure for tagging native Mlp1. The process was heavily modified from that indicated by Bähler et al. (1998) to increase the size of the homology arms. The adapted process also requires shorter oligonucleotide primers. The adapted method was inspired by the Gregan et al. (2006) knockout protocol, and used PCR conditions used in similar protocol by Noguchi (2006). Homology arms are generated by two PCR reactions using the oligonucleotides (A) Mlp1_AF_B and(B)Mlp1_AR_B, and (C)Mlp1_BF_B and (D)Mlp1_BR_B. Subsequently the two arms are purified and are used in five rounds of PCR to produce a cassette flanked with the homology arms, which is then amplified with the outermost oligonucleotides. The linear product is transformed into *S. pombe* and colonies are selected for G418 resistance.

fluorescent microscopy (Figure 5.8). Due to the low intensity of GFP fluorescence compared to the mitochondrial markers, emission filters were used to filter out emission from the mitochondrial stain when visualising GFP localization. Strains negative for Mlp1-GFP were used to confirm that the observed light was due to excitation of GFP (Data not shown). Mlp1-GFP showed strong co-localization with mitotracker-red, indicating that it is mitochondrially localized. Thus Mlp1 shows the same pattern of localization as its *S. cerevisiae* homolog.

Following the confirmation of the Mlp1 mitochondrial localization, an attempt was made to establish co-localization of Mlp1 and Dph1 to the mitochondria. Yeast containing tagged forms of both Mlp1 and Dph1 were visualised by fluorescence microscopy (Figure 5.9). Dph1 appears to show diffuse localization throughout the cell, including enrichment within the nucleus and at the septum. No enrichment was visible at the mitochondria, but neither was Dph1 excluded from regions of Mlp1 localization. Attempts were made to improve the resolution through deconvolution, however both signals were too faint to make this effective.

5.5 $\triangle$*mlp1* Strains Show No Defect in Mitochondrial Morphology

If Mlp1 and Dph1 have a functional role at the mitochondria, phenotypes resulting from their removal may be visible as defects in mitochondrial morphology. This is especially true if the protein has a role in degrading mitochondrial fission or fusion regulatory proteins, such as Fzo1 (Section 6.3.1). To address this possibility, the mitochondrial morphology in strains mutant for both *mlp1* and *dph1* were studied.

Live *S. pombe* were stained with the mitochondrial stain MitoTracker Red and were visualized by fluorescence microscopy. Stacks of images were deconvoluted to improve the image resolution and thus better distinguish mitochondrial structure. Figures 5.10 and 5.11 show images of the mitochondria in wild-type, Δ*mlp1* and Δ*dph1* genetic backgrounds.

A comparison of the images reveals that a range of morphologies exist within each strain. None of the strains showed a single consistent phenotype, and observations while producing the de-convoluted images suggested that the range of phenotypes was comparable for each strain (Data not shown). To gain a better perspective on how the distribution of phenotypes varies between the mutants, the mitochondrial morphologies were organized into categories which could be used to classify the phenotype of an

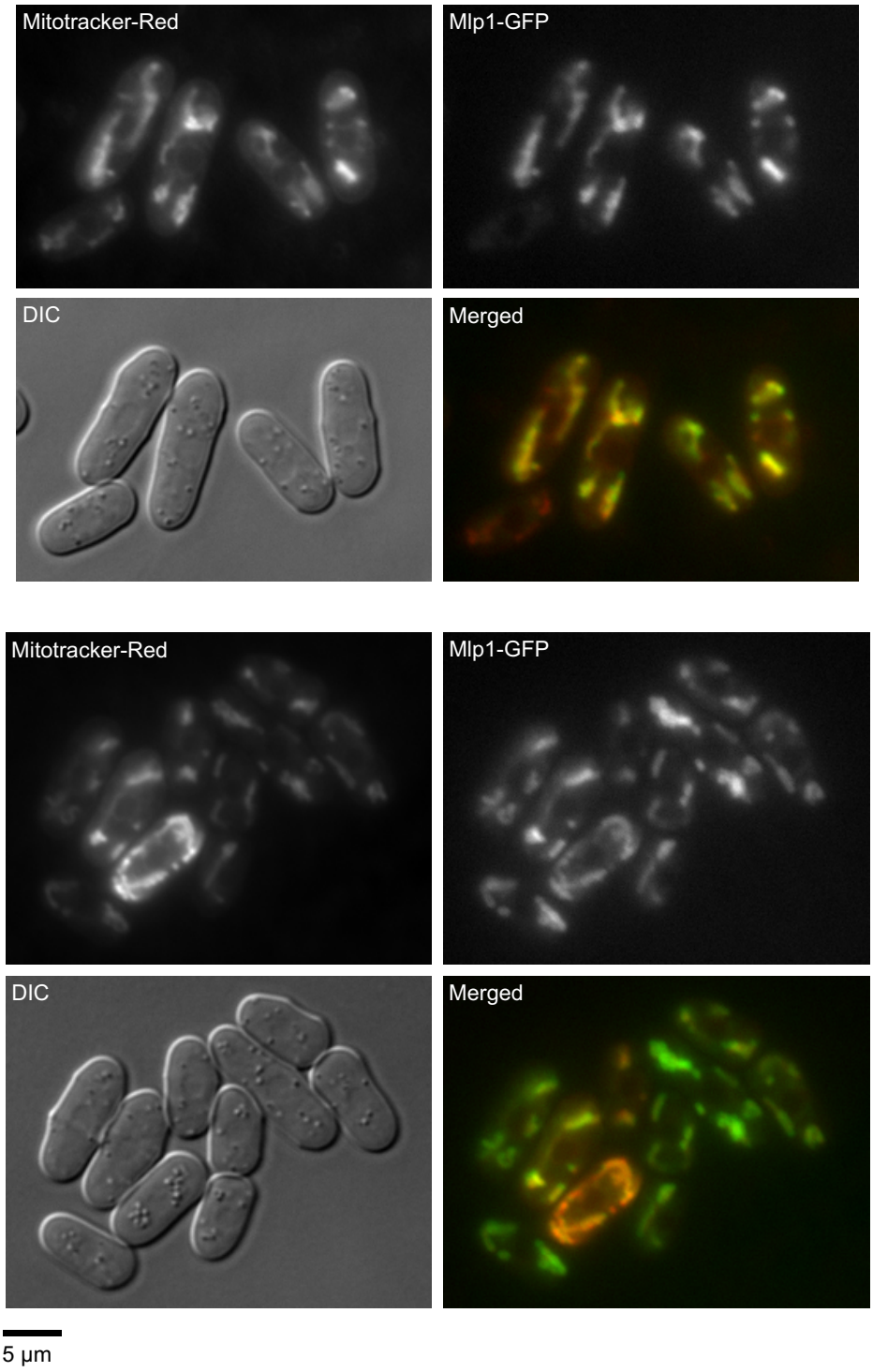

Figure 5.8: Two sets of representative images showing Mlp1 localization to the mitochondrial. Mlp1 is shown as an endogenously expressed form tagged with a C-terminal GFP. Mitochondria are stained with mitotracker-red. DIC is used to show the overall cell morphology.

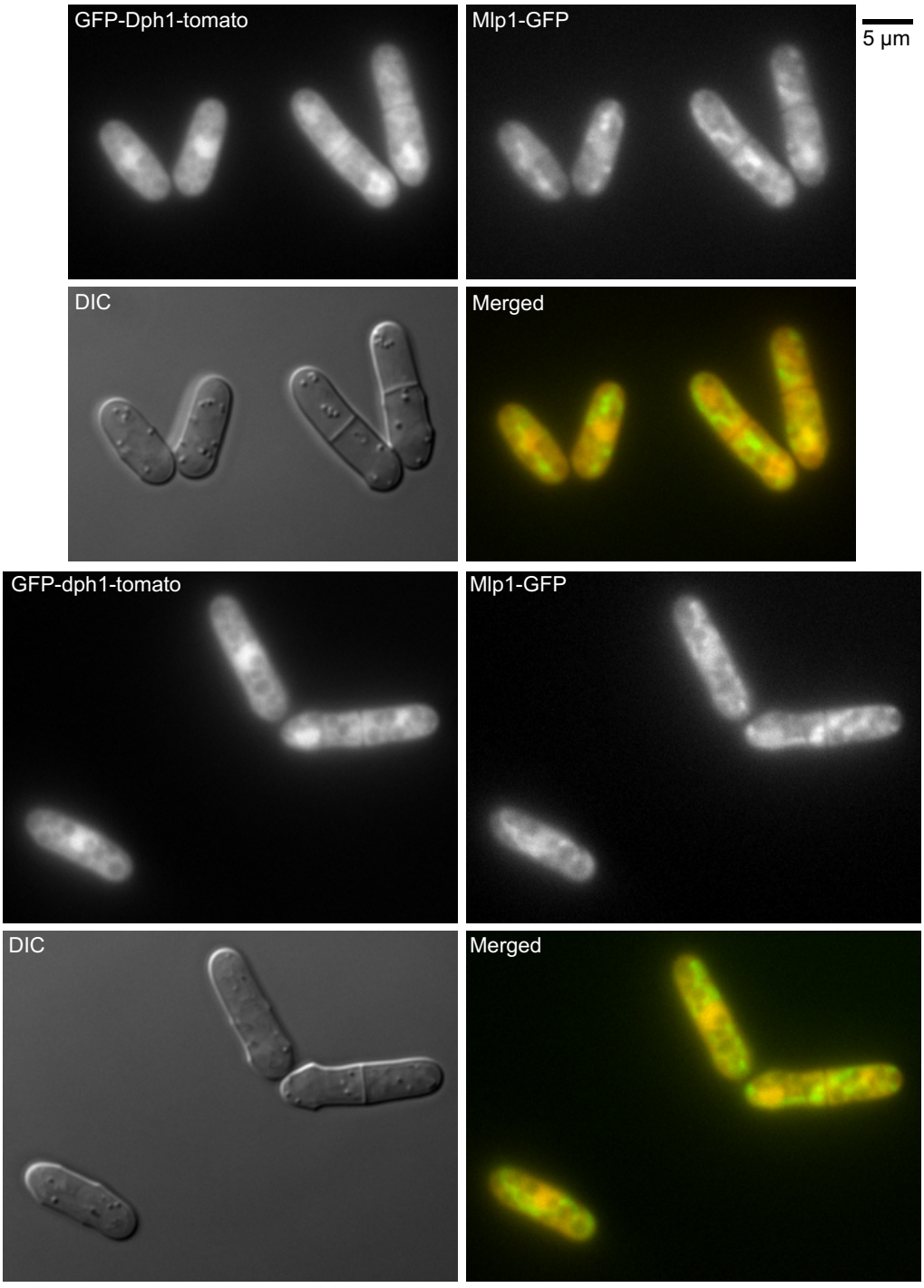

Figure 5.9: Two sets of representative images showing Mlp1 and Dph1 localization. Mlp1 is shown as an endogenously expressed form tagged with a C-terminal GFP. Dph1 is shown as an endogenously expressed form tagged with a GFP tomato variant. DIC is used to show the overall cell morphology.

individual cell. Categories were based on those used in Pevala et al. (2007). As categorisation of morphologies is subjective, strains were classified blind to avoid biasing the results. A minimum of 100 cells were selected for each strain and selections were performed randomly.

The results of the morphology classification are shown in table 5.1 and are represented graphically in figure 5.12. The loss of Dph1 results in a slight increase in the proportion of cells showing a condensed phenotype when compared to wild-type. Conversely, the distribution of mitochondrial morphologies observed for the Δ*mlp1* strain approximate those seen for the wild-type strain, indicating that the loss of Mlp1 has no appreciable effect on mitochondrial morphology.

5.6 Discussion

5.6.1 Protein Interactions

Further support for a role of Dph1 at the mitochondria is provided by the mitochondrial purifications, which find a substantial proportion of Dph1 localised to mitochondrial enriched fractions. Of note is that this localization is not Mlp1 dependent, indicating that other factors may help localize Dph1 to the mitochondria.

It is unfortunate that it was not possible to re-constitute the interaction between Mlp1 and Dph1 with recombinant proteins, as this would provide an additional line of evidence for the interaction demonstrated in the yeast two-hybrid assays. However, the failure to demonstrate an interaction does not indicate that no interaction exists. A major issue with the recombinant interaction experiments is the lack of a suitable positive control for Mlp1 interaction. Although Mlp1 induction can be detected, and the protein clearly binds to the GST beads, the correct folding of the remainder of the protein has not been determined. Folding is likely to be a particular issue for Mlp1, as it possesses a hydrophobic transmembrane domain, which may cause issues when expressed in prokaryotes.

Additional problems are imposed if interaction with Mlp1 is dependent on post-translational modification, or on the presence of other elements of a protein complex. Both Mlp1 and Dph1 have homologs in *S. cerevisiae*, suggesting that there may also be sufficient conservation of other required elements. Additionally, particularly weak or transient interactions may be difficult to detect by this method.

An alternative route to confirming the interaction is adopting a more *in vivo* approach.

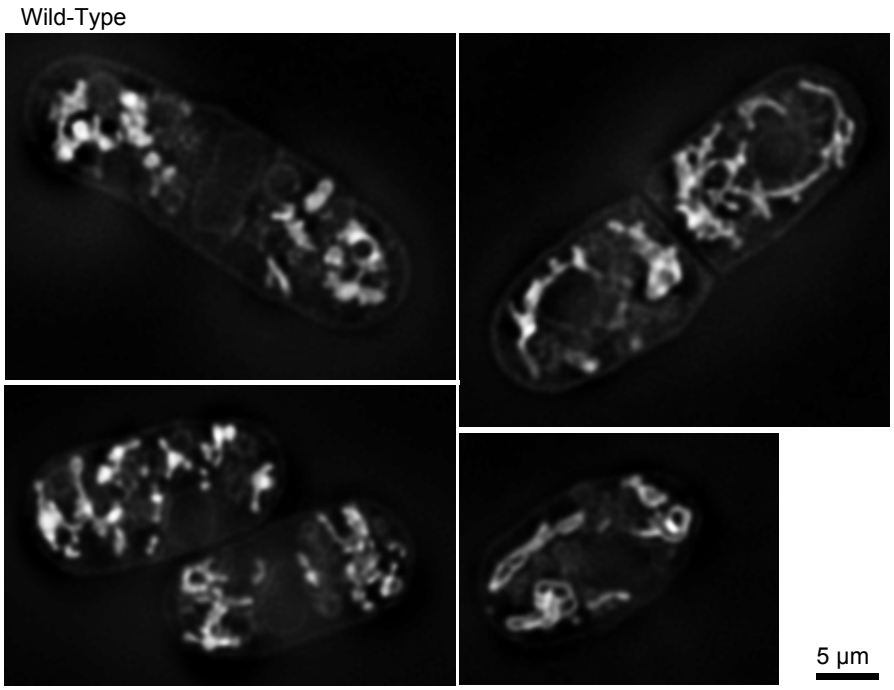

Figure 5.10: Wild-type *S. pombe* stained with MitoTracker Red to highlight mitochondrial morphology. Image resolution was improved by deconvolution.

	Mitochondrial Morphology			
	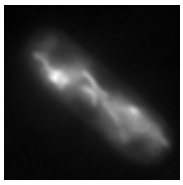	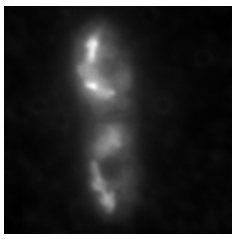	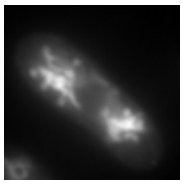	
Strain	Normal	Condensed	Fragmented	Dead
Wild-Type	66.67%	27.96%	1.08%	4.30%
Δ*mlp1*	64.81%	24.07%	2.78%	8.33%
Δ*dph1*	47.66%	42.06%	2.80%	7.48%

Table 5.1: Mitochondrial morphologies were divided into three distinct phenotypes with representative samples shown in the table. For each strain the mitochondrial morphology of a minimum of 100 cells was categorised, and the percentage distribution was calculated and is shown below. A graphical representation of the same data is shown in figure 5.12.

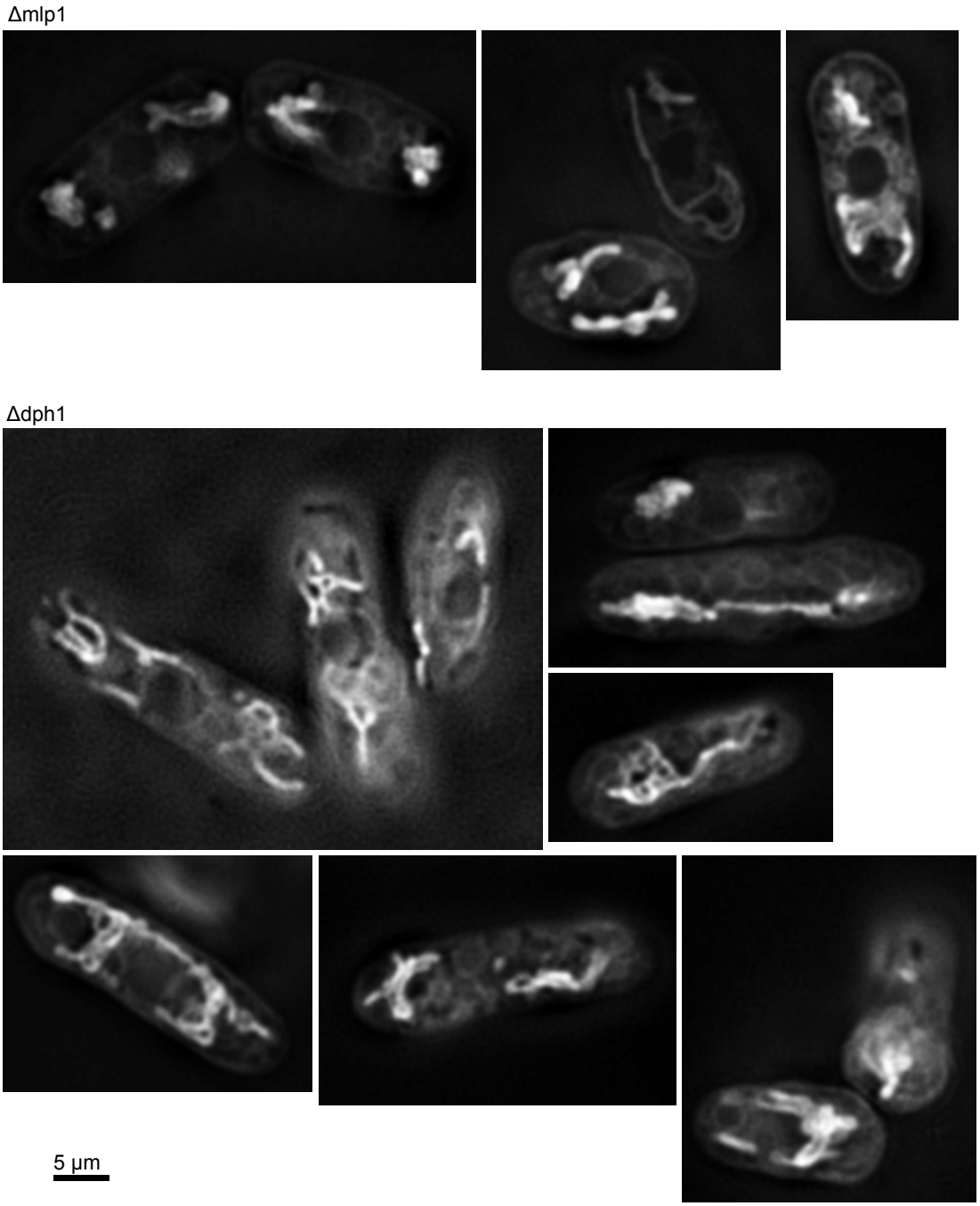

Figure 5.11: Δ*mlp1* and Δ*dph1 S. pombe* stained with MitoTracker Red to highlight mitochondrial morphology. Image resolution was improved by deconvolution.

Immunoprecipitation of Dph1 or Mlp1 from *S. pombe* extract may be more successful at identifying interactions, especially if they are dependent on the presence of other factors. As an additional benefit, this approach could also be used to study the involvement of Cdc48, as implied by the interaction of Ubx1 and Ubx2 in the yeast two-hybrid experiments. Preliminary experiments (Section B.4) suggest that this result may be complicated by the membrane associated nature of Mlp1, and early results were inconclusive. Other approaches include the use of fluorescence resonance energy transfer (FRET) which uses transfer of excitation energy between fluorophores in close proximity, to detect association between two proteins *in vivo*.

Observation of Dph1 localization via its fluorescent tag, revealed a distribution throughout the cell, with particular enrichment at the nucleus and septum. While no particular enrichment of Dph1 was co-incident with the Mlp1 staining at the mitochondria, nor was Dph1 staining excluded from the same areas. Attempts to improve the Dph1 localisation image through deconvolution were not possible, as the fluorescence intensity was insufficient, and the extended exposure times required resulted in the signal becoming bleached before an image stack could be completed.

5.6.2 Mitochondrial Ubiquitin Levels

The detection of substantial levels of ubiquitinated proteins at the mitochondria is consistent with other work, which indicates that the cytosolic face of the mitochondria bears ubiquitinated proteins (Margineantu et al., 2007). However, it is unclear what fraction of these ubiquitinated proteins correspond with potential proteasome substrates, rather than other forms of ubiquitination, such as lysine-27 linked chains associated with mitophagy (Section 1.7). While Margineantu et al. (2007) saw a reduced level of mitochondria ubiquitination upon Hsp90 inhibition, substantial levels of ubiquitination remained.

The level of ubiquitinated proteins at the mitochondria appears to be unaffected on the loss of Mlp1, indicating that it is not possible to detect substantial stabilization of mitochondrial ubiquitin in Mlp1 knockout strains. However, this does not exclude the possibility of a more restricted role for Mlp1, or one which only becomes apparent during increased levels of protein misfolding. Repeating similar experiments under conditions which traditionally result in increased misfolding, such as elevated temperatures, may be informative. Furthermore, the use of antibodies specific to lysine-48 linked ubiquitin, or other proteasome directed chains, will increase the specificity of the assay for proteins targeted to the proteasome, and may help pick up stabilization otherwise obscured by

other forms of ubiquitination.

If Mlp1 acts on a smaller subset of proteins, it will be necessary to identify individual substrates. Potential targets for this search are discussed in section 6.3.

5.6.3 Mitochondrial Morphology

The presence of Mlp1 at the mitochondria, confirmed in this study, lead to the consideration of defects in mitochondrial morphology in the knockout strains. Such defects would be especially likely if Mlp1 were involved in the regulation of components of the fission and fusion machinery, such as the regulator of mitochondrial fusion, Fzo1 (Hermann et al., 1998; Fritz et al., 2003; Cohen et al., 2008). Other components of the ubiquitin proteasome system have previously been linked to mitochondrial defects in *S. cerevisiae* (Altmann and Westermann, 2005).

Mitochondrial morphology showed a range of phenotypes in any given genetic background, and a comparison of the distribution of these phenotypes between wild-type and Δ*mlp1* cells revealed no perturbation in mitochondrial morphology. Conversely, Δ*dph1* strains showed a slight increase in the proportion of cells showing a condensed phenotype, although given Dph1's role in protein degradation it is unclear as to whether this is a direct or indirect effect. The lack of morphology defects in Mlp1 indicates that the protein is not essential for maintaining mitochondrial morphology. However, it is unclear whether this is because the protein is not involved in degrading regulatory proteins, it is redundant to other proteins, or whether it is involved in two or more antagonistic pathways, and will therefore only result in an observable phenotype when one of these pathways is perturbed. Work in *S. cerevisiae* has shown that knockout of proteins that would be expected to act in the same pathway, such as Cdc48 co-factors Npl4 and Ufd1, can have opposing effects on mitochondrial morphology, suggesting that some factors may play roles in opposing pathways.

5.7 Summary

Mlp1 mitochondrial localisation was confirmed, and Dph1 was demonstrated to have a substantial mitochondrial associated fraction. Δ*mlp1* strains were studied, and were shown to have no defects in mitochondrial morphology, or mitochondrial ubiquitin levels. Conversely, the loss of Dph1 resulted in a slight shift towards more condensed mitochondrial morphologies, consistent with previous studies indicating that the ubiquitin proteasome system affects mitochondrial morphology.

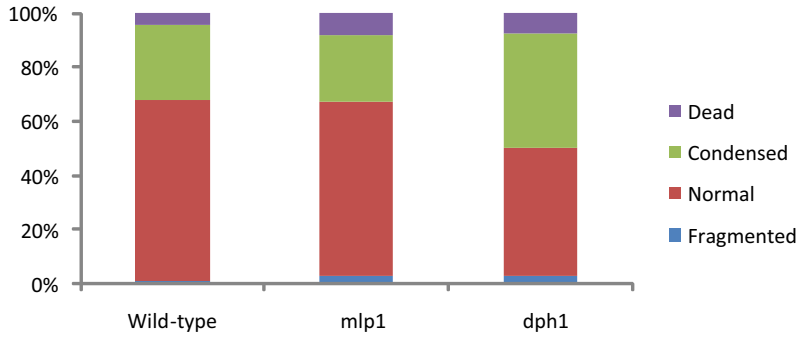

Figure 5.12: Graphical representation of the data shown in table 5.1.

Chapter 6

Discussion

6.1 Ubx4 and Ubx5

Attempts to dissect the role of the Cdc48 co-factors Ubx4 and Ubx5 did not provide any significant novel insights into their function. In particular, while a yeast two-hybrid screen re-capitulated the known interaction between Ubx4 and Cdc48, no further interactors were identified. Section 3.6 discusses the implications of this result, and possible ways to overcome some of the limitations of the initial approach.

Of note are discoveries regarding the role of the *S. cerevisiae* homolog of $ubx4^+$, which were published while this work was underway (Alberts et al., 2009). Ubx4 was shown to play an important role in ERAD, where it appeared to be required for the release of ERAD substrates from $Cdc48^{Npl4-Ufd1}$. The mechanism by which this occurs has not yet been identified, however it is possible that the binding of Ubx4 alone to Cdc48 may be sufficient to modify its function. If Ubx4 in general acts as a Cdc48 modulator, rather than an adapter, the failure to identify other Ubx4 binding partners may be unsurprising. However, as the UBL domain was dispensable for this function, it suggest that Ubx4 is likely to have further unidentified roles, which may involve other proteins in addition to Cdc48.

In line with the findings of Alberts et al. (2009), *S. pombe* $\Delta ubx4$ strains showed the same temperature sensitivity observed in the *S. cerevisiae ubx4* knock-outs. Conversely however, the cycloheximide sensitivity observed in the same study was not recapitulated in *S. pombe*. At present, it is not possible to judge if this difference is a result of differences in the function of the *S. pombe* and *S. cerevisiae* Ubx4 proteins, more general differences in the characteristics of the two species, or is a result in differences in experimental method. In particular, Alberts et al. (2009) assayed stress sensitivity in

strains expressing CPY*, which may result in an increased sensitivity to some stresses in specific backgrounds.

The key questions that now need to be answered with respect to Ubx4, are whether its role in ERAD is conserved in *S. pombe*. The study of the stability of ERAD substrates, such as CPY*, in $\Delta ubx4$ backgrounds would be an excellent way of addressing this. Additionally, Alberts et al. (2009) found that the UBL domain was not required for Ubx4's role in ERAD, indicating the possibility of as yet undiscovered functions, such as in coordinating interaction with Rpn10 or the proteasome. Meanwhile, the function of Ubx5 remains even more elusive and substantial further work will be required.

6.2 Dph1 interactors

The association between Mlp1 and Dph1 identified in the yeast two-hybrid assay, highlighted a novel link between the ubiquitin proteasome system and elements of the outer mitochondrial membrane associated with protein localisation (Nakai et al., 1993; Schnall et al., 1994). Further links with ubiquitin associated proteins were provided by the Cdc48 co-factors, Ubx1 and Ubx2, which also interacted with Mlp1. These interactions implicated Mlp1 in ubiquitin regulated pathways, and in particular the ubiquitin proteasome system. It was speculated the Mlp1 may act in a mitochondrially associated ubiquitin-proteasome mediated degradation pathway, analogous to the ERAD pathway of the endoplasmic reticulum. The AAA-ATPase Cdc48 has already been demonstrated to play an important role in the ERAD pathway, and not only is Mlp1 also a AAA-ATPase, but its interaction with Ubx1 and Ubx2 imply possible Cdc48 involvement.

Unfortunately it was not possible to reconstitute the interaction between Mlp1 and Dph1 in another system, and this is one of the key priorities in future perusal of the findings in this study. The transmembrane nature of Mlp1, and possible involvement of other proteins or translational modifications, is likely to be a key factor inhibiting the current approach. Alternative approaches that may prove more successful were discussed in section 5.6.1. In addition to these approaches, the isolation of proteins associated with Mlp1 will allow for the identification of further components which interact with it, potentially providing more insight into a MAD pathway. In particular, an association of Cdc48 with Mlp1 can be rapidly assayed, and mass spectroscopy may be used to help to identify any unknown prominent bands which may co-precipitate with Mlp1.

6.3 Potential Substrates

Consideration of the total mitochondrial ubiquitin levels did not reveal substantial widescale stabilization of ubiquitin conjugates in Δ*mlp1* strains. However, the methods used identified any mitochondrial associated ubiquitination, not just that associated with proteasome mediated degradation. The identification of mitochondrially localised proteins that are degraded in a proteasome dependent manner will be essential for testing elements of the proposed mitochondria associated degradation pathway. Model proteasomal substrates such as CPY* and 6myc-Hmg2p have proved extremely useful in the dissection of the ERAD pathway; the identification of similar substrates in mitochondria will be essential, both for testing the role of Mlp1 and for identifying other MAD components. Furthermore, parallels in the ERAD pathway suggest that several substrates may be necessary to fully dissect the components of a MAD pathway, as substrates in different mitochondrial compartments may require a different selection of factors.

In addition to the testing of the putative substrates suggested below, more direct methods are available for identifying potential substrates. This approach will be particularly useful for identifying the extent of MAD pathway regulated proteins within the mitochondria. Proteomics methods can be used to look directly for protein stabilization in the mitochondria on either inhibition of the proteasome, or deletion of *mlp1*. Mass spectroscopy approaches such as SILAC (stable isotope-labelled amino acids) may be used to both identify protein stabilization, and to quantify it. Such approaches have already been used for identifying substrates of other proteolytic processes, such as substrates of ClpXP (Schilling and Overall, 2007).

Alternatively, genetic interactions have been productive in detecting potential substrates of Dsk2 and Rad23 in *S. cerevisiae*. Liu et al. (2009) found that overexpression of some Dsk2 or Rad23 substrates would result in growth defects when the corresponding shuttle factor was compromised; similar experiments could be conducted in a Δ*mlp1* background. While such an approach is not as direct as a proteomic approach, and would be ineffective at identifying all MAD substrates, it does identify substrates which provide a clear phenotype when the pathway is disrupted.

6.3.1 Fzo1

Mitofusin or *fuzzy onions* (Fzo1) is a transmembrane GTPase localized to the outer-membrane of the mitochondria. The protein is involved in the regulation

of mitochondrial fusion, and hence helps to modulate mitochondrial morphology (Hales and Fuller, 1997; Hermann et al., 1998). In *D. melanogaster* expression is developmentally regulated. It appears during meiosis II during spermatogenesis, where it coordinates the fusion of mitochondria to form Nebenkern bodies: mitochondrial aggregates along the flagellar axon (Hales and Fuller, 1997). In *S. cerevisiae* the homolog, Fzo1p, appears to play a more diverse role, maintaining mitochondrial structure during vegetative growth, and coordinating the fusion of parent mitochondrial networks during mating. The loss or mutation of Fzo1p results in defects in mitochondrial morphology, and impaired growth (Hermann et al., 1998).

Levels of Fzo1p appear to be post-translationally regulated and both the F-box protein MDM30 and the ubiquitin proteasome system have been linked to Fzo1p degradation (Fritz et al., 2003; Escobar-Henriques et al., 2006; Cohen et al., 2008). In support of this, proteasome inhibition or mutation results in mitochondrial morphology defects consistent with Fzo1p stabilization (Escobar-Henriques et al., 2006; Cohen et al., 2008). However the way these two processes interact is controversial. Escobar-Henriques et al. (2006) suggested the existence of two separate pathways, an Mdm30p dependent, proteasome independent pathway that was operational during vegetative growth, and a proteasome dependent Mdm30p independent pathway activated on α-mating factor induced arrest. Conversely, Cohen et al. (2008) found that during vegetative growth Mdm30p ubiquitinates Fzo1p as part of an SCF^{Mdm30p} complex, directing the protein to the proteasome via lysine-48 linked ubiquitin chains. These two findings are difficult to reconcile, and suggest that there may be more than one mechanism of Fzo1p degradation at play. However, they do indicate that the ubiquitin proteasome system is likely to play at least a partial role in regulating levels of Fzo1p.

This suggests that Fzo1 may provided a suitable substrate localised in the outer mitochondrial membrane. Preliminary work has been conducted to develop a strain expressing a C-terminally GFP tagged form of Fzo1p, under its native promoter (Section D.1). However early observations of this strain reveal possible mitochondrial morphology defects, indicating that the tag may be disrupting Fzo1 function, diminishing its suitability as a substrate; the use of N-terminal GFP tags may help alleviate this problem. Alternatively, other approaches include the use of different tags, such as the smaller 6×histidine tag, or the use of antibodies raised against Fzo1 directly.

6.3.2 Sod1

The gene *sod1* encodes a Cu-Zn superoxide dismutase that catalyses the breakdown of superoxide radicals, which would otherwise be toxic to the cell. Its loss in *S. pombe* results in a slow growth phenotype, with cysteine, or methionine and lysine auxotrophies. Cells are more sensitive to oxidative stresses, and more readily induce protective factors (Mutoh et al., 2002).

Mutations in SOD1 are associated with the neurodegenerative disease amyotrophic lateral sclerosis (ALS) (Rosen et al., 1993), which results in progressive degeneration of motor neurons and eventually death. Patient survival from the time of diagnosis is on average between just three and five years. A large number of mainly dominant mutations have been identified in SOD1, which is responsible for 20% of familial ALS cases (Reviewed in Majoor-Krakauer et al., 2003).

SOD1 mutants show a wide range of activities, from the catalytically inactive G85R, to G37A mutants which show full catalytic activity. Heterozygous mutants generally have between 60 and 80% wild-type activity (Borchelt et al., 1994; Andersen et al., 1995). This finding prompted the realisation that ALS was unlikely to be a result of the defects in SOD1 enzymatic activity. Instead, mutations in SOD1 appear to result in the formation of SOD1 protein aggregates, particularly in the spinal cord; aggregates form with age, and correlate with the onset of ALS symptoms (Wang et al., 2002).

SOD1 has been identified in association with the endoplasmic reticulum, where mutant SOD1 in particular triggers an unfolded protein response, such as the induction of ATF6 signalling in affected cell lines (Kikuchi et al., 2006; Atkin et al., 2006). In addition, ER associated apoptotic factors, such as Caspase-12 are induced, providing a mechanism to explain motor-neuron degeneration (Kikuchi et al., 2006; Atkin et al., 2006).

In addition to its accumulation in the ER, mutant SOD1 also appears to accumulate at the mitochondria in affected tissues, where it forms aggregates (Pasinelli et al., 2004; Liu et al., 2004; Rakhit et al., 2007). Much of the mitochondrial SOD1 appears to be tightly associated with the cytosolic side of the outer-membrane, although some also accumulates in the inter membrane space (Liu et al., 2004). The mitochondrial outer-membrane E3 ligase MITOL appears to bind to and ubiquitinate mitochondrial associated mutant SOD1, which is then degraded in a proteasome dependent manner. Overexpression of MITOL is sufficient to reduce the levels of mutant SOD1 at the mitochondria (Yonashiro et al., 2009). This association with the mitochondria, ubiquitination by a mitochondrial E3 ligase, and destruction by the proteasome suggests that mutant Sod1 may provide a suitable substrate for a putative mitochondria

associated degradation pathway.

S. pombe Sod1 shows 55% sequence identity to the human SOD1 (Figure 6.1). Four well characterised ALS causing SOD1 mutations, taken from both human and mouse models, were mapped onto the alignment, and were found to correspond to residues conserved between humans, mice and *S. pombe*. A series of *S. pombe* mutant constructs have been designed to recreate the ALS causing mutations in the *S. pombe* Sod1, in the hope of creating a suitable *S. pombe* model.

Sod1 provides a potential inter-membrane space substrate, which has additional implications for disease. Its use as a potential substrate will be dependent on the misfolding and mitochondrial accumulation phenotype being reproduced in *S. pombe*. In contrast to Fzo1, Sod1 also provides a clear substrate for a misfolded protein removal pathway, instead of the regulated degradation of Fzo1.

6.3.3 OSCP/Atp5

OSCP is a mitochondrial matrix protein, which was used as a substrate in the study of Hsp90 by Margineantu et al. (2007); the homolog in *S. pombe* is known as Atp5. The protein encodes a subunit of the F1F0-ATP synthase complex, and is stabilized upon Hsp90 inhibition. Importantly, the protein appeared to undergo retro-translocation, as post-processed forms of the protein could be detected on the outer mitochondrial membrane, despite processing occurring in the mitochondrial matrix. Additionally the protein was found to be ubiquitinated in an Hsp90 dependent manner, and was stabilized on proteasome inhibition. This implicates mitochondrially localised OSCP as a substrate of the ubiquitin proteasome system (Margineantu et al., 2007).

Assuming the same conditions are conserved in *S. pombe* Atp5 would make an excellent candidate for a mitochondrial matrix substrate. Additionally, Hsp90 provides an attractive candidate for a positive control, and may be worth investigating in concert with other MAD substrate candidates.

6.3.4 Studying the Substrates

Measuring substrate stability provides a means of assaying the activity of the degradation pathway. Once a suitable substrate has been identified, it will provide a base for future screens to identify other components in the same pathway.

One method of measuring protein stabilization of fluorescent proteins is through fluorescence-activated cell sorting (FACS). FACS uses flow cytometry to separate

Figure 6.1: Comparative alignment of *S. pombe* Sod1 with mouse and human homologs (Larkin et al., 2007; Beitz, 2000). Arrows indicate residues associated with disease in mouse and human models that have been considered in this study; the appropriate mutation is indicated. Mutations are indicated with respect to the *S. pombe* sequence.

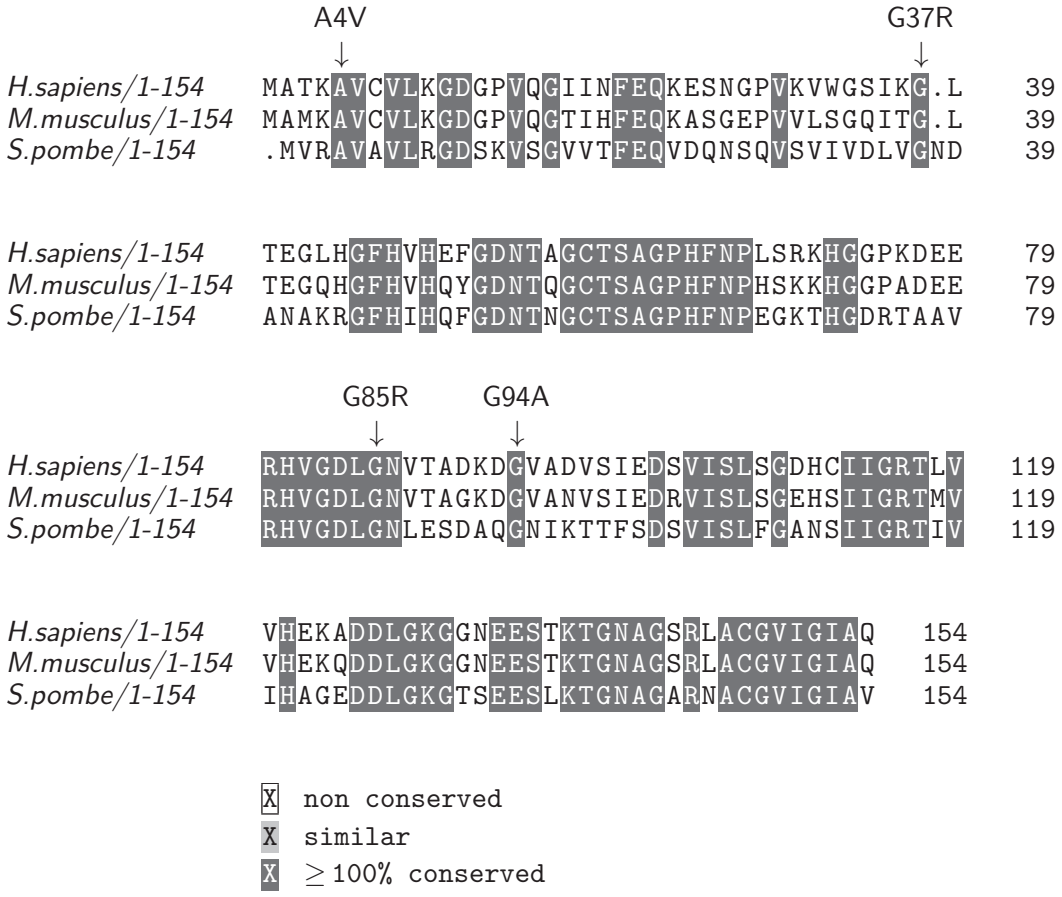

a population of cells such that their fluorescence may be measured individually. The process allows for the sorting of these cells according to their fluorescence, enabling mixed populations to be sorted according to the level of protein stabilisation. Initial FACS experiments could be used to measure the stabilization of the potential substrates in a variety of genetic backgrounds. Proteasome mutants, such as the temperature sensitive *mts3.1* mutant strain (Gordon et al., 1996), provide a positive control to demonstrate that the potential substrate is stabilized when the proteasome is compromised. Hsp90 inhibitors provide a similar positive control for OSCP stabilization, and may also prove useful for other mitochondrial substrates. These experiments may then be followed by similar measurements in the Δ*mlp1* and Δ*dph1* strains, to check whether a similar level of stabilization is observed. In addition to this, Cdc48^{ts} mutants are available for assessing the role of Cdc48, and both *ubx1* and *ubx2* deletion mutants are viable (Kim et al., 2010), providing a means of assessing the importance of their interaction with Mlp1. Early attempts at conducting FACS analysis with the Fzo-GFP and Sod1 mutant substrates were inconclusive, and further optimisation of the protocol with *S. pombe* will be required.

If a substrate is found with sufficient stabilization, such that there is minimal overlap between the fluorescence in stabilizing and non-stabilizing backgrounds, then FACS may form the basis of a screen for elements of a MAD pathway. The fluorescent substrate may be transformed or crossed into a *S. pombe* knockout library, resulting in a mixed cell population expressing the substrate in a wide range of genetic background. Subsequent isolation of cells in which the substrate is stabilized may be used to identify genes involved in the degradation pathway. In addition to elements of a putative MAD pathway, this approach would also be expected to identify proteins in the ubiquitin cascade.

As an alternative to FACS analysis, protein stabilization may be measured more directly via western blotting of total protein extracts. The GFP tags added for the FACS analysis would provide suitable epitopes for antibody detection in situations in which more direct antibodies are not yet available. Additionally, inhibition of protein synthesis with cycloheximide, followed by the measurement of substrate levels over a time-course, will allow for the measurement of protein half-life in mutant and non-mutant backgrounds. This will allow confirmation that any increase in steady-state levels is a result of protein stabilization, rather than an increase in transcription or translation.

6.4 Other approaches

The first components of the ERAD pathway were identified when they were found to rescue Sec61 mutants (Biederer et al., 1996). Sec61 is an essential protein which forms part of the pore through which proteins are transported into the ER. At elevated temperatures, mutant Sec61 is subject to degradation by the ubiquitin proteasome system, resulting in an accumulation of precursor polypeptides in the cytosol, and inviability. On disruption of elements of the ERAD pathway, such as Ubc7, this degradation is blocked, and the phenotype is suppressed (Biederer et al., 1996). The identification of a similar substrate in the mitochondria would prove useful for identifying other elements of a MAD pathway, and would provide a good base for a screen for other MAD pathway proteins. Alternatively, the fusion of a metabolic marker to a non-essential substrate, may be used to create an artificial substrate that may be used in a similar manner. Similar approached have been used successfully to dissect the ERAD pathway in *S. cerevisiae*. A fusion of the metabolic protein Leu2 to the ERAD substrate CPY* was used to assay protein stabilization in the event of ERAD disruption; in the event of protein stabilisation cells would be able to grow in the absence of leucine (Schäfer and Wolf, 2005).

Experiments by Takeda et al. (2010) showed that during G0, *S. pombe* demonstrate increased synergy between the proteasome, and mitochondrial autophagy. The proteasome showed a cellular redistribution from the nuclear periphery to even distribution throughout the cytoplasm, and it was suggested that this was to respond to the increased threat of reactive oxygen species (ROS) induced damage at the mitochondria. Inactivation of the proteasome in G0 results in a massive upregulation of the autophagy pathway, and lethality. These findings suggest that the importance of a MAD pathway, may increase in cells in G0, and indicates potential interactions with the autophagy pathway. It may prove informative to consider the viability of Δ*mlp1* cells maintained in G0, the maintenance of their mitochondria in these conditions, and potential genetic interactions with the mitophagy pathway in G0.

Screening for genetic interactions with Mlp1 may also be used to identify further components of associated pathways. If Mlp1 functions in an essential pathway, but is redundant to other proteins, then a screen for synthetic lethality with other mutants will be useful in identifying elements of parallel pathways. Alternative approaches involve more subtle screens, which compare the growth rates of strains containing single and double mutations to identify both positive and negative genetic interactions (Roguev et al., 2007, 2008). Epistatic mutations, those showing the same phenotype in single

and double mutants, are indicative of proteins acting in the same pathway, and may help identify components of the pathway both upstream and downstream of Mlp1. Not only will this approach be useful in dissecting the pathway in which Mlp1 is involved, but it may prove useful in clarifying the role of Mlp1, especially if it is found to not play a primary role in the MAD pathway.

6.5 Alternative Roles for Mlp1

As yet, it has not been possible to explicitly tie Mlp1 to the putative MAD pathway, so it remains possible that Mlp1 is performing a different function at the mitochondria. The association between Mlp1 and protein localisation has already been demonstrated (Nakai et al., 1993; Schnall et al., 1994), and it is possible that its primary role is one of regulating protein localization, such as helping to re-target proteins mis-localised to the outer mitochondrial membrane. The association with Dph1 may instead be responsible for removing and degrading proteins which remain associated with Mlp1 for an extended period of time, in a manner comparable to the targeting of chaperone bound proteins to the ERAD pathway. Alternatively, Dph1 may associate with Mlp1 to prevent it from acting on ubiquitinated proteins, maintaining them in a retro-translocation pathway. In the event that no substrate stabilization can be identified, these alternative possibilities will have to be investigated.

6.6 A Speculative Model of the MAD Pathway

While it is still premature to begin developing a robust model of a mitochondria associated degradation pathway, parallel pathways in other organelles, and the emerging picture of factors involved in the proteasome dependent degradation of mitochondrial proteins, make it possible to begin speculating as to the nature of such a pathway. An outline of one possible model is shown in figure 6.2. Unidentified factors and those whose role in MAD has not yet been demonstrated by experimental evidence, are illustrated with a dotted outline.

Mitochondria are structurally more complicated than the endoplasmic reticulum, and can be divided into four separate compartments, the outer mitochondrial membrane (OMM), inter-membrane space (IMS), inner mitochondrial membrane (IMM) and mitochondrial matrix (MM). The mechanisms of recognition and removal of misfolded proteins in each compartment are likely to require distinct elements, and in some cases may even function independently. Further diversity may result from different families of

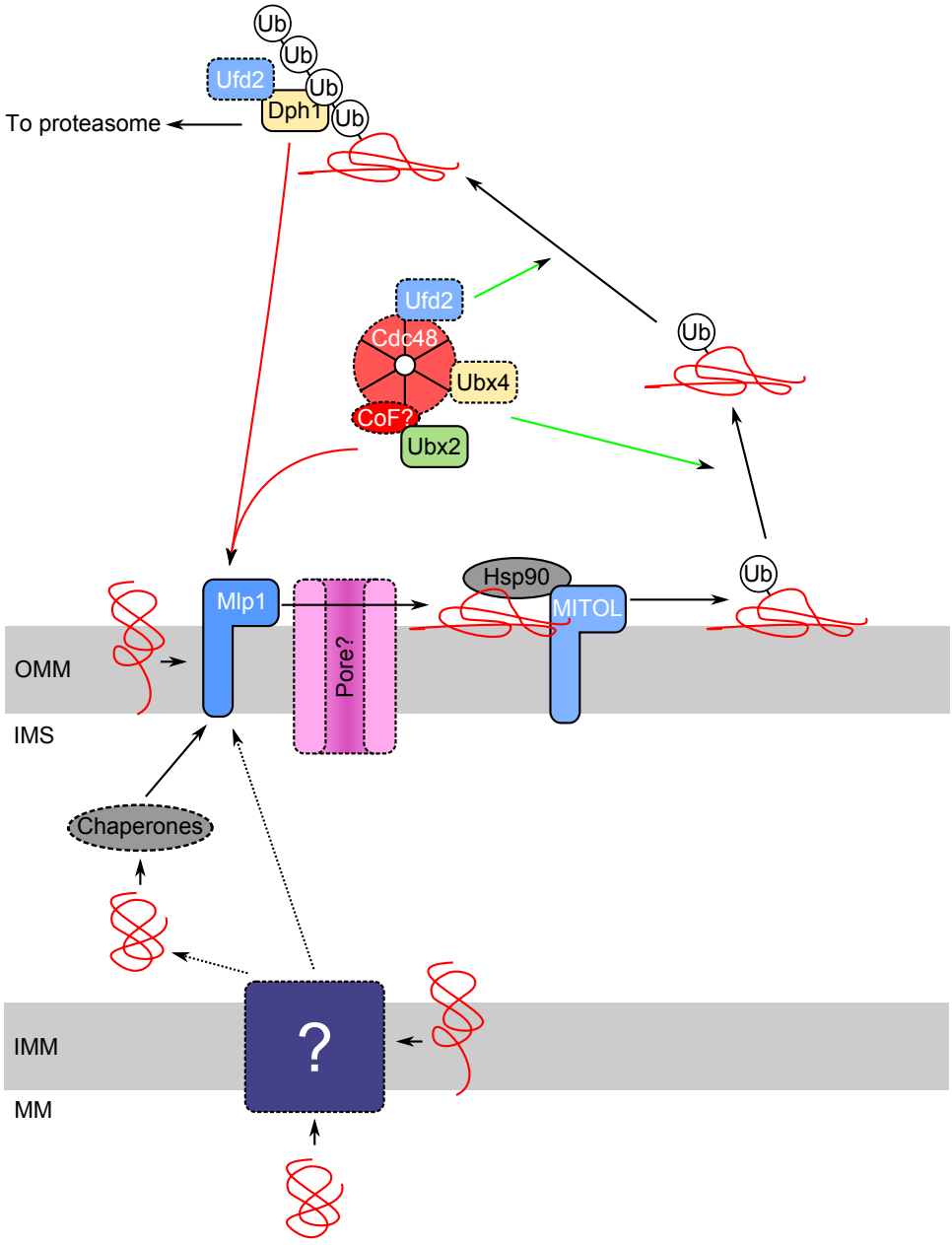

Figure 6.2: A putative model of the MAD pathway.

proteins in each compartment, such as different factors required in the recognition and removal of membrane proteins based on their orientation. The model shown here shows a system by which multiple pathways feed into a shared downstream processing system, in a manner analogous to the shared processing machinery of the ERAD pathway. Retrotranslocation across the inner mitochondrial membrane may be directly couple to transport across the outer-mitochondrial membrane, or else proteins may be passed to recognition machinery in the inter-membrane space. Currently this upstream pathway remains enigmatic, yet it is likely to make use of chaperones in the recognition and delivery of substrates.

In the model presented here, substrates are delivered to Mlp1, which promotes retrotranslocation of substrates across the outer mitochondrial membrane. It is likely that further components will be found to be necessary for this process, including an as yet unidentified pore complex. Just as Sec61p has been implicated in the retrotranslocation of ER proteins, the mitochondrial import machinery may be repurposed for this function. Additionally, Mlp1 appears to act as a scaffold, recruiting other elements of the MAD pathway, ensuring efficient coupling of upstream and downstream processes. The Cdc48 complex is likely to be recruited via the co-factor Ubx2; other Cdc48 co-factors may be necessary for its activity, just as *S. cerevisiae* Ubx2 interaction with ER localised E3 ligases recruits the $Cdc48^{Npl4-Ufd1}$ complex during ERAD in *S. cerevisiae*.

Retrotranslocated substrates are likely to remain associated with the outer mitochondrial membrane, where they are recognised by the chaperone Hsp90, as implied by Margineantu et al. (2007). Hsp90 subsequently recruits ubiquitin E3 ligases, such as the mitochondria associated MITOL, which prompt substrate ubiquitination. Finally, this model predicts that Cdc48 will be required for the release of substrates from the mitochondrial membrane, and their delivery to the shuttle factor Dph1. As with the ERAD pathway, this process is likely to be coupled with ubiquitin chain extension via E4 ligases such as Ufd2. Ubx4 may be found to recapitulate its role in ERAD, catalysing the release of substrates from Cdc48.

In practise, the mitochondria associated degradation pathway will likely involve many more factors than those outlined here. For example, the association of Dph1 with mitochondria in a Δ*mlp1* background indicates other pathways of Dph1 recruitment are likely to be available, although this may represent binding to ubiquitinated proteins at the mitochondrial membrane. Other factors are likely to play a regulatory role, up-regulating the pathway in times of stress, and governing the balance between the ERAD and MAD pathways. These additional factors can be expected to be identified

over the coming years as the understanding of proteasome dependent destruction of mitochondrial proteins increases. These findings will also help test the model presented here, and further clarify the role of some of the factors already implicated in the process.

6.7 Summary

Initial experiments with the Cdc48 co-factors Ubx4 and Ubx5 recapitulated the known interaction between Cdc48 and Ubx4, and revealed minor sensitivities and resistances to a range of stress factors. However, no convincing novel interactions or striking stress sensitivity or resistance phenotypes were identified.

The interaction between Mlp1 and the proteasome shuttle factor provided an interesting link between the mitochondria and the ubiquitin proteasome system. This link was further reinforced by the discovery of potential interaction with two Cdc48 co-factors, Ubx1 and Ubx2. Mlp1 contains a AAA-ATPase domain, which is commonly associated with protein unfolding and anti-chaperone activity; overexpression of its ortholog in *S. cerevisiae* is sufficient to result in the re-localization of outer mitochondrial membrane proteins (Nakai et al., 1993; Schnall et al., 1994). It was proposed that Mlp1 may act in a mitochondrial associated degradation pathway, involved in the delivery of mitochondrial proteins to the proteasome.

Dph1 was found to have a wide distribution throughout the cell, and was enriched in the mitochondrial fraction. Attempts to recapitulate an *in vivo* interaction between Dph1 and Mlp1 have been so far unsuccessful, and will be an important target for future work. Several potential substrates for the proposed MAD pathway have been suggested. Such substrates will be useful in dissection the potential role of Mlp1, as well as in the identification of other elements in a MAD pathway.

Appendix A

Primers

Name	Sequence
AD	TTTCAGTATCTACGATTCATAG
AD3'	TACCACTACAATGGATG
Dph1_AF	GTGGAGCTGGTTTAGGTGGA
Dph1_AR	TTAATTAACCCGGGGATCCGAAGATCACTCAACAAAGATTC
Dph1_BF	GTTTAAACGAGCTCGAATTCCCTGGAAAGTCATCGTACTCTGT
Dph1_BR	CGGACGGAACTTTGGAATTT
Dwch_ubx4	CTTGGTGTCCAACGGTTCGT
Dwch_uni	TCTGGGCCTCCATGTCGCTGG

Name	Sequence
Dwch_uni2	GCTGCGCACGTCAAGACTGTC
Upch_ubx4	GCCAAGAGCCTCCTGATGGT
Upch_uni	GTCGTTAGAACGCGGCTACA
Upch_uni2	GGCTGGCTTAACTATGCGGC
JG1L	AGGATCCTTATGAACGCACCATCCACCAT
JG1R	ACTGTCGACCTATGCATACAAATCATCAG
JG2A	GAAGCGTATCGTCCTATTCG
JG2D	GTCCCGATCAGATTGATCCT
JG2G	TCCCAACGAACATTGGGAAC
JG21uo	AAAATCTAGATGGGAGTGTATCACCCTGGC
JG21do	AAAATCTAGAGTGCGGCTTTGCCTCTCTTT
JG21ui	AAAAGTCGACTCCTAATTTGCGAACGGTAGAGG
JG21di	AAAAAGATCTATTGCTGGTGCTTGGGGTTT
JG25F	CGGGGATCCGTATGGCGACTATTTACGCGTG
JG25R	GCAGGTCGACTTACCTTTGTGCATAAACAG
JG26F	CGGGGATCCGTATGGTTTTGAAATGTTTGGA
JG26R	GCAGGTCGACTTACCATTGCGGAATAAGAA
JG27C	AACCTGCCTTGGATACTTGG
JG27N	GCTCTCAACTGCGATGTTTG
Mlp1_AF_B	GTGGTCAGTCACGGGTTCTT

Name	Sequence
Mlp1_AR_B	TTAATTAACCCGGGGATCCGCTCGACGTCTATACCGGAAAC
Mlp1_BF_B	GTTTAAACGAGCTCGAATTCGCGTTTGTACAACAGCCAAT
Mlp1_BR_B	TGTATGTTCTTTTGAACTGTCACG
MSP3'F	GGGATCCGTATGAATCCGACGACTAAAAG
MSP_AAA3'F	GGGATCCGTTGTCCAAAGGGTTTACTCTTG
MSP_CT3'F	GGGATCCGTGAGCTTTTTGACAAGCATGG
MSP3'F2	CCGAATTCTCATGAATCCGACGACTAAAAG
MSP_NT5'R	GCAGGTCGACGTCACGACAAAAGTCCGCCATGGG
MSP_AAA5'R	GCAGGTCGACGTCAAAGAGGTATGGAGAATACTT
MSP_AAAE5'R	GCAGGTCGACGTCATCTGCGTGGAACTGATAAAG
MSP5'R	GCAGGTCGACGTCACTCGACGTCTATACCGG
Dph1_5'_BamHI	CCGGATCCTCATGACCAATATATCGTTGAC
Dph1_dUBL_BamHI	CCGGATCCTCGGACAAAATCCTGCAGCC
Dph1_sti_Fw	GCCGAATTCACCGAAGAGCTTGCCAATATG
Dph1_dSTI_BamHI	CCGGATCCTCGGTGCTGCCGGTATTGAC
Dph1_dSTI_XhoI	ATCTCGAGTTACGAGGGTGGAACAGGATT
Dph1_sti_Rv	GCCGTCGACTTACATTTGTTGATGTAGTTG
Dph1_dUBA_XhoI	ATCTCGAGTTAACGCTCTTCTGGAGGGCG
Dph1_3'_XhoI	GCCTCGAGTTAAAGATCACTCAACAAAG

Table A.1: Table of primers

Appendix B

Supplementary Figures

Additional figures not included in the main body of the thesis may be found in this section.

B.1 Growth Curves

Growth assays of the $\Delta ubx4$ and $\Delta ubx5$ strains compared to wild-type were repeated three times to ensure consistency. These experiments are discussed in more detail in section 3.3. The repeats are shown in figure B.1

B.2 Sensitivity Assays

Sensitivity assays for the $\Delta ubx4$, $\Delta ubx5$ and $dcd4\mathit{8}^{ts}$ strains and associated crosses are summarised and discussed in section 3.4. Figures B.2 to B.8 show photographs of the sensitivity assays, presenting the raw data for more detailed analysis.

B.3 Dph1 Antibody

The specificity of the Dph1 antibody was assayed against total protein extract from wild-type *S. pombe* and from $\Delta dph1$ strains. The resulting western blot is shown in figure B.9.

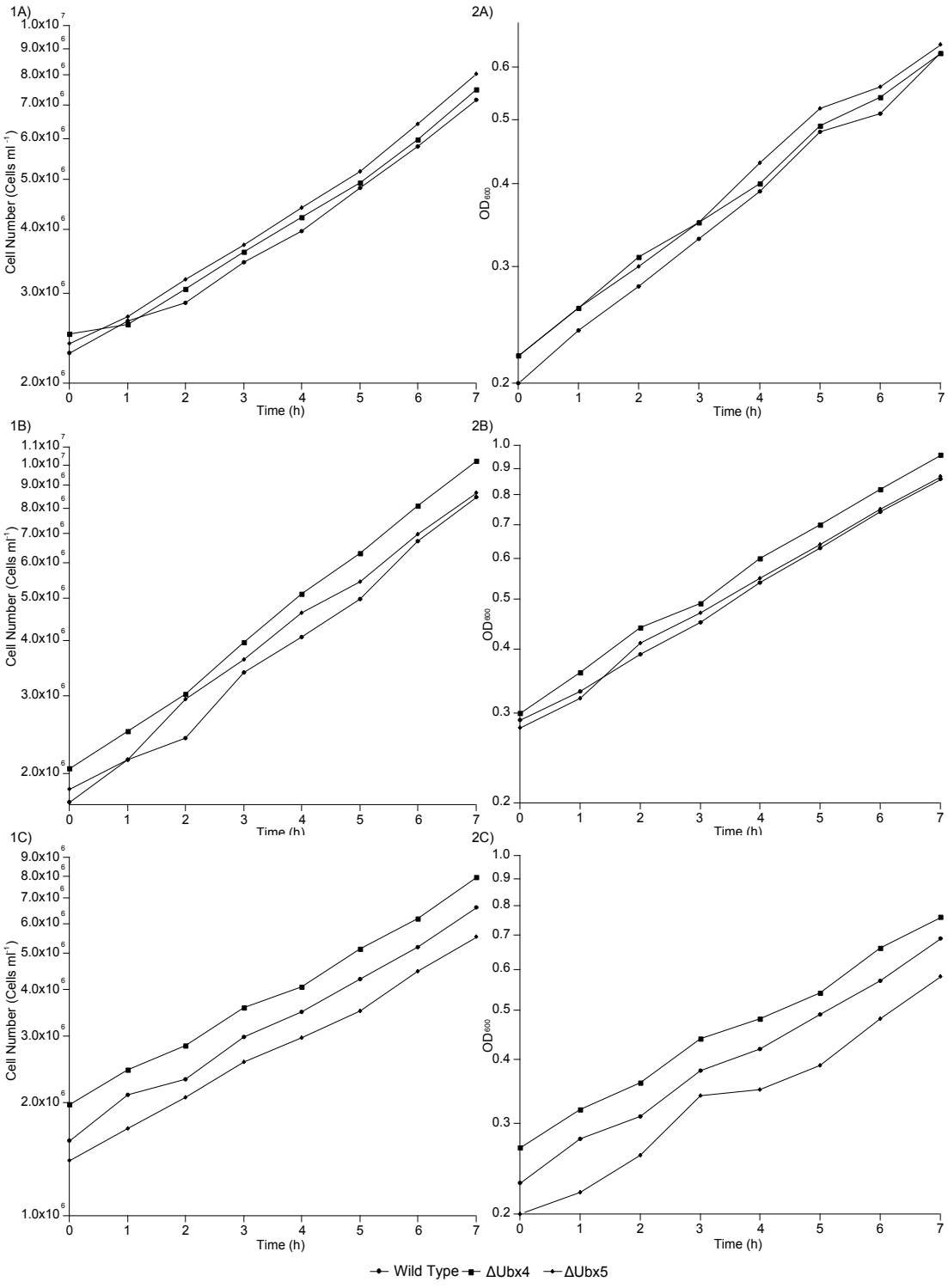

Figure B.1: Growth curve comparisons of the Δubx4 and Δubx5 strains with wild-type *S. pombe* at 25°C. Conducted on three different occasions A, B and C. Growth is indicated by (1) cell density and (2) Absorbance $OD_{6}00$. The Y axis is a logarithmic scale.

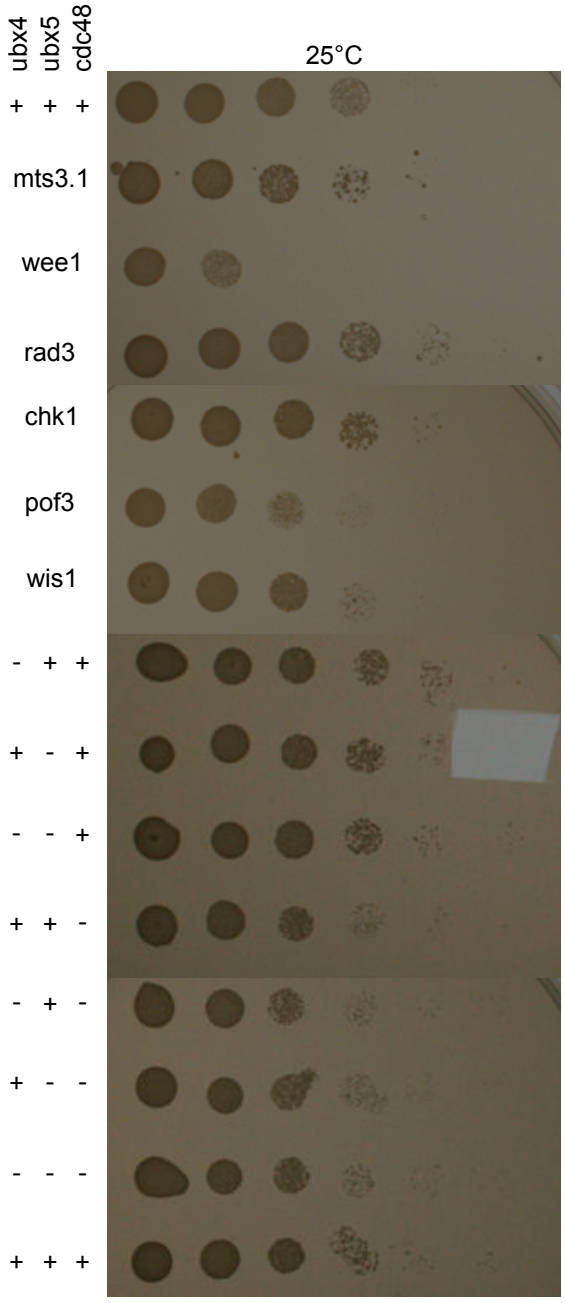

Figure B.2: Colony growth on non-selective media

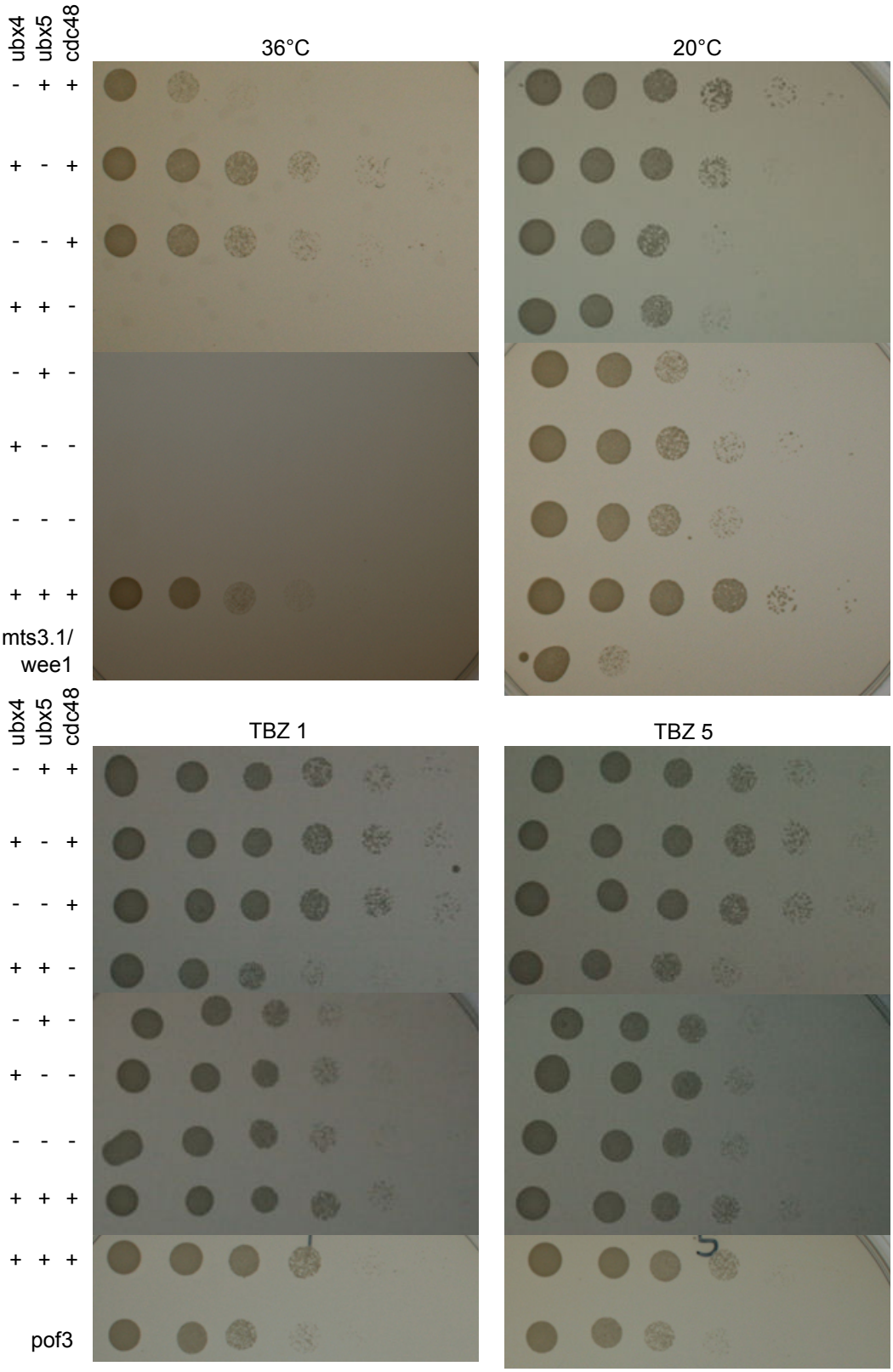

Figure B.3: Colony growth at 20°C, 36°C and on TBZ containing media.

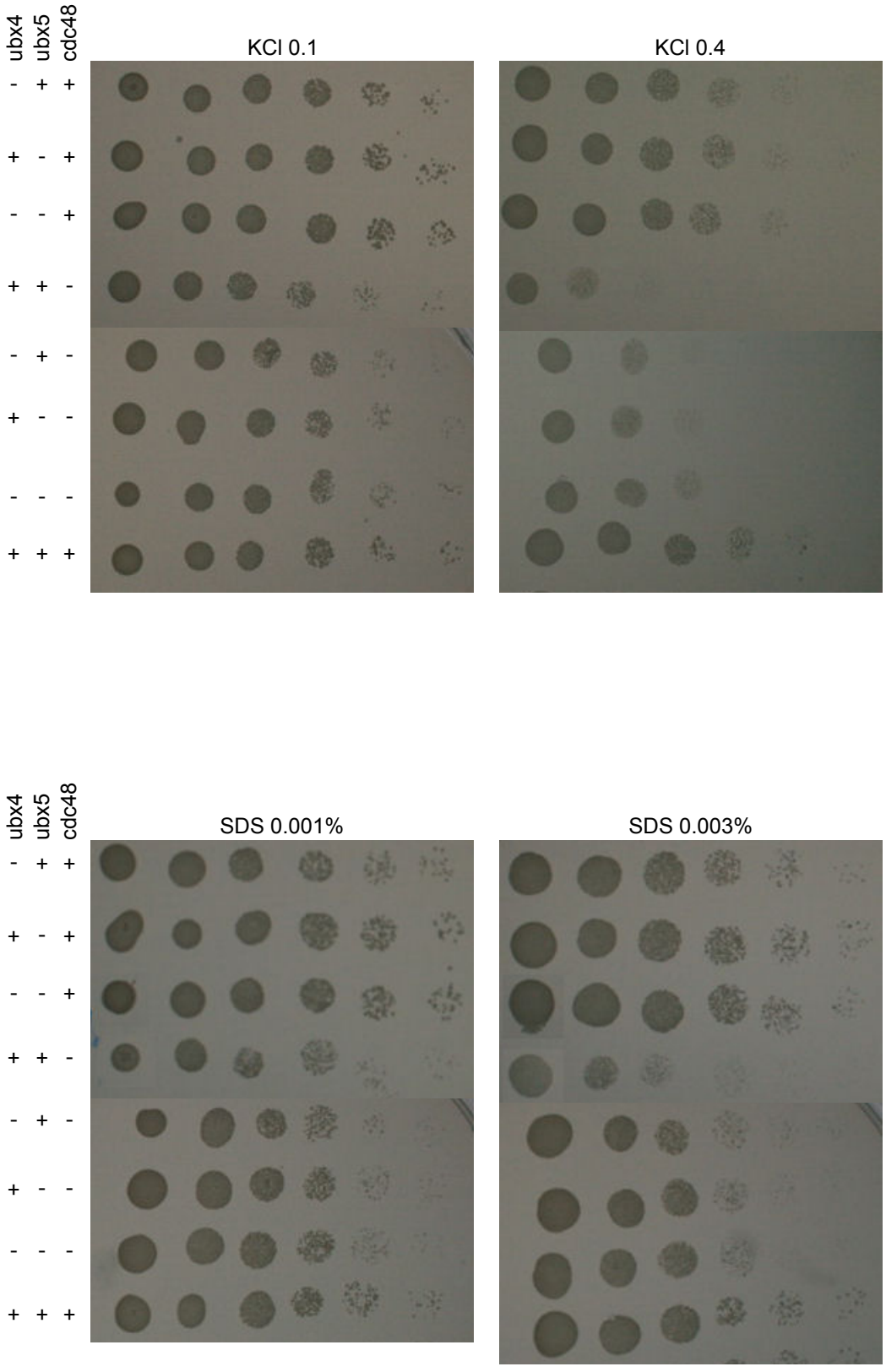

Figure B.4: Colony growth on potassium chloride and SDS containing media.

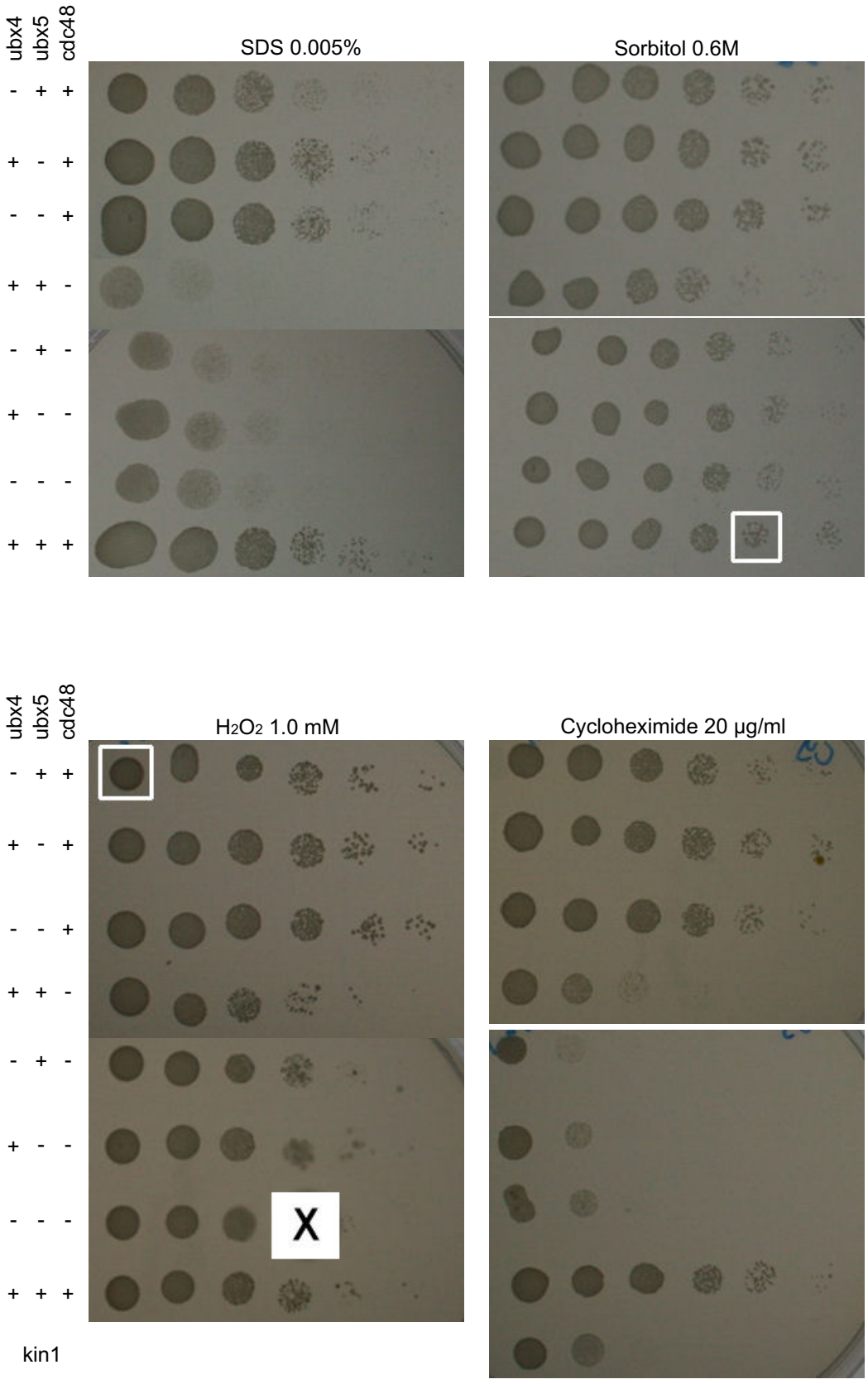

Figure B.5: Colony growth on SDS, sorbitol, hydrogen peroxide and cycloheximide media

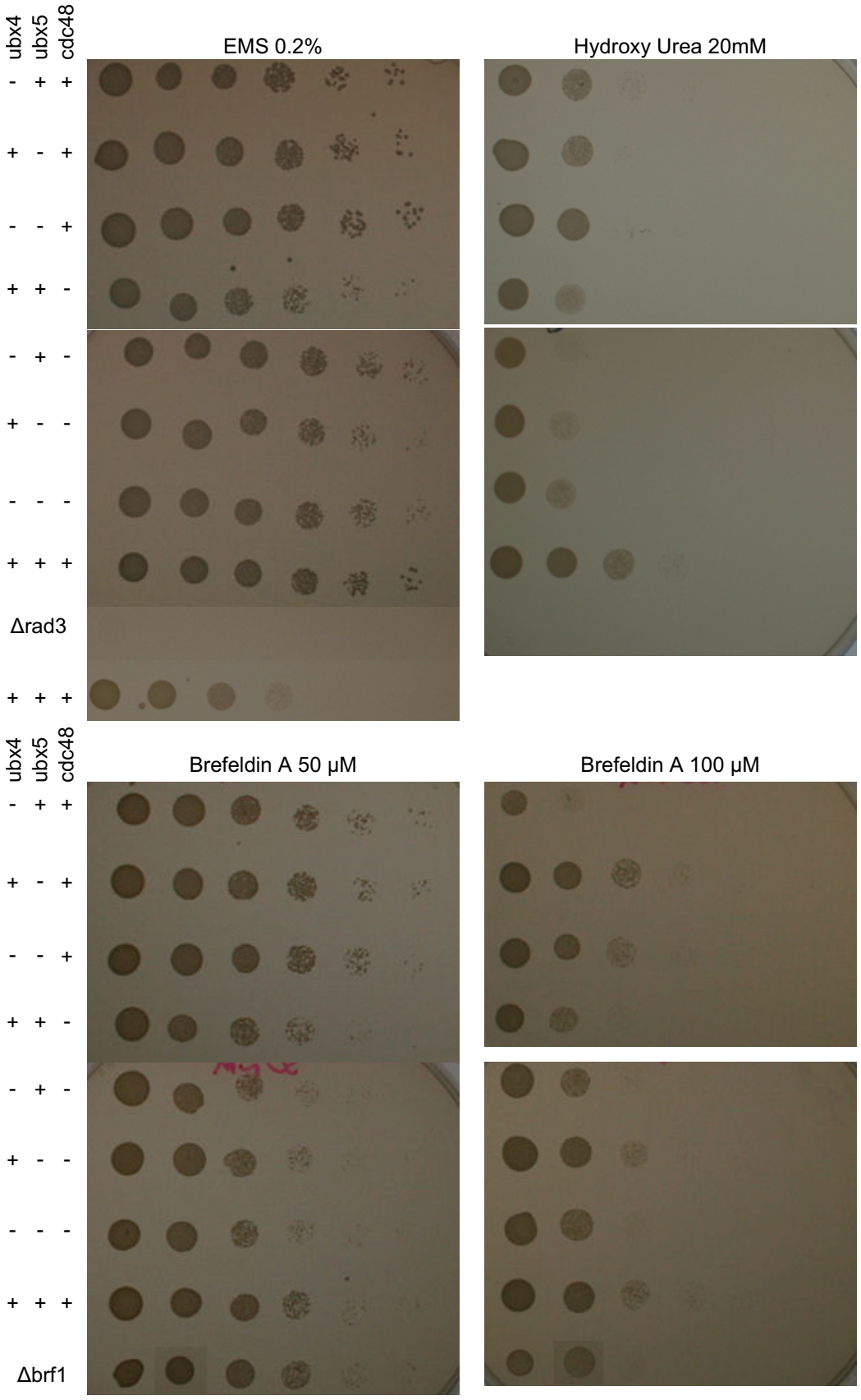

Figure B.6: Colony growth on EMS, hydroxyurea and brefeldin A containing media

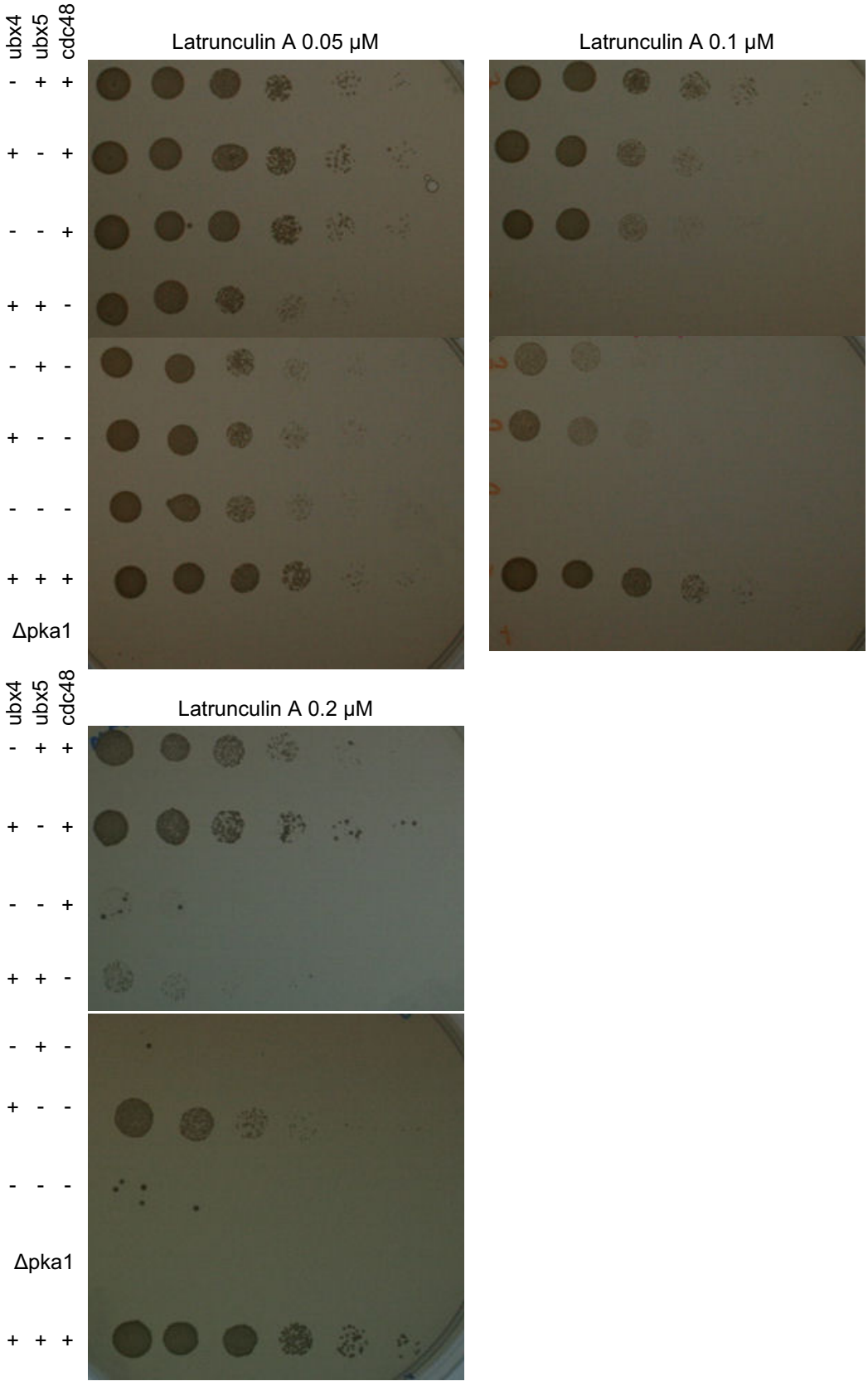

Figure B.7: Colony growth on latrunculin A containing media

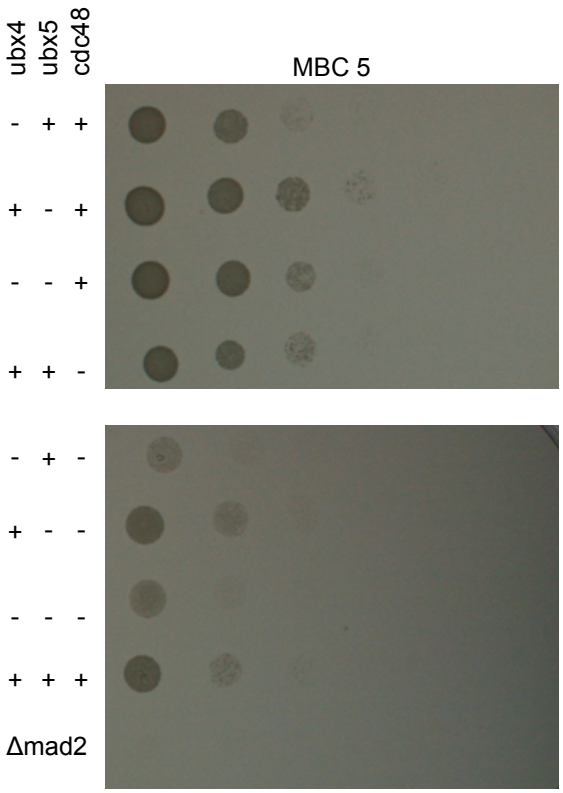

Figure B.8: Colony growth on MBC containing media

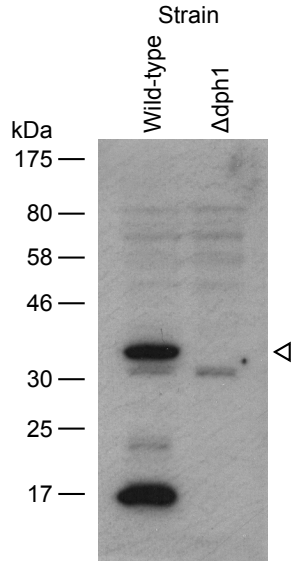

Figure B.9: Western blot of total protein extract from wild-type and Δ*dph1 S. pombe* probed with Dph1 antibody. Dph1 is indicated with the open arrowhead.

B.4 *In vivo* pulldowns

Preliminary experiments appeared to identify an *in vivo* interaction between Dph1 and HA tagged Mlp1 in *S. pombe* protein extracts (Figure B.10). Subsequent attempts to reproduce the initial results were unsuccessful, and additionally failed to demonstrate interaction between Dph1 and Pus1, indicating technical problems with the experiment. High levels of detergent were found to be necessary for the release of Mlp1 from the mitochondria (data not shown), which may have in turn disrupted Dph1 interactions.

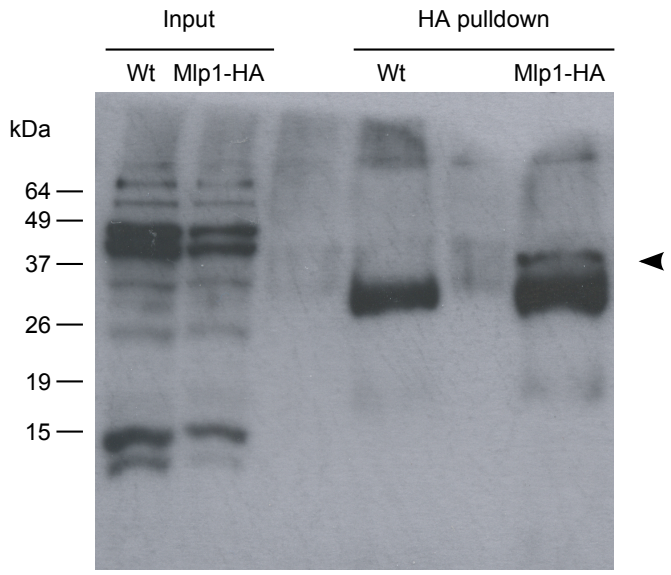

Figure B.10: An *in vivo* interaction between Dph1 and HA tagged Mlp1. Protein extracts were prepared from *S. pombe* expressing either wild-type Mlp1 protein, or a form tagged with the HA epitope tag at the C-terminus. Both proteins were under expression of the native promoter. Extracts were subject to immunoprecipitation with antibodies raised against the HA tag. Subsequently, bound proteins were eluted, were separated by SDS-PAGE, and were subject to western blotting. Blots were probed with Dph1 antibodies. A band corresponding to the size of Dph1 was found to precipitate only in the presence of HA tagged Mlp1.

Appendix C

Yeast Two-Hybrid

Colony	Bait	Colony Size	-WLH	-WLHA	XGAL	Score	Band Size (kb)	Sequence	Retests	Cdc48	His5
A1	Ubx4	++++	+++	+++	++++	13	3	Cdc48	Yes	+	-
B4	Ubx4	++++	+++	+++	++++	13	3			+	-
C6	Ubx4	++++	+++	+++	++++	13	3			+	-
C7	Ubx4	++++	+++	+++	++++	13	3.5	Ribosomal Protein S6 + Cdc48 PCR band		+	
C8	Ubx4	++++	+++	+++	++++	13	0.7			+	
D5	Ubx4	++++	+++	+++	++++	13	0.7			+	

Colony	Bait	Colony Size	-WLH	-WLHA	XGAL	Score	Band Size (kb)	Sequence	Retests	Cdc48	His5
E3	Ubx4	++++	+++	+++	++++	13				+	
A3	Ubx4	++	+++	+++	+++	12	3			+	
A6	Ubx4	++++	+++	+++	+++	12	0.2	Empty + Cdc48		+	-
N8	Ubx4	+++	++++	+++	+	11	1				
J2	Ubx5	++++	+++	++	+++	10					
A5	Ubx4	++++	+++	++	++	9		40S ribosomal protein S15 (rps15)	No		
A8	Ubx4	++	+++	++	++	9	0.7	60S acidic ribosomal protein P2A subunit	No	-	-
I3	Ubx5	++++	+++	+	+++	8	2.8				
I6	Ubx5	++++	+++	+	+++	8	0	Empty			
I7	Ubx5	++++	+++	+	+++	8	0.7 / 2.5				
J8	Ubx5	++++	++	++	+	7	1.5				
K8	Ubx5	++++	++++	-	+++	7	1.8				
D2	Ubx4	++++	+++	-	+++	6	1.1				
E4	Ubx4	+++	+++	-	+++	6			FP		
F6	Ubx4	++	+++	-	+++	6					
G6	Ubx4	+-	+++	-	+++	6					
H2	Ubx5	++++	+++	-	+++	6	1				
J1	Ubx5	++++	+++	+	+	6					

Colony	Bait	Colony Size	-WLH	-WLHA	XGAL	Score	Band Size (kb)	Sequence	Retests	Cdc48	His5
K1	Ubx5	+++	++++	-	++	6					
K3	Ubx5	+++	++++	-	++	6					
M2	Ubx5	+++	++++	-	++	6					
O4	Ubx5	++	+++	-	+++	6					
A7	Ubx4	+-	+	++	-	5					
B5	Ubx4	+++	+++	-	++	5		Nonsense (His5?)	FP		
C9	Ubx4	++++	+	++	-	5					
D1	Ubx4	++++	+++	-	++	5	3.5				
D4	Ubx4	++++	+++	-	++	5	2.9				
D7	Ubx4	++++	+++	-	++	5	1.8				
D9	Ubx4	++++	+++	-	++	5					
E1	Ubx4	++++	+++	-	++	5	1				
E2	Ubx4	++++	+++	-	++	5	2.1				
E6	Ubx4	+++	+++	-	++	5	1.1				
E7	Ubx4	+++	+++	-	++	5					
F3	Ubx4	+++	+++	-	++	5					
F4	Ubx4	+++	+++	-	++	5					
F5	Ubx4	+++	+++	-	++	5					
G3	Ubx4	+-	+++	-	++	5					
G4	Ubx4	+-	+++	-	++	5					

Colony	Bait	Colony Size	-WLH	-WLHA	XGAL	Score	Band Size (kb)	Sequence	Retests	Cdc48	His5
G7	Ubx4	+-	+++	-	++	5					
G9	Ubx4	+-	+++	-	++	5					
H5	Ubx5	+++	+++	-	++	5					
H6	Ubx5	+++	+++	-	++	5					
I1	Ubx5	++++	+++	-	++	5					
I2	Ubx5	++++	+++	-	++	5	0.5	Thioredoxin Reductase (Trr1)	FP	-	-
I4	Ubx5	++++	+++	-	++	5					
I5	Ubx5	++++	+++	+	-	5					
I8	Ubx5	++++	+++	-	++	5					
J3	Ubx5	++++	+++	-	++	5					
J6	Ubx5	++++	+++	-	++	5					
J7	Ubx5	++++	+++	-	++	5					
K2	Ubx5	+++	+++	-	++	5					
K9	Ubx5	+++	++	-	+++	5					
L8	Ubx5	+++	++++	-	+	5					
L9	Ubx5	+++	+++	-	++	5					
M3	Ubx5	+++	+++	-	++	5					
M4	Ubx5	+++	+++	-	++	5					
M6	Ubx5	+++	++++	-	+	5					
N1	Ubx5	+++	+++	-	++	5					

Colony	Bait	Colony Size	-WLH	-WLHA	XGAL	Score	Band Size (kb)	Sequence	Retests	Cdc48	His5
N2	Ubx5	+++	+++	-	++	5					
N4	Ubx5	++++	+++	-	++	5					
N9	Ubx4	+++	+++	-	++	5					
O1	Ubx4	+++	++++	-	+	5					
O9	Ubx5	++	++++	-	+	5					
Q1	Ubx5	++	+++	-	++	5					
R1	Ubx5	++	++++	-	+	5					
J9	Ubx5	++++	-0.5	++	-	4.5					
A4	Ubx4	+-	-	++	-	4					
B6	Ubx4	+++	++	-	++	4		Genomic region CII 4258955-4259374	No		
B8	Ubx4	++	++	-	++	4			No		
D6	Ubx4	++++	+++	-	+	4	1.6				
D8	Ubx4	++++	++	+	-	4	0	Empty			
E5	Ubx4	++	+	-	+++	4					
F2	Ubx4	+++	++	-	++	4					
G1	Ubx4	++	++	-	++	4					
G8	Ubx4	+-	+++	-	+	4					
H3	Ubx5	++++	+++	-	+	4	2.8	NRRL Y-12796 26S ribosomal RNA gene	No	-	+

Colony	Bait	Colony Size	-WLH	-WLHA	XGAL	Score	Band Size (kb)	Sequence	Retests	Cdc48	His5
H4	Ubx5	+++	++	-	++	4					
H7	Ubx5	+++	++	-	++	4					
J4	Ubx5	++++	++	-	++	4					
K4	Ubx5	+++	++	-	++	4					
L2	Ubx5	+++	+++	-	+	4					
L3	Ubx5	+++	+++	-	+	4					
L4	Ubx5	+++	+++	-	+	4					
M7	Ubx5	+++	+++	-	+	4					
P7	Ubx5	++	++	-	++	4					
Q2	Ubx5	++	+	-	+++	4					
Q6	Ubx5	++	++	-	++	4					
Q9	Ubx5	++	++	-	++	4					
C1	Ubx4	+++	+++	-	-+	3.5	2				
A9	Ubx4	+	+	-	++	3			No		
B1	Ubx4	+	+	-	++	3		40S ribosomal protein S3a (Rps1-2)	No		
B2	Ubx4	++++	+	-	++	3			FP		
B3	Ubx4	++++	+++	-	-	3		40S ribosomal protein S5 (rps5-2)	No		
C2	Ubx4	+++	+++	-	-	3	200	Empty Shuttle Vector, Also Larger!	No	-	-

Colony	Bait	Colony Size	-WLH	-WLHA	XGAL	Score	Band Size (kb)	Sequence	Retests	Cdc48	His5
C3	Ubx4	+++	+	-	++	3	0.7 / 2				
C4	Ubx4	+++	+	-	++	3	2.1				
C5	Ubx4	++	+	-	++	3	0.8				
E8	Ubx4	+++	+	-	++	3					
E9	Ubx4	+++	+	-	++	3					
F8	Ubx4	++	+	-	++	3					
G2	Ubx4	++	+	-	++	3					
H1	Ubx5	++++	+++	-	-	3	1.5	40S ribosomal protein S18 (rps18-1)		-	+
H8	Ubx5	+++	+++	-	-	3					
K5	Ubx5	+++	++	-	+	3					
L5	Ubx5	+++	++	-	+	3					
M5	Ubx5	+++	+++	-	-	3					
N3	Ubx5	+++	+	-	++	3					
O2	Ubx4	++	++	-	+	3					
O7	Ubx5	++	++	-	+	3					
O8	Ubx5	++	++	-	+	3					
P1	Ubx5	++	++	-	+	3					
P2	Ubx5	++	++	-	+	3					
P5	Ubx5	++	+	-	++	3					

Colony	Bait	Colony Size	-WLH	-WLHA	XGAL	Score	Band Size (kb)	Sequence	Retests	Cdc48	His5
R3	Ubx5	++	+	-	++	3					
R7	Ubx5	++	+	-	++	3					
R9	Ubx5	++	+	-	++	3					
F7	Ubx4	++	-+	-	++	2.5	2				
G5	Ubx4	+-	-+	-	++	2.5					
L6	Ubx5	+++	++	-	-+	2.5					
D3	Ubx4	++++	+	-	+	2	0	Empty			
F1	Ubx4	+++	+	-	+	2					
F9	Ubx4	++	+	-	+	2					
H9	Ubx5	+++	++	-	-	2					
J5	Ubx5	++++	++	-	-	2					
K6	Ubx5	+++	++	-	-	2					
L1	Ubx5	+++	+	-	+	2					
L7	Ubx5	+++	+	-	+	2					
O3	Ubx5	++	+	-	+	2					
O6	Ubx5	++	-	-	++	2					
R4	Ubx5	++	-	-	++	2					
P3	Ubx5	++	+	-	-+	1.5					
B7	Ubx4	++	+	-	-	1			No		
B9	Ubx4	+++	+	-	-	1					

Colony	Bait	Colony Size	-WLH	-WLHA	XGAL	Score	Band Size (kb)	Sequence	Retests	Cdc48	His5
K7	Ubx5	+++	+	-	-	1					
N5	Ubx5	++	-	-	+	1					
P8	Ubx5	++	-	-	+	1					
P9	Ubx5	++	-	-	+	1					
Q4	Ubx5	++	-	-	+	1					
R2	Ubx5	++	+	-	-	1					
R8	Ubx5	++	+	-	-	1					
I9	Ubx5	++++	-+	-	-	0.5					
M9	Ubx5	+++	-	-	-+	0.5					
A2	Ubx4	+-	-	-	-	0					
M1	Ubx5	+++	-	-	-	0					
M8	Ubx5	+++	-	-	-	0					
N6	Ubx5	++	-	-	-	0					
N7	Ubx5	++	-	-	-	0					
O5	Ubx5	++	-	-	-	0					
P4	Ubx5	++	-	-	-	0					
P6	Ubx5	++	-	-	-	0					
Q3	Ubx5	++	-	-	-	0					
Q5	Ubx5	++	-	-	-	0					
Q7	Ubx5	++	-	-	-	0					

Colony	Bait	Colony Size	-WLH	-WLHA	XGAL	Score	Band Size (kb)	Sequence	Retests	Cdc48	His5
Q8	Ubx5	++	-	-	-	0					
R5	Ubx5	++	-	-	-	0					
R6	Ubx5	++	-	-	-	0					

Table C.1: Collated results of a yeast two hybrid screen with Ubx4 and Ubx5 proteins. Results are sorted in approximate order of interaction strength. Growth was scored by eye and is indicated in the table by an increasing number of + symbols. Colony size represents growth on the initial selection, and the columns -WHL and -WHLA indicate subsequent growth on less stringent and more stringent selection respectively. XGAL indicates the results of the β-galactosidase assay. The score is an attempt to summarise the overall strength of each interaction; it is the sum of the fourth and sixth columns, as indicated by the number of + symbols, plus twice the fifth column. Cdc48 and His5 represent the results of PCRs used to detect copies of the corresponding alleles. Cdc48 PCRs were conducted with primers AD and JG1R, or AD3' and JG2D.

Appendix D

Substrate Creation

D.1 Fzo1-GFP

Fzo1 was tagged with C-terminal GFP under the control of its native promoter. Morag Robertson transformed wild-type *S. pombe* with a GFP cassette targeted to the *fzo1* gene, to provide a selection of colonies which were positive for the insert. Subsequent analysis by PCR was used to identify those colonies in which the cassette had integrated at the correct site (Figure D.1).

To confirm correct expression of the GFP tagged Fzo1, and to ensure that the tag had not affected the localization of the protein, Fzo1-GFP strains were studied by fluorescence microscopy, MitoTracker red was used to stain the mitochondria (Figure D.2). The Fzo1-GFP signal co-localized with the MitoTracker red mitochondrial marker, indicating that Fzo1 was correctly localized to the mitochondrial as expected.

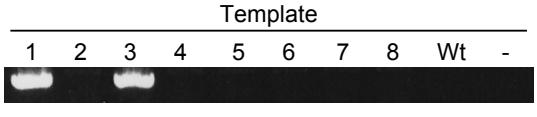

Figure D.1: DNA extracted from eight potential Fzo-GFP expressing strains was tested by PCR with oligonucleotides in *fzo1* itself and the tagging cassette. A PCR product would only be apparent in strains containing the cassette integrated at the *fzo1* locus. Strains 1 and 3 contain a correctly integrated GFP cassette.

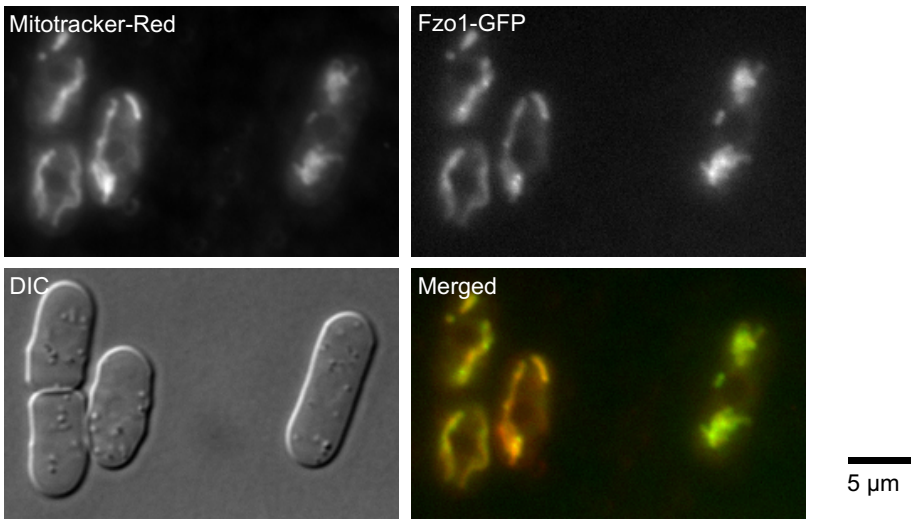

Figure D.2: Fzo1 localization to the mitochondria. Fzo1 is shown as an endogenously expressed form tagged with a C-terminal GFP. Mitochondria are stained with MitoTracker red. DIC is used to show the overall morphology.

Bibliography

Acharya, U., Jacobs, R., Peters, J. M., Watson, N., Farquhar, M. G., and Malhotra, V. (1995). The formation of Golgi stacks from vesiculated Golgi membranes requires two distinct fusion events. *Cell*, 82(6):895–904.

Agatep, R., Kirkpatrick, R. D., Parchaliuk, D. L., Woods, R. A., and Gietz, R. D. (1998). Transformation of Saccharomyces cerevisiae by the lithium acetate/single-stranded carrier DNA/polyethylene glycol protocol. *Technical Tips Online*, 3(1):133–137.

Alberts, S. M., Sonntag, C., Schäfer, A., and Wolf, D. H. (2009). Ubx4 modulates cdc48 activity and influences degradation of misfolded proteins of the endoplasmic reticulum. *The Journal of biological chemistry*, 284(24):16082–9.

Altmann, K. and Westermann, B. (2005). Role of essential genes in mitochondrial morphogenesis in Saccharomyces cerevisiae. *Molecular biology of the cell*, 16(11):5410–17.

Altschul, S. F., Gish, W., Miller, W., Myers, E. W., and Lipman, D. J. (1990). Basic local alignment search tool. *Journal of molecular biology*, 215(3):403–10.

Andersen, P. M., Nilsson, P., Ala-Hurula, V., Keränen, M. L., Tarvainen, I., Haltia, T., Nilsson, L., Binzer, M., Forsgren, L., and Marklund, S. L. (1995). Amyotrophic lateral sclerosis associated with homozygosity for an Asp90Ala mutation in CuZn-superoxide dismutase. *Nature genetics*, 10(1):61–6.

Atkin, J. D., Farg, M. A., Turner, B. J., Tomas, D., Lysaght, J. A., Nunan, J., Rembach, A., Nagley, P., Beart, P. M., Cheema, S. S., and Horne, M. K. (2006). Induction of the unfolded protein response in familial amyotrophic lateral sclerosis and association of protein-disulfide isomerase with superoxide dismutase 1. *The Journal of biological chemistry*, 281(40):30152–65.

Azad, A. K., Tani, T., Shiki, N., Tsuneyoshi, S., Urushiyama, S., and Ohshima, Y.

(1997). Isolation and molecular characterization of mRNA transport mutants in Schizosaccharomyces pombe. *Molecular biology of the cell*, 8(5):825–41.

Bähler, J., Wu, J., Longtine, M. S., Shah, N. G., Mckenzie III, A., Steever, A. B., Wach, A., Philippsen, P., and Pringle, J. R. (1998). Heterologous modules for efficient and versatile PCR-based gene targeting inSchizosaccharomyces pombe. *Yeast*, 14(10):943–951.

Bailly, V., Lauder, S., Prakash, S., and Prakash, L. (1997). Yeast DNA repair proteins Rad6 and Rad18 form a heterodimer that has ubiquitin conjugating, DNA binding, and ATP hydrolytic activities. *The Journal of biological chemistry*, 272(37):23360–5.

Baker, R., Tobias, J. W., and Varshavsky, A. (1992). Ubiquitin-specific proteases of Saccharomyces cerevisiae. Cloning of UBP2 and UBP3, and functional analysis of the UBP gene family. *Journal of Biological Chemistry*, 267(32):23364–23375.

Bays, N. W., Wilhovsky, S. K., Goradia, A., Hodgkiss-Harlow, K., and Hampton, R. Y. (2001). HRD4/NPL4 is required for the proteasomal processing of ubiquitinated ER proteins. *Molecular biology of the cell*, 12(12):4114–4128.

Beitz, E. (2000). TEXshade: shading and labeling of multiple sequence alignments using LATEX2 epsilon. *Bioinformatics*, 16(2):135–9.

Biederer, T., Volkwein, C., and Sommer, T. (1996). Degradation of subunits of the Sec61p complex, an integral component of the ER membrane, by the ubiquitin-proteasome pathway. *The EMBO journal*, 15(9):2069–76.

Bimbó, A., Jia, Y., Poh, S. L., Karuturi, R. K. M., den Elzen, N., Peng, X., Zheng, L., O'Connell, M., Liu, E. T., Balasubramanian, M. K., and Liu, J. (2005). Systematic deletion analysis of fission yeast protein kinases. *Eukaryotic cell*, 4:799–813.

Boone, C., Bussey, H., and Andrews, B. J. (2007). Exploring genetic interactions and networks with yeast. *Nature reviews. Genetics*, 8(6):437–49.

Borchelt, D. R., Lee, M. K., Slunt, H. S., Guarnieri, M., Xu, Z. S., Wong, P. C., Brown, R. H., Price, D. L., Sisodia, S. S., and Cleveland, D. W. (1994). Superoxide dismutase 1 with mutations linked to familial amyotrophic lateral sclerosis possesses significant activity. *Proceedings of the National Academy of Sciences*, 91(17):8292–6.

Bruderer, R. M., Brasseur, C., and Meyer, H. H. (2004). The AAA ATPase p97/VCP interacts with its alternative co-factors, Ufd1-Npl4 and p47, through a common bipartite binding mechanism. *The Journal of biological chemistry*, 279(48):49609–49616.

Buchberger, A., Howard, M. J., Proctor, M., and Bycroft, M. (2001). The UBX domain: a widespread ubiquitin-like module. *Journal of molecular biology*, 307(1):17–24.

Cao, K., Nakajima, R., Meyer, H. H., and Zheng, Y. (2003). The AAA-ATPase Cdc48/p97 regulates spindle disassembly at the end of mitosis. *Cell*, 115(3):355–367.

Carvalho, P., Goder, V., and Rapoport, T. A. (2006). Distinct ubiquitin-ligase complexes define convergent pathways for the degradation of ER proteins. *Cell*, 126(2):361–73.

Chang, H. C. and Lindquist, S. (1994). Conservation of Hsp90 macromolecular complexes in Saccharomyces cerevisiae. *The Journal of biological chemistry*, 269(40):24983–8.

Chang, H. C., Nathan, D. F., and Lindquist, S. (1997). In vivo analysis of the Hsp90 cochaperone Sti1 (p60). *Molecular and cellular biology*, 17(1):318–25.

Chiron, S., Gaisne, M., Guillou, E., Belenguer, P., Clark-Walker, G. D., and Bonnefoy, N. (2007). Studying mitochondria in an attractive model: Schizosaccharomyces pombe. *Methods in molecular biology (Clifton, N.J.)*, 372:91–105.

Clonetech Laboratories (2001). *Protocol No. PT3024-1*, chapter Appendix C, pages 53–55. Clontech, Palo Alto, CA, version no edition.

Cohen, M. M. J., Leboucher, G. P., Livnat-Levanon, N., Glickman, M. H., and Weissman, A. M. (2008). Ubiquitin-proteasome-dependent degradation of a mitofusin, a critical regulator of mitochondrial fusion. *Molecular biology of the cell*, 19(6):2457–64.

Coué, M., Brenner, S. L., Spector, I., and Korn, E. D. (1987). Inhibition of actin polymerization by latrunculin A. *FEBS letters*, 213(2):316–318.

Dantuma, N. P., Heinen, C., and Hoogstraten, D. (2009). The ubiquitin receptor Rad23: at the crossroads of nucleotide excision repair and proteasomal degradation. *DNA repair*, 8(4):449–60.

Davidse, L. C. and Flach, W. (1978). Interaction of thiabendazole with fungal tubulin. *Biochimica et biophysica acta*, 543(1):82–90.

DeLaBarre, B. and Brunger, A. T. (2003). Complete structure of p97/valosin-containing protein reveals communication between nucleotide domains. *Nature structural biology*, 10(10):856–863.

DeLaBarre, B. and Brunger, A. T. (2005). Nucleotide dependent motion and mechanism of action of p97/VCP. *Journal of molecular biology*, 347(2):437–52.

DeLaBarre, B., Christianson, J. C., Kopito, R. R., and Brunger, A. T. (2006). Central pore residues mediate the p97/VCP activity required for ERAD. *Molecular cell*, 22(4):451–62.

Deng, M. and Hochstrasser, M. (2006). Spatially regulated ubiquitin ligation by an ER/nuclear membrane ligase. *Nature*, 443(7113):827–31.

Deveraux, Q., Ustrell, V., Pickart, C. M., and Rechsteiner, M. (1994). A 26 S protease subunit that binds ubiquitin conjugates. *The Journal of biological chemistry*, 269(10):7059–61.

Díaz-Martínez, L. A., Kang, Y., Walters, K. J., and Clarke, D. J. (2006). Yeast UBL-UBA proteins have partially redundant functions in cell cycle control. *Cell division*, 1:28.

Dohmen, R. J., Madura, K., Bartel, B., and Varshavsky, A. (1991). The N-end rule is mediated by the UBC2(RAD6) ubiquitin-conjugating enzyme. *Proceedings of the National Academy of Sciences*, 88:7351–5.

Elder, R. T., Song, X.-q., Chen, M., Hopkins, K. M., Lieberman, H. B., and Zhao, Y. (2002). Involvement of rhp23, a Schizosaccharomyces pombe homolog of the human HHR23A and Saccharomyces cerevisiae RAD23 nucleotide excision repair genes, in cell cycle control and protein ubiquitination. *Nucleic acids research*, 30(2):581–91.

Escobar-Henriques, M., Westermann, B., and Langer, T. (2006). Regulation of mitochondrial fusion by the F-box protein Mdm30 involves proteasome-independent turnover of Fzo1. *The Journal of cell biology*, 173(5):645–50.

Fernández-Sáiz, V. and Buchberger, A. (2010). Imbalances in p97 co-factor interactions in human proteinopathy. *EMBO reports*, 11(6):479–85.

Finley, D., Ozkaynak, E., and Varshavsky, a. (1987). The yeast polyubiquitin gene is essential for resistance to high temperatures, starvation, and other stresses. *Cell*, 48(6):1035–46.

Finn, R. D., Mistry, J., Tate, J., Coggill, P., Heger, A., Pollington, J. E., Gavin, O. L., Gunasekaran, P., Ceric, G., Forslund, K., Holm, L., Sonnhammer, E. L. L., Eddy, S. R., and Bateman, A. (2010). The Pfam protein families database. *Nucleic acids research*, 38(Database issue):D211–22.

Fritz, S., Weinbach, N., and Westermann, B. (2003). Mdm30 is an F-box protein

required for maintenance of fusion-competent mitochondria in yeast. *Molecular biology of the cell*, 14(6):2303–13.

Fu, H., Sadis, S., Rubin, D. M., Glickman, M., van Nocker, S., Finley, D., and Vierstra, R. D. (1998). Multiubiquitin chain binding and protein degradation are mediated by distinct domains within the 26 S proteasome subunit Mcb1. *The Journal of biological chemistry*, 273(4):1970–81.

Funakoshi, M., Sasaki, T., Nishimoto, T., and Kobayashi, H. (2002). Budding yeast Dsk2p is a polyubiquitin-binding protein that can interact with the proteasome. *Proceedings of the National Academy of Sciences of the United States of America*, 99(2):745–50.

Geisler, S., Holmström, K. M., Skujat, D., Fiesel, F. C., Rothfuss, O. C., Kahle, P. J., and Springer, W. (2010). PINK1/Parkin-mediated mitophagy is dependent on VDAC1 and p62/SQSTM1. *Nature cell biology*, 12(2):119–31.

Germain, D. (2008). Ubiquitin-dependent and -independent mitochondrial protein quality controls: implications in ageing and neurodegenerative diseases. *Molecular microbiology*, 70(6):1334–41.

Glickman, M. H., Rubin, D. M., Coux, O., Wefes, I., Pfeifer, G., Cjeka, Z., Baumeister, W., Fried, V. A., and Finley, D. (1998). A subcomplex of the proteasome regulatory particle required for ubiquitin-conjugate degradation and related to the cop9-signalosome and eif3. *Cell*, 94(5):615–23.

Gordon, C., McGurk, G., Dillon, P., Rosen, C., and Hastie, N. D. (1993). Defective mitosis due to a mutation in the gene for a fission yeast 26S protease subunit. *Nature*, 366(6453):355–7.

Gordon, C., McGurk, G., Wallace, M., and Hastie, N. D. (1996). A conditional lethal mutant in the fission yeast 26 S protease subunit mts3+ is defective in metaphase to anaphase transition. *The Journal of biological chemistry*, 271(10):5704–11.

Gregan, J., Rabitsch, P. K., Rumpf, C., Novatchkova, M., Schleiffer, A., and Nasmyth, K. (2006). High-throughput knockout screen in fission yeast. *Nature protocols*, 1(5):2457–2464.

Guan, K. and Dixon, J. (1991). Eukaryotic proteins expressed in : An improved thrombin cleavage and purification procedure of fusion proteins with glutathione -transferase. *Analytical Biochemistry*, 192(2):262–267.

Guyant-Marechal, L., Laquerriere, A., Duyckaerts, C., Dumanchin, C., Bou, J., Dugny,

F., Le Ber, I., Frebourg, T., Hannequin, D., and Campion, D. (2006). Valosin-containing protein gene mutations: clinical and neuropathologic features. *Neurology*, 67(4):644–651.

Hales, K. G. and Fuller, M. T. (1997). Developmentally regulated mitochondrial fusion mediated by a conserved, novel, predicted GTPase. *Cell*, 90(1):121–9.

Hanna, J., Leggett, D. S., and Finley, D. (2003). Ubiquitin depletion as a key mediator of toxicity by translational inhibitors. *Molecular and cellular biology*, 23(24):9251–61.

Hänzelmann, P., Stingele, J., Hofmann, K., Schindelin, H., and Raasi, S. (2010). The yeast E4 ubiquitin ligase Ufd2 interacts with the ubiquitin-like domains of Rad23 and Dsk2 via a novel and distinct ubiquitin-like binding domain. *The Journal of biological chemistry*, 285(26):20390–8.

Hartmann-Petersen, R. (2003). Ubiquitin binding proteins protect ubiquitin conjugates from disassembly. *FEBS Letters*, 535(1-3):77–81.

Hartmann-Petersen, R., Wallace, M., Hofmann, K., Koch, G., Johnsen, A. H., Hendil, K. B., and Gordon, C. (2004). The Ubx2 and Ubx3 cofactors direct Cdc48 activity to proteolytic and nonproteolytic ubiquitin-dependent processes. *Current biology*, 14(9):824–828.

Haubenberger, D., Bittner, R. E., Rauch-Shorny, S., Zimprich, F., Mannhalter, C., Wagner, L., Mineva, I., Vass, K., Auff, E., and Zimprich, A. (2005). Inclusion body myopathy and Paget disease is linked to a novel mutation in the VCP gene. *Neurology*, 65(8):1304–1305.

Hay, R. T. (2005). SUMO: a history of modification. *Molecular cell*, 18(1):1–12.

Hermann, G. J., Thatcher, J. W., Mills, J. P., Hales, K. G., Fuller, M. T., Nunnari, J., and Shaw, J. M. (1998). Mitochondrial fusion in yeast requires the transmembrane GTPase Fzo1p. *The Journal of cell biology*, 143(2):359–73.

Hershko, a. and Ciechanover, A. (1998). The ubiquitin system. *Annual review of biochemistry*, 67:425–79.

Hershko, A., Heller, H., Elias, S., and Ciechanover, A. (1983). Components of ubiquitin-protein ligase system. Resolution, affinity purification, and role in protein breakdown. *The Journal of biological chemistry*, 258(13):8206–14.

Hertz-Fowler, C., Peacock, C. S., Wood, V., Aslett, M., Kerhornou, A., Mooney, P., Tivey, A., Berriman, M., Hall, N., Rutherford, K., Parkhill, J., Ivens, A. C.,

Rajandream, M.-A., and Barrell, B. (2004). GeneDB: a resource for prokaryotic and eukaryotic organisms. *Nucleic acids research*, 32(Database issue):D339–43.

Heubes, S. and Stemmann, O. (2007). The AAA-ATPase p97-Ufd1-Npl4 is required for ERAD but not for spindle disassembly in Xenopus egg extracts. *Journal of cell science*, 120(Pt 8):1325–9.

Hilton, J. L., Kearney, P. C., and Ames, B. N. (1965). Mode of action of the herbicide, 3-amino-1,2,4-triazole(amitrole): inhibition of an enzyme of histidine biosynthesis. *Archives of biochemistry and biophysics*, 112(3):544–7.

Hiyama, H., Yokoi, M., Masutani, C., Sugasawa, K., Maekawa, T., Tanaka, K., Hoeijmakers, J. H., and Hanaoka, F. (1999). Interaction of hHR23 with S5a. The ubiquitin-like domain of hHR23 mediates interaction with S5a subunit of 26 S proteasome. *The Journal of biological chemistry*, 274(39):28019–25.

Hofmann, K. and Falquet, L. (2001). A ubiquitin-interacting motif conserved in components of the proteasomal and lysosomal protein degradation systems. *Trends in biochemical sciences*, 26(6):347–50.

Huang, H., Kahana, A., Gottschling, D. E., Prakash, L., and Liebman, S. W. (1997). The ubiquitin-conjugating enzyme Rad6 (Ubc2) is required for silencing in Saccharomyces cerevisiae. *Molecular and cellular biology*, 17(11):6693–9.

Hulo, N., Bairoch, A., Bulliard, V., Cerutti, L., De Castro, E., Langendijk-Genevaux, P. S., Pagni, M., and Sigrist, C. J. A. (2006). The PROSITE database. *Nucleic Acids Research*, 34(suppl_1):D227–230.

Huyton, T., Pye, V. E., Briggs, L. C., Flynn, T. C., Beuron, F., Kondo, H., Ma, J., Zhang, X., and Freemont, P. S. (2003). The crystal structure of murine p97/VCP at 3.6Å. *Journal of Structural Biology*, 144(3):337–348.

Ikai, N. and Yanagida, M. (2006). Cdc48 is required for the stability of Cut1/separase in mitotic anaphase. *Journal of structural biology*, 156(1):50–61.

Jain, E., Bairoch, A., Duvaud, S., Phan, I., Redaschi, N., Suzek, B. E., Martin, M. J., McGarvey, P., and Gasteiger, E. (2009). Infrastructure for the life sciences: design and implementation of the UniProt website. *BMC bioinformatics*, 10(1):136.

James, P., Halladay, J., and Craig, E. A. (1996). Genomic libraries and a host strain designed for highly efficient two-hybrid selection in yeast. *Genetics*, 144(4):1425–36.

Janiesch, P. C., Kim, J., Mouysset, J., Barikbin, R., Lochmuller, H., Cassata, G.,

Krause, S., and Hoppe, T. (2007). The ubiquitin-selective chaperone CDC-48/p97 links myosin assembly to human myopathy. *Nature cell biology*, 9(4):379–390.

Kanehara, K., Xie, W., and Ng, D. T. W. (2010). Modularity of the Hrd1 ERAD complex underlies its diverse client range. *The Journal of cell biology*, 188(5):707–16.

Kaye, F. J., Modi, S., Ivanovska, I., Koonin, E. V., Thress, K., Kubo, A., Kornbluth, S., and Rose, M. D. (2000). A family of ubiquitin-like proteins binds the ATPase domain of Hsp70-like Stch. *FEBS letters*, 467(2-3):348–55.

Kikuchi, H., Almer, G., Yamashita, S., Guégan, C., Nagai, M., Xu, Z., Sosunov, A. A., McKhann, G. M., and Przedborski, S. (2006). Spinal cord endoplasmic reticulum stress associated with a microsomal accumulation of mutant superoxide dismutase-1 in an ALS model. *Proceedings of the National Academy of Sciences*, 103(15):6025–30.

Kim, D.-U., Hayles, J., Kim, D., Wood, V., Park, H.-O., Won, M., Yoo, H.-S., Duhig, T., Nam, M., Palmer, G., Han, S., Jeffery, L., Baek, S.-T., Lee, H., Shim, Y. S., Lee, M., Kim, L., Heo, K.-S., Noh, E. J., Lee, A.-R., Jang, Y.-J., Chung, K.-S., Choi, S.-J., Park, J.-Y., Park, Y., Kim, H. M., Park, S.-K., Park, H.-J., Kang, E.-J., Kim, H. B., Kang, H.-S., Park, H.-M., Kim, K., Song, K., Song, K. B., Nurse, P., and Hoe, K.-L. (2010). Analysis of a genome-wide set of gene deletions in the fission yeast Schizosaccharomyces pombe. *Nature biotechnology*, 28(6):617–23.

Kim, I., Mi, K., and Rao, H. (2004). Multiple Interactions of Rad23 Suggest a Mechanism for Ubiquitylated Substrate Delivery Important in Proteolysis. *Molecular Biology of the Cell*, 15(July):3357–3365.

Klopotowski, T. and Wiater, A. (1965). Synergism of aminotriazole and phosphate on the inhibition of yeast imidazole glycerol phosphate dehydratase. *Archives of biochemistry and biophysics*, 112(3):562–6.

Koegl, M., Hoppe, T., Schlenker, S., Ulrich, H. D., Mayer, T. U., and Jentsch, S. (1999). A novel ubiquitination factor, E4, is involved in multiubiquitin chain assembly. *Cell*, 96(5):635–44.

Kondo, H., Rabouille, C., Newman, R., Levine, T. P., Pappin, D., Freemont, P., and Warren, G. (1997). P47 Is a Cofactor for P97-Mediated Membrane Fusion. *Nature*, 388(6637):75–8.

Koppen, M., Bonn, F., Ehses, S., and Langer, T. (2009). Autocatalytic processing of m-AAA protease subunits in mitochondria. *Molecular biology of the cell*, 20(19):4216–24.

Koppen, M. and Langer, T. (2007). Protein degradation within mitochondria: versatile activities of AAA proteases and other peptidases. *Critical reviews in biochemistry and molecular biology*, 42(3):221–242.

Krogh, A., Larsson, B., von Heijne, G., and Sonnhammer, E. L. (2001). Predicting transmembrane protein topology with a hidden Markov model: application to complete genomes. *Journal of molecular biology*, 305(3):567–80.

Lambertson, D., Chen, L., and Madura, K. (1999). Pleiotropic defects caused by loss of the proteasome-interacting factors Rad23 and Rpn10 of Saccharomyces cerevisiae. *Genetics*, 153(1):69–79.

Langer, T., Käser, M., Klanner, C., and Leonhard, K. (2001). AAA proteases of mitochondria: quality control of membrane proteins and regulatory functions during mitochondrial biogenesis. *Biochemical Society transactions*, 29(4):431–36.

Larkin, M. A., Blackshields, G., Brown, N. P., Chenna, R., McGettigan, P. A., McWilliam, H., Valentin, F., Wallace, I. M., Wilm, A., Lopez, R., Thompson, J. D., Gibson, T. J., and Higgins, D. G. (2007). Clustal W and Clustal X version 2.0. *Bioinformatics (Oxford, England)*, 23(21):2947–8.

Lass, A., McConnell, E., Nowis, D., Mechref, Y., Kang, P., Novotny, M. V., and Wójcik, C. (2007). A novel function of VCP (valosin-containing protein; p97) in the control of N-glycosylation of proteins in the endoplasmic reticulum. *Archives of biochemistry and biophysics*, 462(1):62–73.

Lässle, M., Blatch, G. L., Kundra, V., Takatori, T., and Zetter, B. R. (1997). Stress-inducible, murine protein mSTI1. Characterization of binding domains for heat shock proteins and in vitro phosphorylation by different kinases. *The Journal of biological chemistry*, 272(3):1876–1884.

Latterich, M., Fröhlich, K. U., and Schekman, R. (1995). Membrane fusion and the cell cycle: Cdc48p participates in the fusion of ER membranes. *Cell*, 82(6):885–893.

Letunic, I., Copley, R. R., Pils, B., Pinkert, S., Schultz, J., and Bork, P. (2006). SMART 5: domains in the context of genomes and networks. *Nucleic acids research*, 34(Database issue):D257–60.

Letunic, I., Doerks, T., and Bork, P. (2009). SMART 6: recent updates and new developments. *Nucleic acids research*, 37(Database issue):D229–32.

Liang, J., Yin, C., Doong, H., Fang, S., Peterhoff, C., Nixon, R. A., and Monteiro,

M. J. (2006). Characterization of erasin (UBXD2): a new ER protein that promotes ER-associated protein degradation. *Journal of cell science*, 119(19):4011–24.

Liu, C., van Dyk, D., Li, Y., Andrews, B., and Rao, H. (2009). A genome-wide synthetic dosage lethality screen reveals multiple pathways that require the functioning of ubiquitin-binding proteins Rad23 and Dsk2. *BMC biology*, 7:75.

Liu, J., Lillo, C., Jonsson, P. A., Vande Velde, C., Ward, C. M., Miller, T. M., Subramaniam, J. R., Rothstein, J. D., Marklund, S., Andersen, P. M., Brännström, T., Gredal, O., Wong, P. C., Williams, D. S., and Cleveland, D. W. (2004). Toxicity of familial ALS-linked SOD1 mutants from selective recruitment to spinal mitochondria. *Neuron*, 43(1):5–17.

Lowe, E. D., Hasan, N., Trempe, J. F., Fonso, L., Noble, M. E. M., Endicott, J. A., Johnson, L. N., and Brown, N. R. (2006). Structures of the Dsk2 UBL and UBA domains and their complex. *Acta crystallographica. Section D, Biological crystallography*, 62(2):177–88.

Määttänen, P., Gehring, K., Bergeron, J. J. M., and Thomas, D. Y. (2010). Protein quality control in the ER: The recognition of misfolded proteins. *Seminars in cell & developmental biology*, 21(5):500–11.

Majoor-Krakauer, D., Willems, P. J., and Hofman, A. (2003). Genetic epidemiology of amyotrophic lateral sclerosis. *Clinical genetics*, 63(2):83–101.

Margineantu, D. H., Emerson, C. B., Diaz, D., and Hockenbery, D. M. (2007). Hsp90 inhibition decreases mitochondrial protein turnover. *PloS one*, 2(10):e1066.

Martín-García, R. and Mulvihill, D. P. (2009). Myosin V spatially regulates microtubule dynamics and promotes the ubiquitin-dependent degradation of the fission yeast CLIP-170 homologue, Tip1. *Journal of cell science*, 122(21):3862–72.

Matiuhin, Y., Kirkpatrick, D. S., Ziv, I., Kim, W., Dakshinamurthy, A., Kleifeld, O., Gygi, S. P., Reis, N., and Glickman, M. H. (2008). Extraproteasomal Rpn10 restricts access of the polyubiquitin-binding protein Dsk2 to proteasome. *Molecular cell*, 32(3):415–25.

Matsuyama, A., Arai, R., Yashiroda, Y., Shirai, A., Kamata, A., Sekido, S., Kobayashi, Y., Hashimoto, A., Hamamoto, M., Hiraoka, Y., Horinouchi, S., and Yoshida, M. (2006). ORFeome cloning and global analysis of protein localization in the fission yeast Schizosaccharomyces pombe. *Nature biotechnology*, 24(7):841–7.

McCollum, D., Feoktistova, A., Morphew, M., Balasubramanian, M., and Gould, K. L.

(1996). The Schizosaccharomyces pombe actin-related protein, Arp3, is a component of the cortical actin cytoskeleton and interacts with profilin. *The EMBO journal*, 15(23):6438–46.

Medicherla, B., Kostova, Z., Schaefer, A., and Wolf, D. H. (2004). A genomic screen identifies Dsk2p and Rad23p as essential components of ER-associated degradation. *EMBO reports*, 5(7):692–7.

Meyer, H. H., Shorter, J. G., Seemann, J., Pappin, D., and Warren, G. (2000). A complex of mammalian ufd1 and npl4 links the AAA-ATPase, p97, to ubiquitin and nuclear transport pathways. *The EMBO journal*, 19(10):2181–92.

Meyer, H. H., Wang, Y., and Warren, G. (2002). Direct binding of ubiquitin conjugates by the mammalian p97 adaptor complexes, p47 and Ufd1-Npl4. *The EMBO journal*, 21(21):5645–52.

Miller, J. and Gordon, C. (2005). The regulation of proteasome degradation by multi-ubiquitin chain binding proteins. *FEBS letters*, 579(15):3224–30.

Moreland, J. L., Gramada, A., Buzko, O. V., Zhang, Q., and Bourne, P. E. (2005). The Molecular Biology Toolkit (MBT): a modular platform for developing molecular visualization applications. *BMC bioinformatics*, 6:21.

Müller, J. M., Meyer, H. H., Ruhrberg, C., Stamp, G. W., Warren, G., and Shima, D. T. (1999). The mouse p97 (CDC48) gene. Genomic structure, definition of transcriptional regulatory sequences, gene expression, and characterization of a pseudogene. *The Journal of biological chemistry*, 274(15):10154–62.

Murzin, A. G., Brenner, S. E., Hubbard, T., and Chothia, C. (1995). SCOP: a structural classification of proteins database for the investigation of sequences and structures. *Journal of molecular biology*, 247(4):536–40.

Mutoh, N., Nakagawa, C. W., and Yamada, K. (2002). Characterization of Cu, Zn-superoxide dismutase-deficient mutant of fission yeast Schizosaccharomyces pombe. *Current genetics*, 41(2):82–8.

Nakai, M., Endo, T., Hase, T., and Matsubara, H. (1993). Intramitochondrial protein sorting. Isolation and characterization of the yeast MSP1 gene which belongs to a novel family of putative ATPases. *The Journal of biological chemistry*, 268(32):24262–9.

Nakatsukasa, K. and Brodsky, J. L. (2008). The recognition and retrotranslocation of

misfolded proteins from the endoplasmic reticulum. *Traffic (Copenhagen, Denmark)*, 9(6):861–70.

Naresh, A., Saini, S., and Singh, J. (2003). Identification of Uhp1, a ubiquitinated histone-like protein, as a target/mediator of Rhp6 in mating-type silencing in fission yeast. *The Journal of biological chemistry*, 278(11):9185–94.

Neuber, O., Jarosch, E., Volkwein, C., Walter, J., and Sommer, T. (2005). Ubx2 links the Cdc48 complex to ER-associated protein degradation. *Nature cell biology*, 7(10):993–8.

Noguchi, E. (2006). 2 Step PCR for Gene Disruption / Tagging. *The Noguchi Lab Protocol*, http://homepage.mac.com/enognog/tag delete transformation.pdf:Accessed on 20/01/2009.

Ogiso, Y., Sugiura, R., Kamo, T., Yanagiya, S., Lu, Y., Okazaki, K., Shuntoh, H., and Kuno, T. (2004). Lub1 participates in ubiquitin homeostasis and stress response via maintenance of cellular ubiquitin contents in fission yeast. *Molecular and cellular biology*, 24(6):2324–2331.

Ogura, T. and Wilkinson, A. J. (2001). AAA+ superfamily ATPases: common structure-diverse function. *Genes to Cells*, 6(7):575–597.

Ortolan, T. G., Tongaonkar, P., Lambertson, D., Chen, L., Schauber, C., and Madura, K. (2000). The DNA repair protein rad23 is a negative regulator of multi-ubiquitin chain assembly. *Nature cell biology*, 2(9):601–8.

Park, S., Isaacson, R., Kim, H. T., Silver, P. A., and Wagner, G. (2005). Ufd1 exhibits the AAA-ATPase fold with two distinct ubiquitin interaction sites. *Structure (London, England : 1993)*, 13(7):995–1005.

Park, S., Rancour, D. M., and Bednarek, S. Y. (2007). Protein domain-domain interactions and requirements for the negative regulation of Arabidopsis CDC48/p97 by the plant ubiquitin regulatory X (UBX) domain-containing protein, PUX1. *The Journal of biological chemistry*, 282(8):5217–5224.

Pasinelli, P., Belford, M. E., Lennon, N., Bacskai, B. J., Hyman, B. T., Trotti, D., and Brown, R. H. (2004). Amyotrophic lateral sclerosis-associated SOD1 mutant proteins bind and aggregate with Bcl-2 in spinal cord mitochondria. *Neuron*, 43(1):19–30.

Pelham, R. J. and Chang, F. (2002). Actin dynamics in the contractile ring during cytokinesis in fission yeast. *Nature*, 419(6902):82–6.

Peng, J., Schwartz, D., Elias, J. E., Thoreen, C. C., Cheng, D., Marsischky, G., Roelofs,

J., Finley, D., and Gygi, S. P. (2003). A proteomics approach to understanding protein ubiquitination. *Nature biotechnology*, 21(8):921–6.

Pevala, V., Kolarov, J., and Polcic, P. (2007). Alterations in mitochondrial morphology of Schizosaccharomyces pombe induced by cell-death promoting agents. *Folia microbiologica*, 52(4):381–90.

Pickart, C. M. (2001). Mechanisms underlying ubiquitination. *Annual review of biochemistry*, 70:503–33.

Quinlan, R. A., Pogson, C. I., and Gull, K. (1980). The Influence of the Microtubule Inhibitor, Methyl Benzimidazol-2-yl-Carbamate (MBC) on Nuclear Division and the Cell Cycle In Saccharomyces cerevisiae. *Journal of Cell Science*, 46:341–352.

Raasi, S. and Wolf, D. H. (2007). Ubiquitin receptors and ERAD: a network of pathways to the proteasome. *Seminars in cell & developmental biology*, 18(6):780–91.

Rabinovich, E., Kerem, A., Fröhlich, K. U., Diamant, N., and Bar-Nun, S. (2002). AAA-ATPase p97/Cdc48p, a cytosolic chaperone required for endoplasmic reticulum-associated protein degradation. *Molecular and cellular biology*, 22(2):626–634.

Rabouille, C., Kondo, H., Newman, R., Hui, N., Freemont, P., and Warren, G. (1998). Syntaxin 5 is a common component of the NSF- and p97-mediated reassembly pathways of Golgi cisternae from mitotic Golgi fragments in vitro. *Cell*, 92(5):603–610.

Rabouille, C., Levine, T. P., Peters, J. M., and Warren, G. (1995). An NSF-like ATPase, p97, and NSF mediate cisternal regrowth from mitotic Golgi fragments. *Cell*, 82(6):905–914.

Rakhit, R., Robertson, J., Vande Velde, C., Horne, P., Ruth, D. M., Griffin, J., Cleveland, D. W., Cashman, N. R., and Chakrabartty, A. (2007). An immunological epitope selective for pathological monomer-misfolded SOD1 in ALS. *Nature medicine*, 13(6):754–9.

Rapo port, S., Dubiel, W., and Müller, M. (1982). Characteristics of an ATP-dependent proteolytic system of rat liver mitochondria. *FEBS letters*, 147(1):93–6.

Rapo port, S., Dubiel, W., and Müller, M. (1985). Proteolysis of mitochondria in reticulocytes during maturation is ubiquitin-dependent and is accompanied by a high rate of ATP hydrolysis. *FEBS letters*, 180(2):249–52.

Richly, H., Rape, M., Braun, S., Rumpf, S., Hoege, C., and Jentsch, S. (2005). A series

of ubiquitin binding factors connects CDC48/p97 to substrate multiubiquitylation and proteasomal targeting. *Cell*, 120(1):73–84.

Roguev, A., Bandyopadhyay, S., Zofall, M., Zhang, K., Fischer, T., Collins, S. R., Qu, H., Shales, M., Park, H.-O., Hayles, J., Hoe, K.-L., Kim, D.-U., Ideker, T., Grewal, S. I., Weissman, J. S., and Krogan, N. J. (2008). Conservation and rewiring of functional modules revealed by an epistasis map in fission yeast. *Science (New York, N.Y.)*, 322(5900):405–10.

Roguev, A., Wiren, M., Weissman, J. S., and Krogan, N. J. (2007). High-throughput genetic interaction mapping in the fission yeast Schizosaccharomyces pombe. *Nature methods*, 4(10):861–6.

Rosen, D. R., Siddique, T., Patterson, D., Figlewicz, D. A., Sapp, P., Hentati, A., Donaldson, D., Goto, J., O'Regan, J. P., and Deng, H. X. (1993). Mutations in Cu/Zn superoxide dismutase gene are associated with familial amyotrophic lateral sclerosis. *Nature*, 362(6415):59–62.

Saeki, Y. (2002). Ubiquitin-like proteins and Rpn10 play cooperative roles in ubiquitin-dependent proteolysis. *Biochemical and Biophysical Research Communications*, 293(3):986–992.

Sawin, K. E. and Nurse, P. (1998). Regulation of cell polarity by microtubules in fission yeast. *Journal of Cell Biology*, 142(2):457–471.

Sawin, K. E. and Snaith, H. A. (2004). Role of microtubules and tea1p in establishment and maintenance of fission yeast cell polarity. *Journal of cell science*, 117(Pt 5):689–700.

Schäfer, A. and Wolf, D. H. (2005). Yeast genomics in the elucidation of endoplasmic reticulum (ER) quality control and associated protein degradation (ERQD). *Methods in enzymology*, 399:459–68.

Schilling, O. and Overall, C. M. (2007). Proteomic discovery of protease substrates. *Current opinion in chemical biology*, 11(1):36–45.

Schnall, R., Mannhaupt, G., Stucka, R., Tauer, R., Ehnle, S., Schwarzlose, C., Vetter, I., and Feldmann, H. (1994). Identification of a set of yeast genes coding for a novel family of putative ATPases with high similarity to constituents of the 26S protease complex. *Yeast*, 10(9):1141–55.

Schubert, U., Antón, L. C., Gibbs, J., Norbury, C. C., Yewdell, J. W., and Bennink,

J. R. (2000). Rapid degradation of a large fraction of newly synthesized proteins by proteasomes. *Nature*, 404(6779):770–4.

Schuberth, C. and Buchberger, A. (2005). Membrane-bound Ubx2 recruits Cdc48 to ubiquitin ligases and their substrates to ensure efficient ER-associated protein degradation. *Nature cell biology*, 7(10):999–1006.

Schuberth, C. and Buchberger, A. (2008). UBX domain proteins: major regulators of the AAA ATPase Cdc48/p97. *Cellular and molecular life sciences : CMLS*, 65(15):2360–71.

Schultz, J., Milpetz, F., Bork, P., and Ponting, C. P. (1998). SMART, a simple modular architecture research tool: Identification of signaling domains. *Proceedings of the National Academy of Sciences*, 95(11):5857–5864.

Seeger, M., Hartmann-Petersen, R., Wilkinson, C. R. M., Wallace, M., Samejima, I., Taylor, M. S., and Gordon, C. (2003). Interaction of the anaphase-promoting complex/cyclosome and proteasome protein complexes with multiubiquitin chain-binding proteins. *The Journal of biological chemistry*, 278(19):16791–6.

Shcherbik, N. and Haines, D. S. (2007). Cdc48p(Npl4p/Ufd1p) binds and segregates membrane-anchored/tethered complexes via a polyubiquitin signal present on the anchors. *Molecular cell*, 25(3):385–397.

Smith, D. M., Benaroudj, N., and Goldberg, A. (2006). Proteasomes and their associated ATPases: a destructive combination. *Journal of structural biology*, 156(1):72–83.

Sonnhammer, E. L., Eddy, S. R., and Durbin, R. (1997). Pfam: a comprehensive database of protein domain families based on seed alignments. *Proteins*, 28(3):405–20.

Sonnhammer, E. L., von Heijne, G., and Krogh, A. (1998). A hidden Markov model for predicting transmembrane helices in protein sequences. *Proceedings / ... International Conference on Intelligent Systems for Molecular Biology ; ISMB. International Conference on Intelligent Systems for Molecular Biology*, 6:175–82.

Studier, F. W. and Moffatt, B. A. (1986). Use of bacteriophage T7 RNA polymerase to direct selective high-level expression of cloned genes. *Journal of molecular biology*, 189(1):113–30.

Szlanka, T., Haracska, L., Kiss, I., Deák, P., Kurucz, E., Andó, I., Virágh, E., and Udvardy, A. (2003). Deletion of proteasomal subunit S5a/Rpn10/p54 causes lethality,

multiple mitotic defects and overexpression of proteasomal genes in Drosophila melanogaster. *Journal of cell science*, 116(6):1023–33.

Takeda, K., Yoshida, T., Kikuchi, S., Nagao, K., Kokubu, A., Pluskal, T., Villar-Briones, A., Nakamura, T., and Yanagida, M. (2010). Synergistic roles of the proteasome and autophagy for mitochondrial maintenance and chronological lifespan in fission yeast. *Proceedings of the National Academy of Sciences of the United States of America*, 107(8):3540–5.

The UniProt Consortium (2010). The Universal Protein Resource (UniProt) in 2010. *Nucleic acids research*, 38(Database issue):D142–8.

Tobias, J. W. and Varshavsky, A. (1991). Cloning and functional analysis of the ubiquitin-specific protease gene UBP1 of Saccharomyces cerevisiae. *Journal of Biological Chemistry*, 266(18):12021–12028.

Turi, T., Webster, P., and Rose, J. (1994). Brefeldin A sensitivity and resistance in Schizosaccharomyces pombe. Isolation of multiple genes conferring resistance. *Journal of Biological Chemistry*, 269(39):24229–24236.

Uchiyama, K., Jokitalo, E., Kano, F., Murata, M., Zhang, X., Canas, B., Newman, R., Rabouille, C., Pappin, D., Freemont, P., and Kondo, H. (2002). VCIP135, a novel essential factor for p97/p47-mediated membrane fusion, is required for Golgi and ER assembly in vivo. *Journal Cell Biology*, 159(5):855–866.

Uchiyama, K., Totsukawa, G., Puhka, M., Kaneko, Y., Jokitalo, E., Dreveny, I., Beuron, F., Zhang, X., Freemont, P., and Kondo, H. (2006). p37 is a p97 adaptor required for Golgi and ER biogenesis in interphase and at the end of mitosis. *Developmental cell*, 11(6):803–816.

van Dyck, L., Dembowski, M., Neupert, W., and Langer, T. (1998). Mcx1p, a ClpX homologue in mitochondria of Saccharomyces cerevisiae. *FEBS letters*, 438(3):250–4.

Vijay-Kumar, S., Bugg, C. E., and Cook, W. J. (1987). Structure of ubiquitin refined at 1.8 A resolution. *Journal of molecular biology*, 194(3):531–44.

Wang, J., Xu, G., and Borchelt, D. R. (2002). High molecular weight complexes of mutant superoxide dismutase 1: age-dependent and tissue-specific accumulation. *Neurobiology of disease*, 9(2):139–48.

Watson, I. R. and Irwin, M. S. (2006). Ubiquitin and ubiquitin-like modifications of the p53 family. *Neoplasia (New York, N.Y.)*, 8(8):655–66.

Welchman, R. L., Gordon, C., and Mayer, R. J. (2005). Ubiquitin and ubiquitin-like

proteins as multifunctional signals. *Nature reviews. Molecular cell biology*, 6(8):599–609.

Wilkinson, C. R. M., Ferrell, K., Penney, M., Wallace, M., Dubiel, W., and Gordon, C. (2000). Analysis of a Gene Encoding Rpn10 of the Fission Yeast Proteasome Reveals That the Polyubiquitin-binding Site of This Subunit Is Essential When Rpn12 / Mts3 Activity Is Compromised. *Biochemistry*, 275(20):15182–15192.

Wilkinson, C. R. M., Seeger, M., Hartmann-Petersen, R., Stone, M., Wallace, M., Semple, C., and Gordon, C. (2001). Proteins containing the UBA domain are able to bind to multi-ubiquitin chains. *Nature cell biology*, 3(10):939–43.

Wilkinson, K. D., Tashayev, V. L., O'Connor, L. B., Larsen, C. N., Kasperek, E., and Pickart, C. M. (1995). Metabolism of the polyubiquitin degradation signal: structure, mechanism, and role of isopeptidase T. *Biochemistry*, 34(44):14535–14546.

Wilson, J. D., Liu, Y., Bentivoglio, C. M., and Barlowe, C. (2006). Sel1p/Ubx2p participates in a distinct Cdc48p-dependent endoplasmic reticulum-associated degradation pathway. *Traffic (Copenhagen, Denmark)*, 7(9):1213–23.

Winder, B. S., Strandgaard, C. S., and Miller, M. G. (2001). The role of GTP binding and microtubule-associated proteins in the inhibition of microtubule assembly by carbendazim. *Toxicological sciences*, 59(1):138–146.

Wood, J. S. (1982). Genetic effects of methyl benzimidazole-2-yl-carbamate on Saccharomyces cerevisiae. *Molecular and cellular biology*, 2(9):1064–79.

Xie, W. and Ng, D. T. W. (2010). ERAD substrate recognition in budding yeast. *Seminars in cell & developmental biology*.

Xie, Y. and Varshavsky, A. (2000). Physical association of ubiquitin ligases and the 26S proteasome. *Proceedings of the National Academy of Sciences*, 97(6):2497–502.

Xu, P., Duong, D. M., Seyfried, N. T., Cheng, D., Xie, Y., Robert, J., Rush, J., Hochstrasser, M., Finley, D., and Peng, J. (2009). Quantitative proteomics reveals the function of unconventional ubiquitin chains in proteasomal degradation. *Cell*, 137(1):133–45.

Yao, T. and Cohen, R. E. (2002). A cryptic protease couples deubiquitination and degradation by the proteasome. *Nature*, 419(6905):403–7.

Ye, Y., Meyer, H. H., and Rapoport, T. A. (2003). Function of the p97-Ufd1-Npl4 complex in retrotranslocation from the ER to the cytosol: dual recognition

of nonubiquitinated polypeptide segments and polyubiquitin chains. *Journal Cell Biology*, 162(1):71–84.

Yonashiro, R., Sugiura, A., Miyachi, M., Fukuda, T., Matsushita, N., Inatome, R., Ogata, Y., Suzuki, T., Dohmae, N., and Yanagi, S. (2009). Mitochondrial ubiquitin ligase MITOL ubiquitinates mutant SOD1 and attenuates mutant SOD1-induced reactive oxygen species generation. *Molecular biology of the cell*, 20(21):4524–30.

Young, P., Deveraux, Q., Beal, R. E., Pickart, C. M., and Rechsteiner, M. (1998). Characterization of two polyubiquitin binding sites in the 26 S protease subunit 5a. *The Journal of biological chemistry*, 273(10):5461–7.

Yu, A. Y. H. and Houry, W. A. (2007). ClpP: a distinctive family of cylindrical energy-dependent serine proteases. *FEBS letters*, 581(19):3749–57.

Yuasa, T., Hayashi, T., Ikai, N., Katayama, T., Aoki, K., Obara, T., Toyoda, Y., Maruyama, T., Kitagawa, D., Takahashi, K., Nagao, K., Nakaseko, Y., and Yanagida, M. (2004). An interactive gene network for securin-separase, condensin, cohesin, Dis1/Mtc1 and histones constructed by mass transformation. *Genes to Cells*, 9(11):1069–1082.